Interactions between CRY1 and CBS mediate bi-directional regulation of circadian clock function and metabolism

by

Sibel Cal Kayitmazbatir

A Dissertation Submitted to the
Graduate School of Sciences and Engineering
in Partial Fulfillment of the Requirements for
the Degree of

Doctor of Philosophy

in

Molecular Biology and Genetics



July, 2019

Interactions between CRY1 and CBS mediate bi-directional regulation of circadian clock function and metabolism

Koç University

Graduate School of Sciences and Engineering

This is to certify that I have examined this copy of a doctoral dissertation by

Sibel Cal Kayitmazbatir

and have found that it is complete and satisfactory in all respects,
and that any and all revisions required by the final
examining committee have been made.

Committee Members:

Prof. Dr. Halil Kavakli

Prof. Dr. Metin Turkay

Assoc. Prof. Dr. Nuri Ozturk

Assoc. Prof. Dr. Umut Sahin

Asst. Prof. Dr. Ayse Koca Caydasi

Date:

11/07/2019

To my dear husband and beloved family...

ABSTRACT

Circadian clock controls the physiology and behavior in order to synchronize them to 24-hr rhythm. Synchronization of physiological events in our body both prevents us from diseases and helps us to overcome the existing problems. Unlike the central clock located in the SCN (suprachiasmatic nucleus) which is regulated by light, peripheral clocks either regulated by central clock or by feeding cues. Despite the many efforts have been done in the field to understand how transcription and translation is controlled by circadian clock, they are not enough to explain the oscillation of 50% of the metabolites. There is little known about how circadian clock molecular machinery controls metabolism or post-translational regulations of core clock components to regulate metabolically-important proteins.

Here we characterize a novel molecular interaction between one of the negative arm proteins of circadian clock (CRY1) and an important metabolic enzyme CBS (cystathionine-β-synthase). Mutations resulting loss-of-function of CBS causes a multi-systemic disorder called homocystinuria. Physical interaction of these two proteins provides bi-directional regulation of both circadian rhythm and metabolism. Other than transcriptional repressor role of CRY1, as a novel post-translational regulatory mechanism, it binds to CBS and regulates metabolism by favoring oligomerization and increasing the activity of it. On the other hand, wild type CBS, but not disease-causing mutant CBS, binds to CRY1 and enhances the repressor activity. Additionally, we also analyzed the effect of mutant CBS which causes homocystinuria in humans. CBS-I278T cannot form oligomers and thus, doesn't have any enzyme activity. This single mutation blocks the interaction of CRY1 and CBS. We verified the physiologic importance of this interaction by performing untargeted metabolomics screen in *Cry1*$^{-/-}$ and *Cbs*$^{-/-}$ liver samples and analyzed the significantly affected pathways. Strikingly, *Cry1*$^{-/-}$ affects the same pathways that are affected by *Cbs*$^{-/-}$. These pathways are transsulfuration pathway, lysine, arginine and proline metabolisms and urea cycle.

Our results provide better understanding about how circadian clock and metabolism regulate each other at post-translational level, with direct protein-protein interactions. We anticipate that our results will provide new circadian perspective to treat CBS-caused homocystinuria disease.

ÖZETÇE

Sirkadiyen ritim; fizyoloji ve davranışları 24 saatlik ritme senkronize ederek kontrol eder. Vücuttaki fizyolojik olayların senkronizasyonu, bizi hastalıklardan korurken hali hazırda var olan problemlerin de üstesinden gelmemize yardımcı olur. Işıkla kontrol edilen ve beynin SCN (suprakiazmatik çekirdek) bölgesinde bulunan merkez saatin aksine, organlarda yer alan periferal saatler merkez saat ya da beslenme sinyalleri ile kontrol edilir. Gen anlatımı ve protein anlatımının biyolojik saat tarafından kontrolü alanında yapılan yoğun çalışmalara rağmen, bu çalışmalar metabolitlerin yüzde 50'sinin osilasyonununun nasıl gerçekleştiğini açıklayamamaktadır. Moleküler seviyede sirkadiyen ritmin metabolizmayı nasıl kontrol ettiği ve protein anlatımı sonrası seviyede metabolik açıdan önemli proteinlerin sirkadiyen ritim tarafından nasıl kontrol edildiği hakkında çok az bilgi bulunmaktadır.

Burada bahsedilen çalışmada, önemli bir metabolik enzim olan Sistation-beta-Sentez (CBS) ile sirkadiyen ritim negatif kontrolünden sorumlu olan kriptokrom 1 (CRY1) arasında yeni bir etkileşim keşfedilmiştir. CBS' in aktivite kaybına sebep olan mutasyonlar homosistinuria isimli çoklu-sistem hastalığına sebep olmaktadır. Bu iki protein arasındaki fiziksel etkileşim sirkadiyen ritim ve metabolizmanın karşılıklı kontrolünü sağlamaktadır. Çalışmamızda, CRY1' in gen anlatımı baskılayıcı rolünün yanında, yeni protein seviyesinde enzim aktivitesi kontrol edici rolü aydınlatılmıştır. CRY1, CBS'e bağlanarak ve onun oligomerizasyon yapısını düzenleyerek aktivitesini arttırmaktadır. Diğer taraftan, CBS CRY1'e bağlanarak onun gen anlatımı seviyesindeki baskılayıcı rolünü güçlendirmektedir. Buna ek olarak, insanlarda homosistinuria hastalığına sebep olan CBS mutasyonu da çalışmamız kapsamında araştırılmıştır. Mutant CBS (CBS-I278T) oligomerize olma yeteneğini kaybetmekle birlikte enzim aktivitesini de sürdürememektedir. Tüm bunların yanında, mutant CBS-I278T, CRY1 ile de etkileşememektedir. CBS-CRY1 etkiletişiminim fizyolojik önemini anlamak amacıyla da Cry1 nakavt ve Cbs nakavt farelerin karaciğer örneklerinde metabolomik çalışmalar gerçekleştirdik. Metabolomik çalışma sonuçları, organizmada CRY1 olmadığında ve CBS olmadığında ayni yolakların önemli ölçüde etkilendiğini gösterdi. Sülfür

metabolizmasi, amino asit metabolizmasi ve üre yolağı CRY1 ve CBS tarafından önemli ölçüde etkilenen yolaklar olarak analiz edildi.

Çalışmalarımız sirkadyen ritmin metabolizmayi protein etkileşimi seviyesinde nasıl kontrol ettiğine dair daha detaylı bilgi birikimine sahip olmamızı sağlamıştır. Çalışmamız sayesinde CBS-kaynaklı homosistinuria hastalığının tedavisinde sirkadyen bakış açisinin kazandırılması gerektiği de gösterilmiştir.

ACKNOWLEDGMENTS

I would like to express my gratefulness to my personal instructor Prof. Dr. I. Halil Kavakli for his support and mentorship from my first day in his lab until my graduation. I am appreciated to him for teaching me how to work as good as the leading scientists around the world in our field. I had chances to work with experienced people thank to his collaborations. I also thank to Dr. Ron Anafi for his collaboration with us on my project.

I would like to thank to my committee members; Halil Kavakli, Metin Turkay, Nuri Ozturk, Ayse Koca Caydasi, and Umut Sahin for their guidance and suggestions during my research. I want to thank to Dr. Ibrahim Baris for his support throughout my PhD years. I am also grateful to Prof. Dr. John B. Hogenesch for his endless support about my research at the last year of my PhD study.

I feel so lucky because I have had the best lab members ever. We worked a lot, but we had fun a lot as well. I am grateful to my friend and sister Eylem Kulkoyluoglu-Cotul. I know we are going to be together until we will be old and cranky. Darya Yarparvar and Selma Bulut, thank you for all of your support and friendship for years. We had suffered a lot, but we handled them all. I am thankful to Yagmur Umay and Safak Isin for their special helps on my last year. I couldn't get it done without you. Finally, I am appreciated to have the best volunteer interns in the lab; Melis Celik and Edin Hepgulum. I know you guys are going to be great scientists.

My dear husband and my family, I couldn't do it without you. Your endless love and support made everything a lot easier and bearable. My dear mom and dad, my best luck in my life is being your child. You have always supported me through each step until here and encouraged me to go for the better. I am grateful for everything you have done for me. My lovely sisters, I know that you are there, and you will be there anytime I need you. Thank you for being on my side on my every decision. My better half, my beloved husband; you have always supported me and tried to make me happy and happier. You have never complained about our limited time that we had to spent in the lab. I am appreciated to you about your patience and respect to my work all the time. I will have to

work more, and I know you will be there supporting me. I love you so much, and I will always do. My family and you are my biggest gratitude in my life.

Translation of the last paragraph for my family:

Sevgili esim ve ailem, siz olmasanız bunu başaramazdım. Sizin sonsuz sevginiz ve desteğiniz her şeyi daha katlanılabilir ve kolay yaptı. Sevgili annem ve babam, sizin çocuğunuz olarak dogmam benim hayatımdaki en büyük şansım. Sizler bu zamana kadarki her adımımda beni desteklediniz ve hep daha iyisini yapmam için beni cesaretlendirdiniz. Benim için yaptığınız her şey için size minnettarım. Canim kardeşlerim, her zaman orda olduğunuzu ve her ihtiyacım olduğunda orda olacağınızı biliyorum. Tüm kararlarımda beni destekleyip yanımda olduğunuz için teşekkür ederim. Benim diğer yarim, sevgili esim; beni hep destekledin ve beni mutlu etmeye ve daha da mutlu etmeye calistin. Sinirli olan zamanımızı labta geçirmemizden hiçbir zaman şikâyet etmedin. Sabrın ve isime olan saygın için sana minnettarım. Bundan sonra da çok çalışmam gerekecek ve hep benim için orda olup beni destekleyeceğini biliyorum. Seni çok seviyorum ve hep seveceğim. Ailem ve sen hayatımdaki en büyük şükürlerimsiniz.

This project has been supported by Tubitak 2214A program between August 2018 and June 2018. Last year of the study was completed at Cincinnati Children's Hospital Medical Center, with the supervision of John B. Hogenesch.

TABLE OF CONTENTS

ABSTRACT v
ÖZETÇE vii
ACKNOWLEDGMENTS ix
LIST OF TABLES xiv
LIST OF FIGURES xv
NOMENCLATURE xix
Chapter 1 INTRODUCTION 1
Chapter 2 LITERATURE REVIEW 3
2.1 Biological Rhythms 3
2.1.1 Ultradian Rhythm 3
2.1.2 Circadian rhythms 4
2.1.3 Infradian Rhythms 5
2.2 Circadian Rhythms from Cyanobacteria to Higher Organisms 8
2.3 Physiology of Circadian Rhythms in Humans-in Health and Disease 11
2.3.1 Circadian Controlled Physiology 11
2.3.2 Circadian Regulation of Diseases 11
2.4 Molecular Regulation of Circadian Rhythms in Mammals 13
2.4.1 Core Circadian Clock Molecular Mechanism 15
2.4.2 Importance of Post-Transcriptional Regulation in Molecular Circadian Clock 19
2.5 One Carbon Metabolism Pathway and Circadian Regulation of Metabolism 19
2.5.1 One Carbon Metabolism and Related Pathways 20
2.5.2 Relationship Between Circadian Clock and Metabolism 27
Chapter 3 THESIS RATIONALE AND AIM 28
Chapter 4 MATERIALS AND METHODS 30
4.1 Cell Lines and Regular Maintenance Protocols 30
4.2 Plasmid Constructs 30
4.3 Mammalian-two-hybrid 31
4.4 Per1:luc Reporter Gene Assay 33

4.5 Cell Based Circadian Assay 33
4.6 Bimolecular Fluorescence Complementation Assay (Bi-FC) 35
4.7 Co-immunoprecipitation (co-IP) 36
4.8 Generating CRY1 Mutant Library 38
4.8.1 Construction of CRY1 Mutant Library Using Degenerate Primers 38
4.8.2 Site Directed Mutagenesis After the Detection of Crucial Amino Acid 39
4.9 Western Blot Immunoblotting 39
4.10 RNA Isolation and Real-Time PCR 40
4.10.1 RNA Isolation 40
4.10.2 cDNA Synthesis 40
4.10.3 Real-Time PCR 40
4.11 Cystathionine-Beta Synthase Enzymatic Activity Detection 41
4.11.1 Liver Lysate Preparation 41
4.11.2 Determination of CBS Enzymatic Activity 41
4.11.3 Measurement of H_2S Formation by Methylene Blue Assay 42
4.12 Cytosol-Nuclear Fractionation 42
4.13 Generation of *Cry1*$^{-/-}$, *Cry2*$^{-/-}$ and *Cbs* $^{-/-}$ Mice 42
4.14 Circadian Behavioral Analysis 43
4.15 Metabolomics Analysis 43
4.16 Mass spectroscopy data processing and enrichment analysis 44
Chapter 5 RESULTS 45
5.1 The Expression of CBS Through 24 Hour Period in Synchronized Cells 45
5.2 Interaction Analysis of CBS with Known Clock Components 47
5.3 Effect of CBS siRNA Knock-Down on Circadian Rhythms of Cells 49
5.4 Circadian Behavioral Analysis of *Cbs*$^{-/-}$ Mice 55
5.5 Further Analysis of The Interaction of CRY1 and CBS 62
5.5.1 Identification of the Crucial Binding Site on CRY1 for Its Interaction with CBS 62
5.5.2 Co-Immunoprecipitation Verified the Physical Interaction Between CRY1 and CBS 68
5.5.3 Bi-Molecular Fluorescence Complementation (Bi-FC) Assay Showed CBS-CRY1 interaction *in vitro* 69
5.5.4 Nucleo-cytoplasmic Fractionation of Liver Proved the Localization of CBS and CRY1 at both Cytosol and Nucleus *in vivo* 73
5.5.5 Disease causing CBS Mutation (I278T) Blocks CBS-CRY1 Interaction ... 76

5.6 Wild Type but Not Mutant CBS Enhances CRY1 Repression 78
5.7 CRY1 is Increasing the Enzymatic Activity of CBS in Liver 82
5.8 CRY1 Favors the Homo-Tetramerization of CBS by Enhancing Its Enzyme Activity 88
5.9 Absences of CBS and CRY1 Affects the Same Pathways in Mouse Liver 90
5.10 Analysis of the Effects of CBS and CRY1 Absences on DNA and RNA Methylations 97
Chapter 6 DISCUSSION 101
Chapter 7 106
CONCLUSIONS AND FUTURE DIRECTIONS 106
Chapter 8 107
REFERENCES 107
Chapter 9 116
APPENDICES 116
9.1 Supplementary Tables 116
9.2 Supplementary documents 120
9.2.1 Metabolites Significantly Changed in CBS knock out liver samples, compared with wild type 120
9.2.2 Thermo Prestained page ruler used in all western blot experiments as molecular weight indicator. 138
9.2.3 Permissions to use published figures in literature review section 139

LIST OF TABLES

Table 1: Medium types used in the cell culture experiments and their compositions 32
Table 2: siRNA target genes, their host species and the catalog numbers of used siRNAs in the experiments. 34
Table 3: Buffers and their compositions which were used in the experiments. All buffers which were used for protein experiments were supplemented with protease inhibitors. 37
Table 4: PCR reaction conditions to apply degenerate PCR.... 38
Table 5: PCR reaction conditions to apply site-directed PCR 39
Table 6: Different mutations detected after degenerate PCR and their interaction with CBS based on mammalian-two hybrid signals. 65
Table 7: Period, relative amplitude and circadian power raw data obtained from locomotor activity analysis 116
Table 8: Q-PCR primer sequences used in this project.... 117
Table 9: Primer sequences which used to make degenerate mutations in the last 20 amino acids of CRY1. Last two primers were used to make site-directed mutagenesis on R602 point.... 118
Table 10: IUPAC codes and their base meanings 119

LIST OF FIGURES

Figure 2-1: Adopted from Franz Weber, 2017. Wake, REM and NREM stages of human sleep with around 90 minutes of cycling profile. 4
Figure 2-2: Figure explaining the 24-hour interval of the peaks of repeating biological event. 5
Figure 2-3: Applied from Driver and Baker, 2007. 28-day representative menstruation cycle and hormone levels during this process is represented at the top graph. The graph below shows the orchestration of morning rectal temperature and REM sleep percentage with menstrual cycle. 6
Figure 2-4: Applied from Walter Arnold et al, 2018. Percentage of activity in arctic animals showing circannual rhythm which peaks at summertime. 7
Figure 2-5: The figure was modified from Reena Saini, 2019. Inputs like light and temperature both directly regulates molecular central clock machinery and peripheral clocks (black solid lines). Peripheral clocks also send signals to central clock and regulate it (red dashed lines). 9
Figure 2-6: The figure was modified from Aleksandar Videnovic et al, 2014. While Feeding, light, and activity regulate central clock, feeding can also regulate peripheral clocks directly. Peripheral clocks also send signal to central clock to regulate central behaviors like sleep-wake cycles. 14
Figure 2-7: Adapted from Jay Dunlap, 1999. Schematic representation of positive and negative elements forming molecular machinery of circadian clock to regulate circadian regulation of behavior and metabolism. 15
Figure 2-8: Adapted from Buhr and Takahashi, 2013. Expressions of core circadian clock genes and their induction synchronized with SCN firing which is regulated by light-dark cycle. 16
Figure 2-9: Adopted from Joseph Takahashi, 2016. Molecular mechanisms regulating circadian clock. Positive regulators BMAL1-CLOCK drives the expressions of clock-controlled genes (ccg) and negative regulators (Per and Cry). 18
Figure 2-10: Folate pathway and important biosynthesis reactions mediated by folate pathway. 21
Figure 2-11: DHFR (dihydro folate reductase) mRNA expression in mouse liver. Data exported from CircaDB database. 22
Figure 2-12: Diagram of methyl cycle showing methionine sources, synthesis and utilization steps. 24
Figure 2-13: A diagram of transsulfuration pathway starting with utilization of homocysteine, continues with synthesis of H_2S and glutathione. 25
Figure 3-1: One carbon metabolism and urea cycle are the central pethways Cystathionine-β-synthase (CBS) is connected to. 29
Figure 4-1: Schematic representation of bimolecular fluorescence complementation .. 35

Figure 5-1: (A) Western blot detection of CBS protein amount oscillation over time after synchronization with Dexamethasone. (B) Quantification of western blot results shows the oscillation of CBS. n=3 biological replicates. 46
Figure 5-2: Circadian expression profile of CBS in mouse liver and lung tissues. Adopted from CircaDB online database. 47
Figure 5-3: Mammalian two hybrid interaction analysis of CBS and known core clock components. Bars indicate the mean luciferase activity± SEM which was normalized by renilla-luciferase expression. n=2 * $p<0.03$, *$p<0.018$. 48
Figure 5-4: (A) Circadian phenotypes of NIH 3T3:P(Bmal1)dluc cells when Cbs and Cry1 were separately knocked-down with siRNAs. (B) Effects of Cbs and Cry1 silencing on period lenght of the cells. (C) siRNA knock-down efficiencies of the genes. 50
Figure 5-5: (A) Circadian phenotypes of U2-OS:P(Bmal1)dluc cells when Cbs and Cry1 were separately knocked-down with siRNAs. (B) Effects of Cbs and Cry1 silencing on period length of the cells. (C) siRNA knock-down efficiencies of the genes. 51
Figure 5-6: Effect of different methionine concentrations on circadian phenotypes of cells. (A) (B) Circadian responses of U2-OS: P(Bmal1)-dluc and NIH 3T3: P(Bmal1)-dluc cells to 0, 1, 5, 10 and 15 mg/mL methionine concentrations. 53
Figure 5-7: Effect of different glutathione on circadian phenotypes of cells in the wild type and CBS knock-down cells. (A) (B) Circadian responses of U2OS: P(Bmal1)-dluc and NIH 3T3: P(Bmal1)-dluc cells glutathione addition to the cells. Addition of glutathione doesn't affect period lengths of the cells. 54
Figure 5-8: Representative actogram and *Cbs*$^{-/-}$ genotype verification at protein level. Protein samples prepared from *Cbs*$^{-/-}$ mouse liver. 56
Figure 5-9: Wild type female actogram results. 57
Figure 5-10: CBS knock-out female actogram results. 58
Figure 5-11: Wild type male actogram results. 59
Figure 5-12: CBS knock-out male actogram results. 60
Figure 5-13: (A) (B) (C) Respectively, circadian period, relative amplitude and circadian power analysis results of *Cbs*$^{-/-}$ mice circadian locomotor activities. Closed red circles represent female samples, closed blue circles represent male samples. 61
Figure 5-14: (A) C-terminal Truncated CRY1 constructs in pBIND vector. (B) Expression of all of the constructs which were detected by anti-GAL4 western blot antibody. 62
Figure 5-15: Repression activity of truncated CRY1 proteins on BMAL1-CLOCK transactivation. 63
Figure 5-16: Mammalian-two hybrid interaction analysis of CBS and truncated CRY1 proteins. 64
Figure 5-17: Even though the new constructs are functionally active, they do not interact with CBS. (A) Expression of wild-type, mutant, and truncated CRY1 constructs which were transfected to HEK293T cell line with PEI. (B) Clustal Omega conservation analysis of R R602 point across different organisms. (C) Mammalian two hybrid interaction analysis of CRY1-WT, CRY1-R602P and CRY1-T1 with PER2. All constructs interact with PER2. 66

Figure 5-18: (A) Repression activities of CRY1-WT, CRY1-R602P and CRY1-T1 on BMAL1-CLOCK transactivation. CRY1-T1 and CRY1-R602P are able to repress the BMAL1-CLOCK transactivation as much as wild type CRY1. (B) Mammalian two hybrid interaction analysis of CRY1-WT, ... 67
Figure 5-19: Proof of physical interaction between CRY1 and CBS by co-immunoprecipitation. The upper panel shows the result of CBS pull down with Flag tag. 2nd panel is the western blot of the input samples used for Flag-tagged pull down. 3rd and 4th panels are the pull down and input blots of His-tagged CRY1 immunoprecipitation. 68
Figure 5-20: Bi-FC result of CBS and CRY1. (A) Upper photos show that CRY1-R602P and CBS do not interact. The lower photos show that CRY1 and CBS interact. We can see from the merged image that this interaction is both in cytosol (orange areas-overlapping of yellow and red) and in nucleus (yellow areas-no overlap with red). (B) Expressions of CBS and CRY1 in upper and lower panels where mutant CRY1 and CBS and wild type CRY1 and CBS co-expressed for Bi-FC visualizations. 71
Figure 5-21: Detection of the interaction localization of CBS and CRY1. (A) Together with Bi-FC detection, co-localization of CBS at the interaction site was determined with Anti-Flag antibody detection. (B) Both cytosolic and nuclear localization of the interaction of CBS and CRY1 were verified with DAPI staining. 72
Figure 5-22: Cytosolic and nuclear fractions of mouse liver samples which were obtained at ZT10 and ZT22. Tubulin was used as cytosolic loading control, Histone-H3 was used as nuclear loading control. (A) Control of the success of fractionation experiment. Both tubulin and Histone-H3 was detected in both fractions. (B) Both CBS and CRY1 were detected in both fractions. (C) (D) Cytosolic and nuclear abundances of CRY1. (E) (F) Cytosolic and nuclear abundances of CBS. (G) CRY1 protein amounts at ZT10 and ZT22 in whole cell lysates. (H) CBS protein amounts at ZT10 and ZT22 in whole cell lysates. 74
Figure 5-23: Disease causing mutation inhibits the interaction of CRY1 and CBS (A) Mammalian-two hybrid experiment showing significantly less interaction between CBS-I278T and CRY1. (B) Co-immunoprecipitation results showing the interaction between wild type CBS and CRY1 and disruption of the interaction between CBS-I278T and CRY1. Top two panels show the western blot of immunoprecipitation samples and bottom two panels show the western blot of the input samples. 77
Figure 5-24: Analysis of the effect of CBS on the repression activity of CRY1. (A) Per1:luc reporter assay analyzing the effect of CBS on CRY1's repression activity on BMAL1-CLOCK transactivation. (B) CBS and CRY1 protein amounts in HEK293T and Neuro-2A cell lines. (C) The effects of CBS-WT, CBS-I278T and GAPDH on BMAL1-CLOCK transactivation, in the absence of CRYs. 79
Figure 5-25: mRNA levels of Dbp and Per2 in Cbs knocked-down samples..... 80
Figure 5-26: Change in the output of E-box promoters in Cbs knock out liver samples. (A) (B) CRY1 protein amount in *Cbs*$^{-/-}$ liver samples and their quantifications. (C) Dbp and Per2 mRNA levels in CBS knock out liver samples. 81

Figure 5-27: (A) Cry1$^{-/-}$ genotype verification by western blot and CRY1 total abundance verification at ZT10 and ZT22. (B) Cry2$^{-/-}$ genotype verification by PCR. (C) Inhibition of CSE activity in Cbs-/- liver samples by 30 mM PAG. 83
Figure 5-28: CBS activity detection system setup. 84
Figure 5-29: CBS protein levels in the samples used in enzyme activity detection experiments at ZT10 and ZT22. 85
Figure 5-30: Analysis of the effect of CRY1 and CRY2 absence on the enzyme activity of CBS. (A) (C) CBS enzyme activity change in CRY1 knock out and CRY2 knock out mouse liver samples at ZT10 and ZT22. (B) (D) CRY1 protein amounts in CRY2 knock out samples at ZT10 and ZT22 with their quantifications. 86
Figure 5-31: (A) Complementation assay showing the increase in the CBS enzyme activity in the presence of CRY1-WT in Cry1-/- liver samples. (B) CBS and CRY1 protein amounts in the assay samples. (C) CBS protein level quantification in complementation assay samples. 87
Figure 5-32: Native-PAGE showing homo-oligomers of CBS when either GFP, CRY1-WT or CRY1-R602P was overexpressed in HEK293T cells. 89
Figure 5-33: Quantification of Native-PAGE showing increased tetramer amount of CBS by only CRY1-WT. The below SDS-PAGE followed by western blot shows comparable expressions of CBS, CRY1 and ACTIN under reducing conditions. 90
Figure 5-34: Metabolites significantly affected by the absence of either CRY1 or CRY2, compared by their wild type littermate controls. 91
Figure 5-35: Metabolites significantly affected by the absence of either CRY1 or CRY2, compared by their wild type littermate controls. 92
Figure 5-36: Metabolites significantly affected by the absence of either CRY1 or CRY2, compared by their wild type littermate controls. 93
Figure 5-37: Heatmap representing the significance of metabolites in both CBS absence, and CRY1 absence compared to their wild type littermate control. 95
Figure 5-38: Pathways significantly affected by the absence of **(A)** CBS, and **(B)** CRY1 and CRY2. **(C)** 15 out of 37 metabolites are same with the metabolites affected by CBS absence. 96
Figure 5-39: 5-mC total DNA methylation in wild type, Cry1 and Cry2$^{-/-}$ and Cbs$^{-/-}$ MEF cells. There is no significant difference between samples. 97
Figure 5-40: m6-A RNA methylation level of Cry1-Cry2$^{-/-}$ and Cbs$^{-/-}$ MEF cells compared with wild type. 99
Figure 5-41: m6-A RNA methylation level of Cry1$^{-/-}$, Cry2$^{-/-}$ and Cbs$^{-/-}$ mouse liver samples compared with wild type. 100
Figure 6-1: CRY1 increases CBS enzyme activity by modulating tetramerization of CBS from dimers. 102
Figure 6-2: Some of the affected metabolites highlighted on one carbon metabolism pathway. 104
Figure 6-3: Model for the regulation between CRY1 and CBS inducing eachother's activities. CRY1 favors CBS tetramerization and enzyme activity in cytosol at ZT10, while CBS increases CRY1 repression activity in nucleus at ZT22. 105

NOMENCLATURE

3MST, 3-mercapto Sulfurtransferase

ACTH, Adrenocorticotropic Hormone

ALKBH5, AlkB homolog 5

AMP, Adenosine monophosphate

Bi-FC, Bi-molecular Fluorescence Complementation

BMAL1, Brain-Muscle-Arnt-like protein 1

BHMT, Betaine-homocysteine S-methyltransferase

CBS, Cystathionine-β-synthase

CCGs, Clock Controlled Genes

cDNA, Complementary deoxyribonucleic acid

CDP, Cytidine diphosphate

CLOCK, Circadian Locomotor Output Cycles Kaput

CK1, Casein kinase 1

CoA, Coenzyme A

CRY1/2, Crptochrome1/2

CSE, Cystathionine-γ-lyase

dAMP, Deoxyadenosine monophosphate

dCMP, Deoxycytidine monophosphate

DBP, D site of albumin promoter (albumin D-box) binding protein

DHF, Dihydrofolate

DHFR, Dihydrofolate Reductase

DMEM, Dulbecco's Modified Eagle Medium

ECL, Enhanced Chemiluminescence

FBXL3/21, F-box/LRR-Repeat Protein

FBS, Fetal Bovine Serum

FSH, Follicle-Stimulating Hormone

FTO, fat mass and obesity associated protein

GAPDH, Glyceraldehyde 3-Phosphate Dehydrogenase

GDP, Guanosine Diphosphate

GFP, green fluorescent protein

H_2S, Hydrogen Sulfide

H_2O_2, Hydrogen Peroxide

H_2O, Dihydrogen Oxide

HEK293T, Human Embryonic Kidney 293T Cells

HNRNP, heterogeneous ribonucleoprotein particle

HRP, Horse Radish Peroxidase

ipRGC, Intrinsically Photosensitive Retinal Ganglion Cells

LC, liquid chromatography

LC-MS, liquid chromatography-mass spectrometry

LH, Lutenizing Hormone

MEF, mouse embryonic fibroblast

METTL3/14/16, methyltransferase like 3/14/16

mRNA, messenger RNA

m^6A-RNA, N6-methylated RNA

MST, 3-mercaptopyruvate Sulfurtransferase

NAD, Nicotinamide Adenine Dinucleotide

NADP, Nicotinamide Adenine Dinucleotide Phosphate

N2A, Neuro-two-A (mouse neuronal cell line)

NIH 3T3:P(Bmal1)-dluc, mouse fibroblast luciferase reporter cell line

NREM, Non-Rapid Eye Movement

PAG, DL-propargylglycine

PBS, Phosphate Buffered Saline

PCR, Polymerase Chain Reaction

Per1:*luc,* luciferase expression under Per1 promotor

REM, Rapid Eye Movement

REV-ERB, Nuclear Receptor Subfamily 1, Group 1

RISC, RNA Induced Silencing Complex

ROR, RAR-related orphan receptor

ROS, Reactive oxygen species

RORE, RAR-related orphan receptor response element

SAH, S-Adenosyl-L-Homocysteine

SAM, S-adenosyl-L-methionine

SDS, Sodium Dodecyl Sulphate

SDS-PAGE, Sodium Dodecyl Sulphate Poly Acrylamide Gel Electrophoresis

SCN, Suprachiasmatic Nucleus

siRNA, Small Interfering RNA

Q-PCR, Quantitative Polymerase Chain Reaction

TBS, Tris Buffered Saline

THF, Tetra-hydro Folate

TTFL, Transcriptional-Translational Feedback Loop

U2-OS:P(Bmal1)-dluc, human osteosarcoma luciferase reporter cell line

UDP, Uracil Diphosphate

UMP, Uracil Monophosphate

YFP, Yellow Fluorescent Protein

YTHDC1, YTH domain containing protein-1

YTHDF1, YTH domain containing family protein-1

$ZnSO_4$, Zinc Sulfate

ZT, Zeitgeber Time

5-mC, 5-methyl cytosine

5hmC, 5-hydroxymethylcytosine

5fC, 5-formylcytosine

5caC, 5-carboxylcytosine

5hmU, 5-hydroxymethyluracil

6mA, n6-methyladenine

Chapter 1

INTRODUCTION

Temporal regulation of many important physiological and behavioral processes in the body occurs by transcriptional regulation of circadian clock [1]. Circadian regulation has been detected in a wide range of organisms from cyanobacteria, yeast, plants and mammals [2]. Memory, heart rate, alertness, immune responses, cognitive functions, and blood pressure are all controlled by circadian clock [3] [4].

It has been shown that 50% of metabolites show circadian regulations [5]. Even temporal transcriptional regulation is able to explain some of the cycling incidences, our current knowledge is not enough to understand how circadian clock regulates metabolism. Recent studies revealed that there has to be post-translational regulations regulating circadian physiology and metabolism [6].

Here, we have identified Cystathionine-β-synthase (CBS) as a novel circadian clock component candidate [7]. CBS catalyzes the first step of transsulfuration pathway utilizing homocysteine and producing cystathionine and hydrogen sulfide. It has been known that any disturbance on CBS protein level, or enzyme activity efficiency, or oligomerization state results in severe metabolic conditions [8]. We have characterized the bi-directional relation of CBS and circadian clock through the interaction of CBS and Cryptochrome 1 (CRY1).

Chapter 2 overviews literature about circadian clock, known molecular regulations of circadian clock, and the relation between circadian clock and metabolism.

Chapter 3 mentions the rational and aim of the study.

Chapter 4 explains materials and methods utilized in the current study in detail.

Chapter 5 provides detailed elucidation of all of the results obtained throughout the study leading us to conclude that CBS-CRY1 interaction is crucial and regulates metabolism and circadian clock in a bi-directional way.

Chapter 6 and chapter 7 provides discussion about obtained results and explains future perspectives concluded from the study.

Chapter 2

LITERATURE REVIEW

2.1 Biological Rhythms

Any biological processes showing re-occurrence in organisms are called biological rhythms. Biological rhythm types are characterized mainly based on the recurrence frequency of the rhythmic event [9]. There are three main types of biological rhythms, circadian, ultradian and infradian rhythms. The recurrence frequency of circadian rhythm is 24-hour which is mainly regulated by day-night cycle of the Earth. Circadian rhythms are the most common type of biological rhythms. In addition to that, we see re-occurring biological events with a frequency of either less or more than 24 hours. More detailed information about all these rhythms will be explained in the following sub-sections. It is important to note that, some bioperiodic events can be regulated by more than one biological rhythm mechanisms. Different mechanisms work together to adjust the organismal physiology to environmental changes.

2.1.1 Ultradian Rhythm

Ultradian rhythms are the biological processes occurring repeatedly with a period of less than 24 hour. Unlike circadian clock, ultradian rhythms are generated endogenously, independent of environmental the entrainment cues and independent of intact circadian rhythm [10] [11]. The most obvious ultradian rhythm is hidden in our sleep. Even though sleep timing is strongly regulated with circadian rhythm, sleep is made-up of sequentially occurring two stages (non-REM (NREM-non rapid eye movement) and REM (rapid eye movement)) with 90 minutes in total length. As seen in **Figure 2-1** [12], from awake to deep sleep, it goes from non-REM to REM. And this cycle repeats every 90 minutes.



Figure 2-1: Adopted from Franz Weber, 2017. Wake, REM and NREM stages of human sleep with around 90 minutes of cycling profile.

Even though growth hormone secretion shows 24 hour circadian oscillation, its secretion shows pulses at every 3 hours [13]. Similarly, ACTH (adrenocorticotropic hormone) and cortisol secretion shows both circadian and ultradian properties with showing pulses at every 90 minutes [14].

2.1.2 Circadian rhythms

Circadian word is composed of two words which are circa and dies. 'Circa' means about and 'dies' means a day. Any biological processes repeated with daily frequency are called circadian rhythms (**Figure 2-2**). If we think the event occurrence as hormone secretion, the maximum concentration of the hormone peaks every 24 hours as represented in **Figure 2-2**. These processes are both endogenously regulated by the central clock in the SCN (suprachiasmatic nucleus) and also by environmental cues like light, food, and social interactions. The occurrence of circadian rhythms in different organisms, the physiology of circadian rhythms, and molecular regulation of physiology by circadian clock are explained in detail in the following sections.

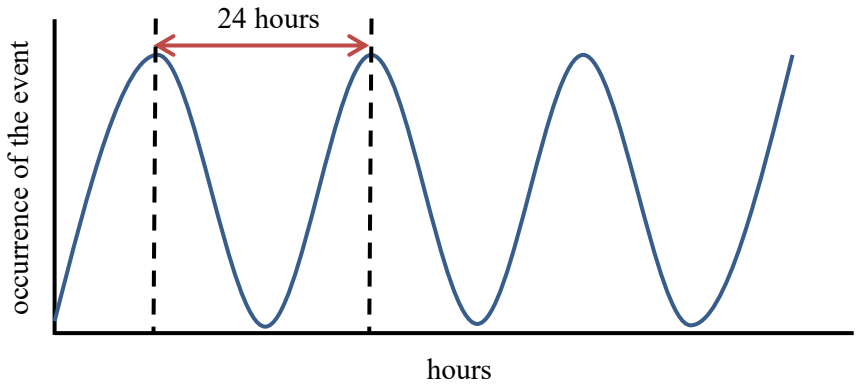


Figure 2-2: Figure explaining the 24-hour interval of the peaks of repeating biological event.

2.1.3 Infradian Rhythms

Infradian rhythms are the bioperiodic processes repeating with a longer period than 24 hours. This group of rhythms includes physiological processes with a period of days (menstrual cycle-28 days), or even months.

2.1.3.1 Menstrual Cycle

As a part of being healthy a woman, menstrual cycle helps women to produce an egg and prepare the uterus for fertilization and reproduction. If a mature egg doesn't get fertilized, the egg and the capillary filled inner layer of uterus is expulsed. This process is called menstrual cycle and it takes around 25-35 days as an average [15]. Menstrual cycle is performed by an orchestration of several hormones. Lutenizing hormone (LH), follicle-stimulating hormone (FSH), estrogen and progesterone have to work in synchrony to perform a healthy cycle.

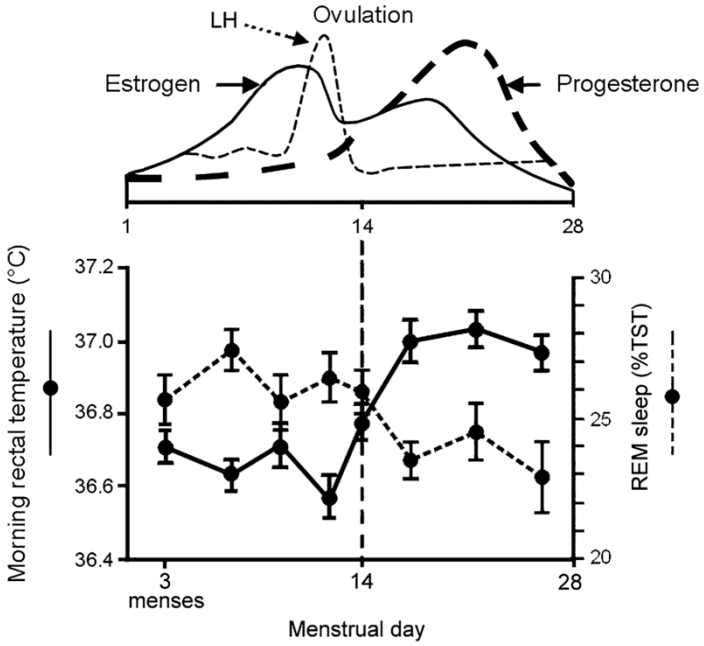


Figure 2-3: Applied from Driver and Baker, 2007. 28-day representative menstruation cycle and hormone levels during this process is represented at the top graph. The graph below shows the orchestration of morning rectal temperature and REM sleep percentage with menstrual cycle.

Even though body temperature is regulated in circadian manner [16], it also shows infradian rhythm which is correlated with progesterone secretion. Similarly, REM sleep is ultradian regulated, but its duration shows monthly rhythm too (**Figure 2-3** [17]). In addition to that, menstrual cycle is also regulated by circadian clock as well. Shift worker women who do not have intact circadian clock, report more irregularity in their menstrual cycle [18].

2.1.3.2 Annual Rhythms

Annual rhythms can be defined as combination of endogenous rhythms and environmental cues with a period of a year [19] [20]. Annual rhythms can be seen in either life cycle of annual plants, or growing patterns of some long-lived plants, or migration [21], reproduction, and hibernation[22] properties of animals, or even some hormone secretion in humans (even though they also show circadian rhythms) [23]. In 1957, annual rhythms were first reported in hibernation profiles of ground squirrels [22]. Hibernation helps animals to overcome harsh environmental conditions despite their core body temperature decreases a lot during winter. Due to their body fat accumulation and sleeping, they can survive from harsh winter conditions [24]. Migration is also necessary for reproduction effectiveness of migrating birds [21]. Thus, annual control of specific events is highly important for hibernating and migrating animals to survive [20].

Studies with arctic animals like arctic reindeers show the importance of arctic photic conditions on the circannual rhythms of animals. Even though they respond to acute light changes with melatonin secretion, their internal circadian clock is weak and even not present [25]. **Figure 2-4** shows the circannual activity pattern of an arctic animal Svalbard reindeer [26]. Relatively milder weather conditions in mid-summer increases the activity pattern which is related with reproductivity of the animals.

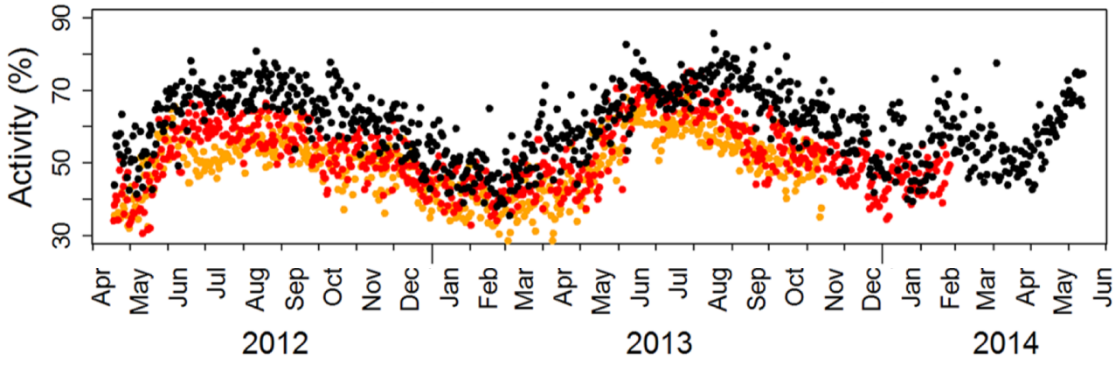


Figure 2-4: Applied from Walter Arnold et al, 2018. Percentage of activity in arctic animals showing circannual rhythm which peaks at summertime.

2.2 Circadian Rhythms from Cyanobacteria to Higher Organisms

As briefly mentioned above, circadian regulated bio-processes are both endogenously and environmentally regulated with day-night cycle of the Earth. Being endogenously regulated means the rhythm continues even under constant environmental conditions. In 1962, Franz Halberg in USA analyzed body temperature, blood cell count, and circulating hormone levels in both mice and men and defined the word ‘circadian’ for the first time [27]. Jurgen Aschoff in Germany (in 1965) [28] and Jean Colin in France (in 1968) [29] did experiments on circadian regulation of physiology and free running phase of circadian clock, too. Free running period shows the endogenous regulation of circadian controlled processes in the body independent of external entrainment cues.

As represented in **Figure 2-5**; inputs like light, temperature, food, social interactions send signals to regulate molecular clock machinery in central clock which further regulate the orchestration of peripheral clocks. However, circadian clock regulation cannot be explained with owner-slave model of interaction between central and peripheral clocks, because peripheral clocks both directly regulated by external inputs and also, they send signals back to central clock and regulate the central clock.

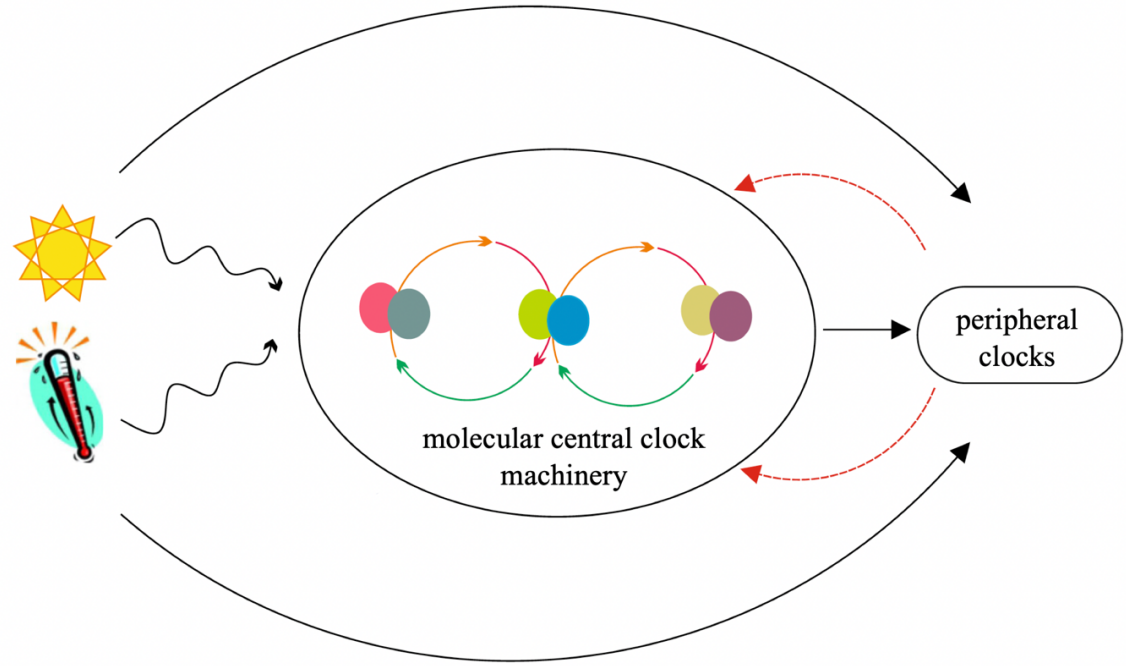


Figure 2-5: The figure was modified from Reena Saini, 2019. Inputs like light and temperature both directly regulates molecular central clock machinery and peripheral clocks (black solid lines). Peripheral clocks also send signals to central clock and regulate it (red dashed lines).

Cyanobacteria are simple prokaryotes, but they show a strong circadian regulation in behaviors of nitrogen fixation and photosynthesis. As represented in **Figure 2-5**, cyanobacteria circadian clock has both endogenous regulation with transcriptional translational feedback loop (TTFL), and acquire signals from environment [30]. Unlike eukaryotes, light is not the main entrainment cue for cyanobacteria. They sense the levels of photosynthetic metabolites and entrain themselves accordingly [31].

Cotyledon and leaf movements are the first realized circadian behavior in plants [32]. Like cyanobacteria and mammals, 10% of Arabidopsis mRNA expression show circadian oscillation [33]. Plants are prone to any kind of stress from environment. Their circadian clock helps them to overcome cold stress [34].

Insects show not only circadian clock, but also circannual and circalunar clocks. Since there is a consistent social behaviors in honeybee populations, they have been widely used to study circadian regulation of social behaviors. Workers in honeybee species find their food sources by using sun as a solar compass [35]. Light signals control migration behavior of a butterfly *Danaus plexippus* [36].

In the current study, we focus on mammalian circadian rhythm and circadian control of metabolism. In the following sections; mammalian circadian physiology, molecular regulation of mammalian circadian clock, and one carbon metabolism pathways have been overviewed to provide background information for understanding the results better.

2.3 Physiology of Circadian Rhythms in Humans-in Health and Disease

Circadian clock regulates numerous physiological and behavioral processes in many different pathways. In this section, I will explain how a healthy circadian clock regulates different physiological pathways throughout the body, and how disrupted circadian clock affects disease occurrence and progression.

2.3.1 Circadian Controlled Physiology

Signals coming from central clock, and feeding are the two main inputs of peripheral circadian clocks. When central circadian clock is disrupted either by SCN lesions or by molecular alterations, feeding timing is impaired in rat and mouse models [37] [38]. Despite underlying transcriptional or translational mechanisms remain to be elucidated, body temperature shows a feedback temporal regulation, because it is both an input and cycling output for body [39] [40]. Similarly, body temperature and sleep are strongly correlated under free running conditions. Sleep timing is directly regulated by central circadian clock, it is an obscure that how sleep, and body temperature is interconnected with each other . Learning and memory is also regulated by circadian clock with the help of hormonal signals. Daily regulation of learning and memory is also controlled by hippocampus by cellular signaling pathways like cyclic-AMP [41]. Time restricted feeding induces weight loss in humans as well as calorie restrictions [42] [43].

2.3.2 Circadian Regulation of Diseases

Circadian clock is all about feedback loop kind of regulations. Sleep is the main behavior regulated by central clock. Additionally, sleep also regulates circadian clock molecular mechanism [44]. Melatonin is secreted at night, providing a healthy sleep. Melatonin administration is also used to treat sleep disorders, as well as phase-shift problems [45].

Cancer is uncontrolled cell growth in numerous different tissues which also has the ability to spread between tissues. Several connections between circadian clock and cancer has been shown [46]. Mutations in the Per gene, or dysregulation in the mRNA expression of Per induces colon and breast cancer in humans [47] [48].

Aging decreases amplitude, thus robustness of circadian clock. Early-aging was shown in Bmal1 knock out mice [49]. Even we cannot totally reverse aging process, we can reduce aging symptoms by treating circadian clock, and by increasing robustness of it.

As outlined above, many behavioral and metabolic diseases are connected with circadian clock. Targeting circadian clock to treat diseases is an important perspective that every scientist needs to keep in mind.

2.4 Molecular Regulation of Circadian Rhythms in Mammals

Before explaining the molecular mechanisms regulating the circadian rhythms in mammals, we should firstly focus on what are the inputs and outputs of the circadian clock machinery. Inputs can regulate circadian clock in two ways: (1) regulating the central clock, (2) regulating the peripheral clocks. Central clock regulating inputs are light [50], feeding schedule [51], social interactions [52], and activity [53]. Feeding is also peripheral clock regulator which in turn sends signals to central clock, too [54].

The direct outputs of central clock are mainly behavioral activities like sleep-wake cycle and cognitive performances. And indirect output of the central clock is peripheral clock regulation. Peripheral clocks are both regulated by feeding and central clock which include circadian regulation of many organs like heart, liver, muscle and kidney [55]. While the role of peripheral clocks is regulating the circadian regulation in peripheral organs, they also send feedback signals to central clock. It has been shown in mice that feeding schedules affect the timing and quality of sleep [56].

Altogether, central and peripheral clocks work in synchrony to regulate circadian behavior and physiology (**Figure 2-6**). We need to be aware that we should help our body to keep them in synchrony with each other, because they are not two independent processes, they are strongly connected with each other.

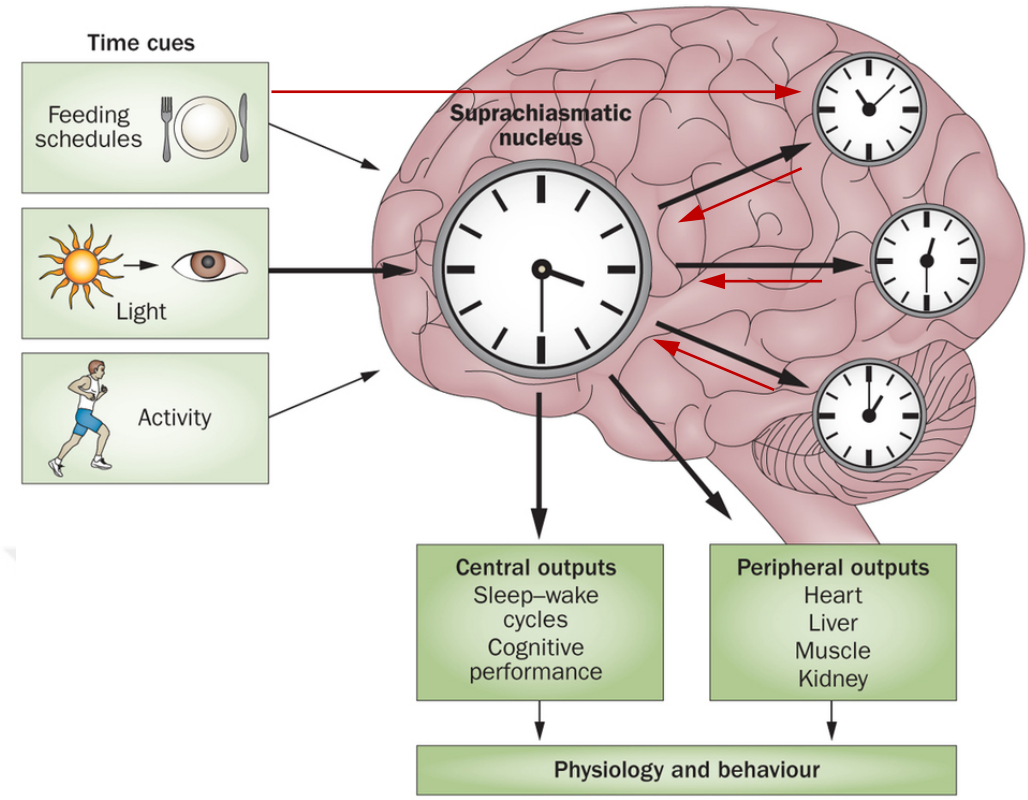


Figure 2-6: The figure was modified from Aleksandar Videnovic et al, 2014. While Feeding, light, and activity regulate central clock, feeding can also regulate peripheral clocks directly. Peripheral clocks also send signal to central clock to regulate central behaviors like sleep-wake cycles.

2.4.1 Core Circadian Clock Molecular Mechanism

Suprachiasmatic nucleus (SCN) is located in the hypothalamus region of brain and it is considered as the circadian clock regulation center of the brain. 20,000 neurons are located in SCN. 78% of the neurons are induced by light stimulation [57] which is sensed by eyes and transmitted through retinohypothalamic tract (RHT) [58]. Even without any environmental stimulation, the individual neurons are able to generate and maintain their internal circadian clock in SCN [59].

Light is sensed via 'intrinsically photosensitive retinal ganglion cells' (ipRGCs) and transmitted to SCN and regulate the expression of positive and negative regulators of molecular circadian clock machinery. There are positive and negative elements (blue and red boxes in the **Figure 2-7**) in molecular circadian clock machinery which in turn controls each other's and clock controlled genes' expressions and regulate the circadian control of behavior and metabolism [60].

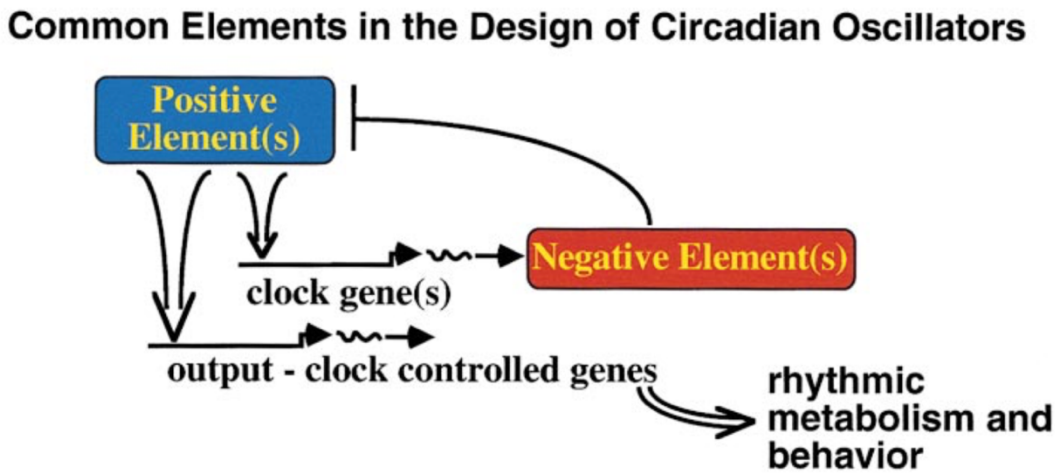


Figure 2-7: Adapted from Jay Dunlap, 1999. Schematic representation of positive and negative elements forming molecular machinery of circadian clock to regulate circadian regulation of behavior and metabolism.

We have mentioned that ipRGC cells sense and transmit the light signal to SCN. After light stimulation, neurons in the SCN starts firing. As shown in **Figure 2-8** [61], Per2 mRNA expression starts with neuron firing in SCN. PER2 protein expression continues mRNA synthesis with ~3 hours delay. 3-6 hours of delay between transcription and translation has been shown to be common [62]. When PER2 protein level increases, Bmal1 mRNA expression starts. Thus, the core molecular mechanism transcriptional translational feedback loop (TTFL) regulating circadian clock starts with light input and neuronal firing in SCN.

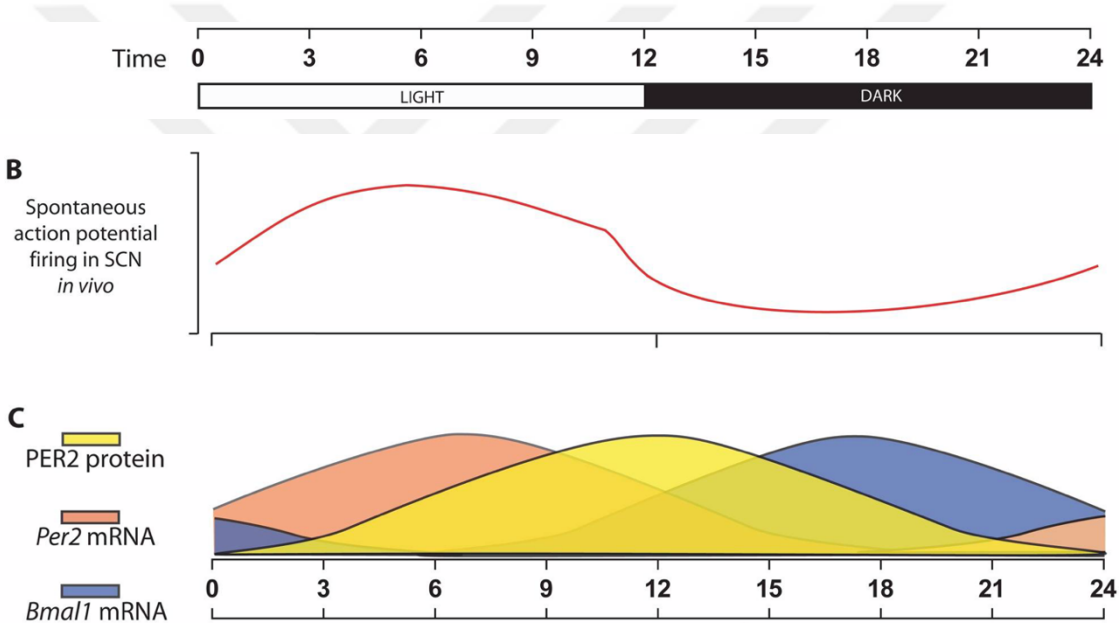


Figure 2-8: Adapted from Buhr and Takahashi, 2013. Expressions of core circadian clock genes and their induction synchronized with SCN firing which is regulated by light-dark cycle.

The molecular mechanism to control the circadian physiology is regulated with and interlocked transcriptional-translational feedback loop (TTFL) which regulates rhythmic gene expression and protein degradation. In the TTFL model, there are 4 different, while strongly related transcriptional and translational control mechanisms **(Figure 2-9** [63] **)**. Mechanism (1) starts with the expression of positive arm proteins BMAL1 and CLOCK which interacts and forms a heterodimer and binds to E-box elements in the promoter region of clock-controlled genes (ccg) and negative arm proteins. Mechanism (2) starts with the expression of negative arm proteins. After the negative arm proteins PER1, PER2, CRY1 and CRY2 are expressed, PERs and CRYs forms a heterodimer in cytosol and translocated to nucleus to repress their own transcription. Mechanism (3) is known as secondary transcriptional loop which involves the control of positive arm protein BMAL1. REV-ERB proteins are expressed under E-Box element and represses BMAL1 expression. On the other hand, ROR proteins are expressed from D-Box elements and induces BMAL1 expression. The last mechanism, mechanism (4) is a protein level regulation of negative arm proteins PERs and CRYs. FBXL3 and FBXL21 proteins mediate CRYs degradation in nucleus and cytosol, respectively. CK1ε/δ proteins regulate the degradation of PERs in cytosol.

TTFL helps us to explain the transcriptional level control of the genes whose transcription is under circadian clock control. In a study investigating the circadian mRNA expression of protein coding genes in different tissues, scientists found that 43% of RNAs in all protein coding genes show circadian regulated mRNA expression in organ specific manner [64]. Even though the TTFL is extremely important to understand the central clock regulation, it cannot explain neither tissue specific regulation of gene expression, nor how circadian clock regulates metabolism.

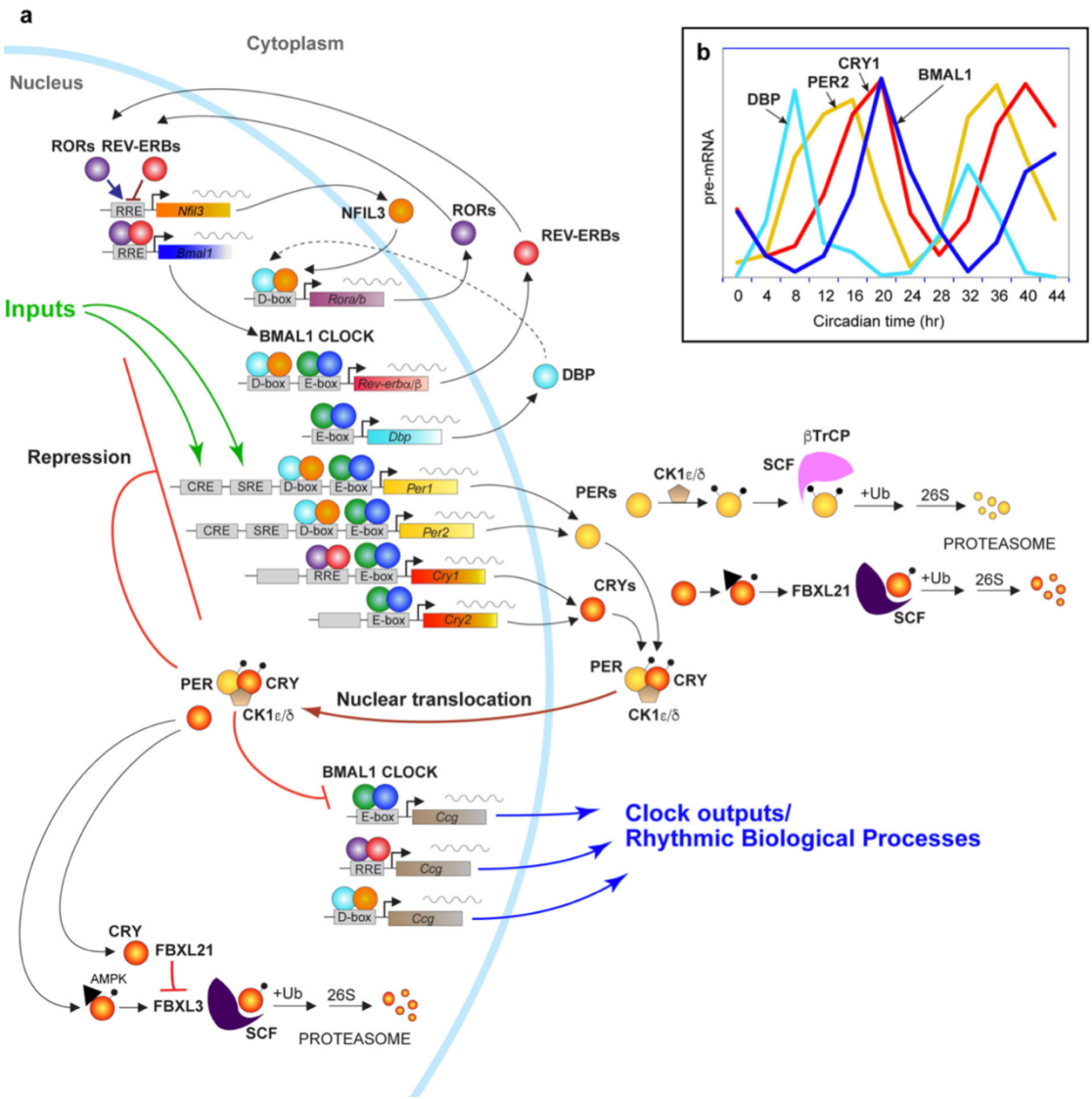


Figure 2-9: Adopted from Joseph Takahashi, 2016. Molecular mechanisms regulating circadian clock. Positive regulators BMAL1-CLOCK drives the expressions of clock-controlled genes (ccg) and negative regulators (Per and Cry).

2.4.2 Importance of Post-Transcriptional Regulation in Molecular Circadian Clock

Despite the molecular clock is active and works throughout many different organs, the amplitudes of the circadian clock in each organ is different than each other. TTFL alone is not enough to explain tissue specific circadian phasing [65]. In addition to that, proteomics studies in SCN revealed that 13% of soluble proteins have rhythmic protein expression, but not rhythmic mRNA expression [66]. Saikumari Krisnaiah and her colleagues performed high resolution metabolite and transcript profiling. They showed that despite only 1.5% of the total transcripts show cycling profile, 38% of metabolites show circadian cycling *in vitro* [5]. It has been shown that circadian clock is affected by the changes in m^6A mRNA methylation disturbances in the cells. Specific inhibition of m^6A-RNA methylation by either chemical or RNA methylase (Mettl3) knock-down; elongated the period length *in vitro* [67]. Thus, it is clear that transcriptional regulation is not enough to totally explain the regulation of metabolism. In the following section, important metabolic diseases.

2.5 One Carbon Metabolism Pathway and Circadian Regulation of Metabolism

Generation and utilization of one carbon units are required for healthy cellular and organismal physiology. Nucleic acid and amino acid synthesis and homeostasis, regulation of epigenetic modifications, and the strength of oxidative stress defense are all controlled by one carbon metabolism. Understanding temporal regulation of metabolism through one carbon pathway is required to have circadian perspective to the treatment of metabolic diseases.

2.5.1 One Carbon Metabolism and Related Pathways

2.5.1.1 Folate Cycle

While is a folate (dietary folate from foods) prominent part of their development, animals need dietary supply of folate because they cannot synthesize it [68]. On the other hand, many bacteria species, algae, yeast and plants can produce their own folate [69]. Plants utilizes GTP and produces folate [70]. Though folic acid (synthetic form of folate) intake is extremely important during pregnancy, adults also needs to get sufficient amount of folic acid to prevent anemia [71].

Necessary amount of daily folic acid intake is 400 micrograms for a pregnant woman, but the average folic acid intake is only 200 micrograms per day-either as dietary folate or folic acid supplement- [72]. Inadequate folic acid intake during pregnancy results in birth defects like neural tube development problems. Open spina bifida (spinal cord defects) and malformed skull are the common birth defects caused by insufficient folic acid supplementation of pregnant woman [73].

The importance of folic acid intake is because of the importance of biosynthesis reactions it is involved in. Folic acid is utilized to produce DHF (dihydro folate) by DHFR (dihydrofolate reductase). Either from DHF or from dietary folate, THF (tetra-hydro folate) is synthesized which is the source of methyl-THF, methylene-THF, or formyl-THF. Methyl-THF, methylene THF, and formyl-THF are utilized to mediate methionine from homocysteine, thymine, and purine biosynthesis reactions, respectively [74] [75] (**Figure 2-10**).

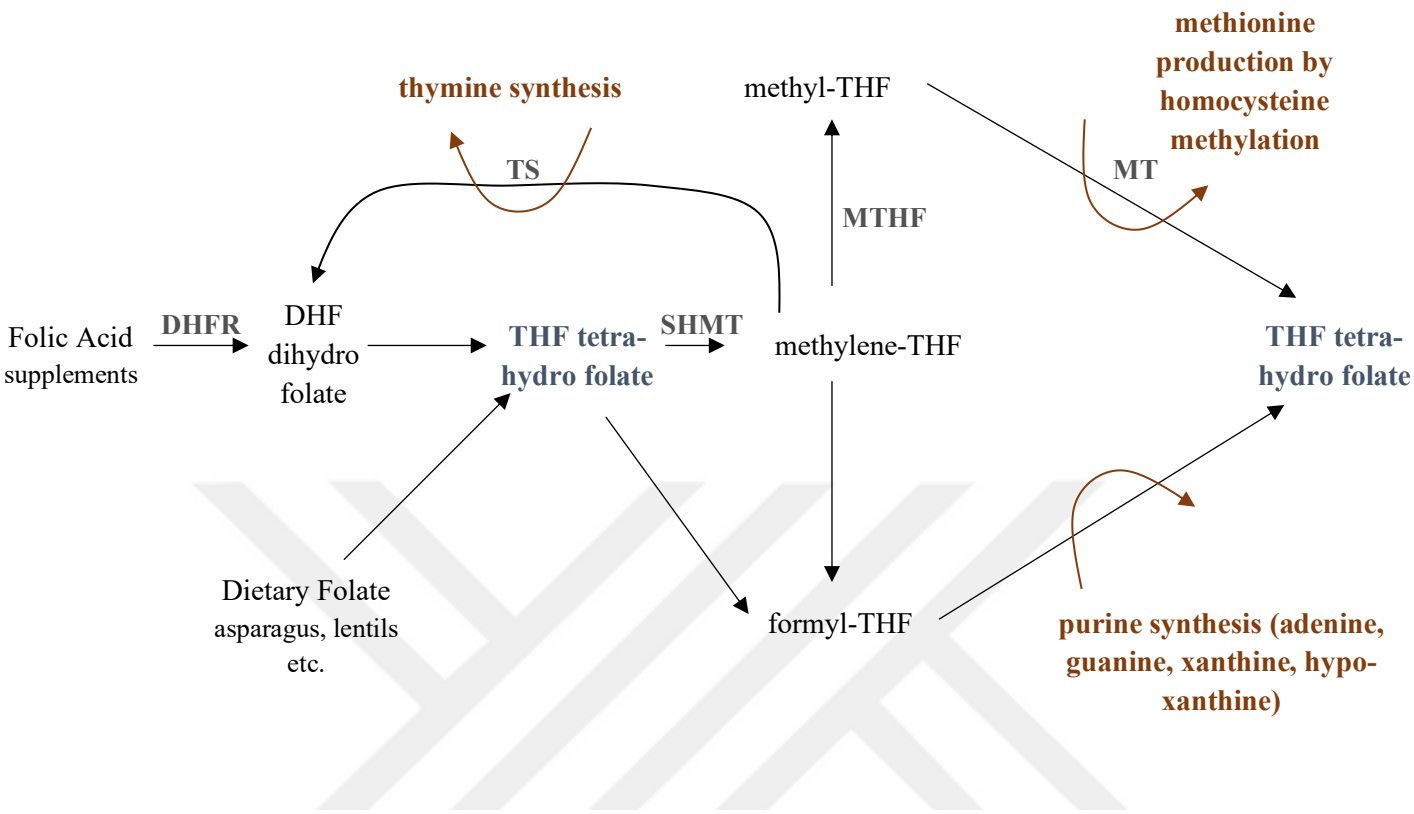


Figure 2-10: Folate pathway and important biosynthesis reactions mediated by folate pathway.

Folic acid metabolism regulates DNA synthesis and methylation through synthesis of thymine, adenine, guanine and methionine [76].

Since mammalian folate cycle has to be supplemented by either dietary folate or folic acid from supplements, feeding schedules become extremely important for proper folate cycle. mRNA expression of DHFR (dihydrofolate reductase) is a circadian regulated (**Figure 2-11**) which is necessary for utilization of folic acid. The expression of DHFR peaks in liver at resting phase of mouse. However, detailed studies are needed to detect temporal regulation of protein levels and as well as enzyme activities throughout a day.

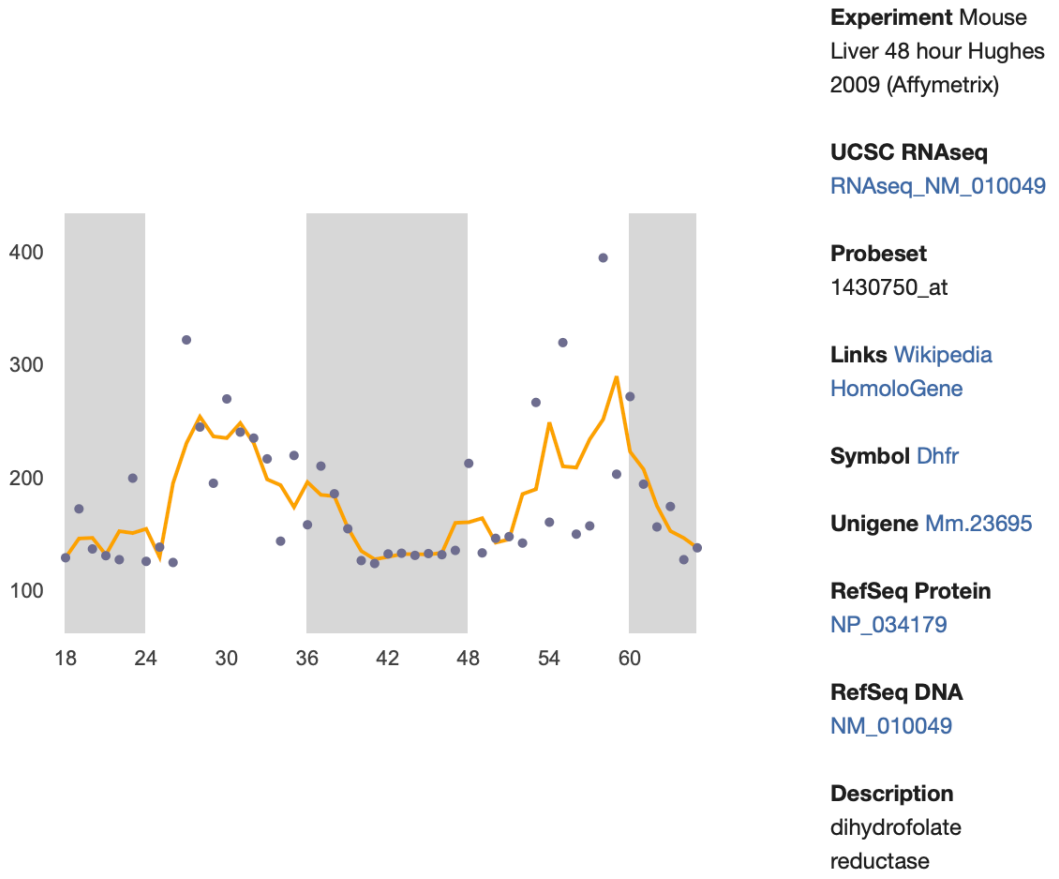


Figure 2-11: DHFR (dihydro folate reductase) mRNA expression in mouse liver. Data exported from CircaDB database.

2.5.1.2 Methyl Cycle

Even though sub-grouped here, the cycles in one-carbon metabolism are strongly connected with each other. Synthesis of methionine was explained in folate cycle subtitle. Here, I will explain how methionine is further metabolized in methyl cycle. As explained in the previous section, methionine can be synthesized from homocysteine by folate cycle. In addition to that, same reaction is catalyzed by BHMT (betaine-homocysteine methyl transferase) in a folate independent mechanism [77]. Even though methionine expression is needed throughout the body, only liver and kidney expresses BHMT [78]. Choline is an essential water-soluble compound which is needed for folate-independent methionine

synthesis and is needed to be taken through our diet. Cod, beef and chicken liver, soybean oil, salmon and broccoli are main choline sources in our diet. Folate-dependent and independent methionine synthesis from homocysteine are not only methionine sources for cells. Protein intake and extracellular methionine are also methionine sources for cells. The control of methionine level is important to regulate DNA, RNA, and protein methylations which further regulates gene expression, post-transcriptional protein synthesis, and post-translational protein activity or stabilization. SAM (S-adenosyl-methionine) is produced from methionine and it is a universal methyl donor for methylation reactions. SAH (S-adenosyl-L-homocysteine) is generated at the end of methylation reactions which is catalyzed by S-adenosyl-L-homocysteine hydrolase enzyme. Homocysteine propagation from SAH feeds back to the methyl cycle (**Figure 2-12**).

As explained above, epigenetic modifications are exogenously controlled by feeding (folate and choline supplementation by diet) and they regulate expressions of core circadian clock mRNAs and proteins. It has been shown in Arabidopsis that, inhibition of H3K4 tri-methylation elevates the binding of repressor complexes on DNA [79]. Even though exact mechanisms are unknown, it is an excellent example for the regulation of central clock by peripheral clocks.

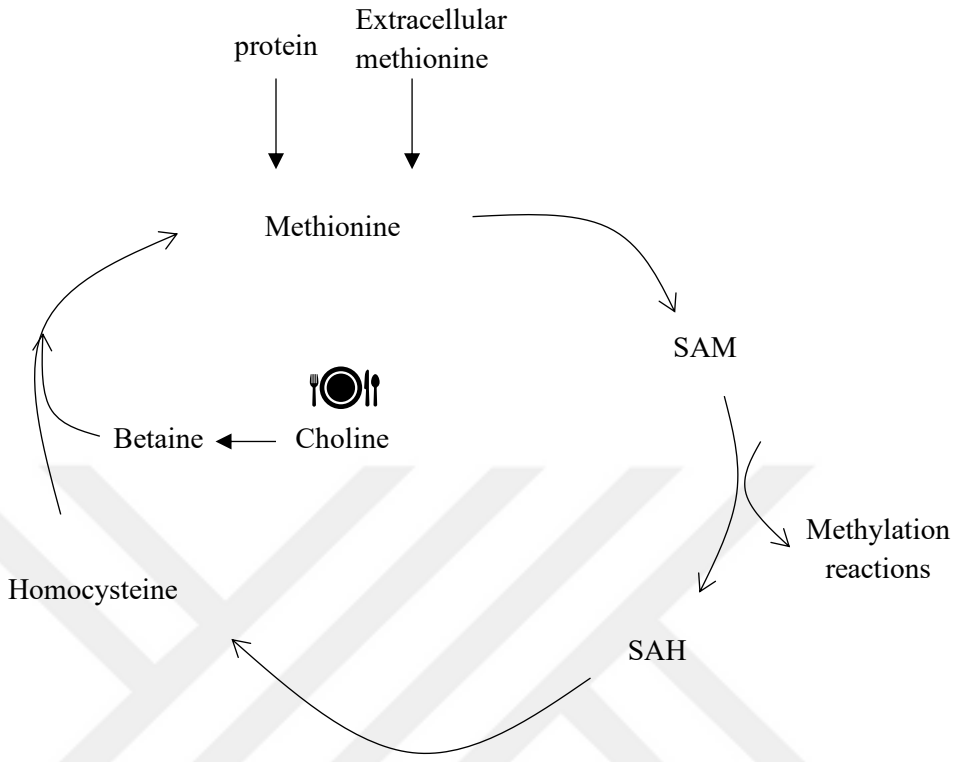


Figure 2-12: Diagram of methyl cycle showing methionine sources, synthesis and utilization steps.

2.5.1.3 Transsulfuration Pathway

Homocysteine is a critical metabolite which is needed for both methyl cycle and transsulfuration pathway. Concentration change of homocysteine in body disturbs these two important pathways. Cystathionine-β-synthase (CBS) is the first enzyme irreversibly catalyzing cystathionine synthesis from homocysteine, by utilizing serine. Cystathionine-γ-lyase (CSE) is both able to perform the same reaction and generation of cysteine from cystathionine. While carbon chain of cysteine comes from serine, its sulfur atom comes from methionine. It is also found in keratin protein. Keratin is needed for healthy hair, skin and nails [80].

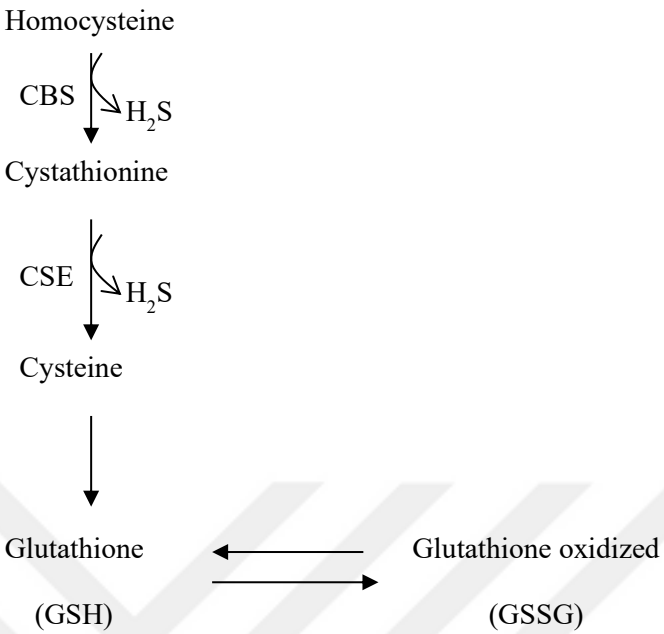


Figure 2-13: A diagram of transsulfuration pathway starting with utilization of homocysteine, continues with synthesis of H_2S and glutathione.

Homocysteine is both a precursor and product of the methyl cycle, and precursor of transsulfuration pathway. Concentrations of homocysteine is prominent for cells and organisms. As seen from **Figure 2-13**, less CBS activity will cause accumulation of homocysteine and blockage of H_2S (hydrogen sulfide) synthesis. Hyper-homocysteinemia by less or no CBS activity causes SAH accumulation which inhibits DNA methylation [81]. Despite the mechanisms relating hyper-homocysteinemia and cancer progression is unclear, in liver cancer [82] and head and neck squamous cell carcinoma [83] elevated homocysteine levels are detected. Additionally, the link between CBS expression and cancer is specific to cancer type. Higher CBS protein expression compared to nearby healthy cells were detected in breast [84], colon [85], prostate [86] and ovarian [87] cancer cells. On the other hand, it has been shown that loss of CBS increased tumorigenesis in glioma tissues [88].

Hydrogen sulfide (H_2S) is a gaseous neuromodulator and muscle relaxant molecule which is produced by three enzymes in most tissues: Cystathionine-β-synthase (CBS), Cystathionine-γ-lyase (CSE), and 3-mercaptopyruvate sulfur transferase (3MST). The differences in activities and expressions of these enzymes are important for H_2S concentrations in cells. Lower concentrations of H_2S serves as antioxidant in neurons [89]. However, less CBS activity and extremely decreased H_2S levels were detected in the brain samples from Alzheimer's disease patients [90]. CBS-produced H_2S could have prominent role in cognitive functions.

Cysteine is an important amino acid which is used for glutathione (GSH) synthesis as antioxidant mechanism of cells [91]. Reactive oxygen species (ROS) are produced through oxidative metabolism. Hydrogen peroxide, hydroxyl radicals, and superoxide anion are examples to ROS. Even though they have been thought to bring only damage to the cells, it has been shown that they also act as signaling molecules at proper concentrations [92] [93]. When their concentration is higher in cells, they react with nucleic acids, carbohydrates, proteins and lipids; destroying their functions [94]. Glutathione (GSH) is the key component of oxidative stress defense mechanism in mammalian tissues. Glutathione is mainly found in a reduced form (GSH). GSH is oxidized to form oxidized di-sulfite glutathione (GSSG) when there are high concentrations of reactive oxygen species in the cells .

CBS is a 63 kDa protein which forms oligomers ranging between dimers to sixteen-mers. CBS enzyme activity is regulated by heme, pyridoxal 5-phosphate and SAM (S-adenosyl-L-methionine) binding. I have mentioned that less or no CBS activity causes homocysteine and SAH accumulation and DNA hypo-methylation. CBS single nucleotide polymorphisms (SNPs) reduces either the activity or expression of CBS protein and causes homocystinuria in humans [8]. CBS-induced homocystinura patients show skeletal and muscle problems, vascular diseases, intellectual disability and insulin resistance [95]. Oligomerization of CBS is extremely important for the enzyme activity of CBS. Most of the SNPs disrupt the oligomerization performance of CBS. I278T is the most common mutation found in humans resulting in CBS-related homocystinuria among over 300 mutations [96]. Treatment of homocystinuria is based on inducing utilization of homocysteine by folic acid, vitamin B_{12} and vitamin B_6 supplementation [97].

2.5.1.4 Urea Cycle

Urea cycle is directly connected with one-carbon pathway. Metabolic side products cause toxicity if they are not deported from the body. Excess nitrogen and ammonia are eliminated and turned into urea and send away from the body with urine. In addition to waste disposal, urea cycle is also important to synthesize amino acids [98]. Arginine biosynthesis occur from citrulline. Ornithine is produced as a by-product of urea synthesis [99].

Any disruptions on urea cycle will result in accumulation of toxic ammonia. Ammonia accumulation causes central nervous system problems and seizures [100].

2.5.2 Relationship Between Circadian Clock and Metabolism

Despite the fact that RNA oscillations of metabolic enzymes are regulated by TTFL (transcriptional translational feedback loop), post-translational modifications also regulate circadian oscillation of metabolism [101]. 28% of metabolites in U2-OS (human osteosarcoma cell line) cellular system shows cycling phenotype, while only 1.5% of transcripts show mRNA level oscillations. Additionally, 50% of metabolites show circadian cycling . It has been shown that protein acetylation oscillation regulates fatty acid, amino acid and glucose metabolisms [102] [103].

With continuously emerging scientific knowledge about how metabolism is regulated by circadian clock, we will be able to time feeding of specific food to regulate metabolism or to cure metabolism related diseases.

Chapter 3

THESIS RATIONALE AND AIM

Circadian clock synchronizes self-sustained endogenous molecular clock and environmental timing cues to increase fitness of organisms. While light and feeding are the main timing cues for central clock, feeding and central clock signals are the main synchronization cues for peripheral clocks. Central clock regulates circadian behaviors like sleep-wake cycle. Peripheral clocks regulates metabolism in different organs [104]. Metabolism is strongly regulated by circadian clock. It has been identified how light input synchronizes central clock and organismal behavior at the molecular level. However, it is still an obscure that how metabolism is controlled by circadian clock [5].

Recent studies revealed that, in addition to known transcriptional and translational regulatory mechanisms, there has to be unknown post-translational control mechanisms to control peripheral clocks and metabolism [6].

CBS has been identified as potential circadian clock component candidate by our collaborators, in 2014 [7]. Then, we aimed to identify the potential interactions of CBS with known clock components. Following the identification of Cryptochrome 1 (CRY1)-CBS interaction, we characterized the interaction and their effects on each other's activities.

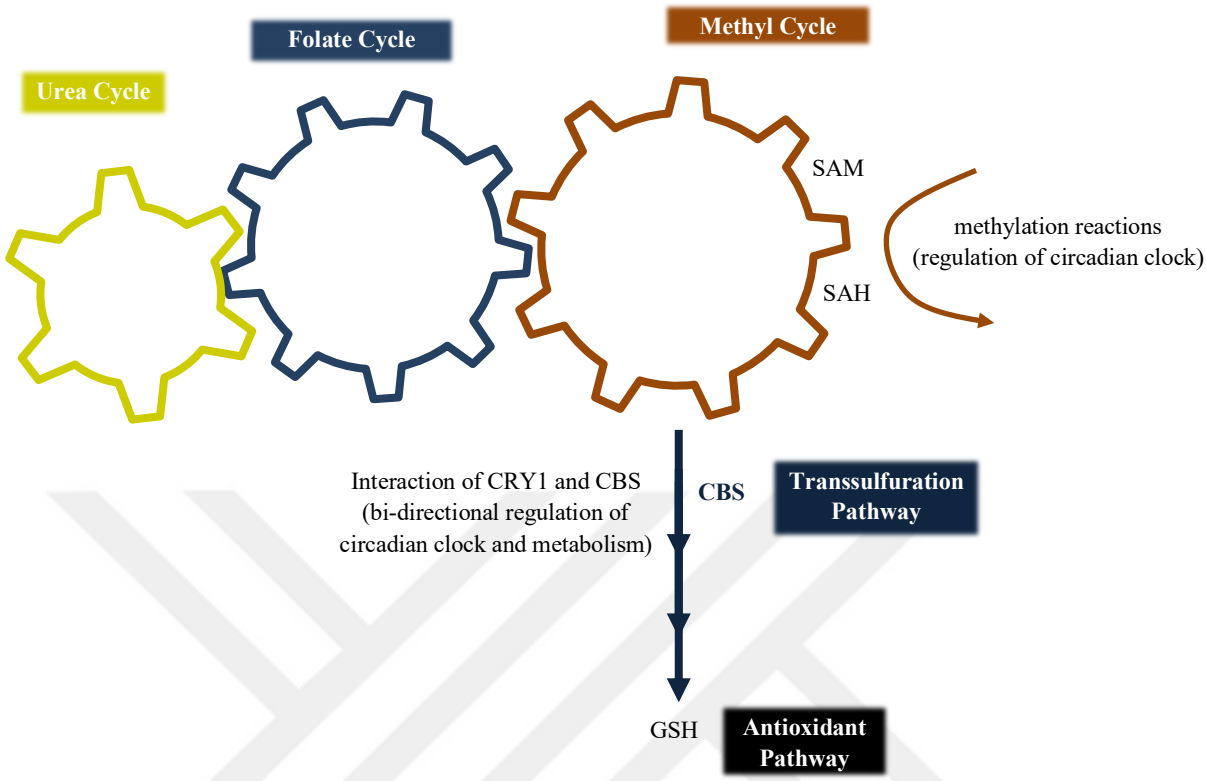


Figure 3-1: One carbon metabolism and urea cycle are the central pethways Cystathionine-β-synthase (CBS) is connected to.

In our study, we aimed to characterize the novel protein-protein interaction to find both how metabolism is regulated by circadian clock, and how circadian clock regulates the metabolism at post-translational level. A novel circadian clock regulatory role of metabolically important enzyme (**Figure 3-1**), Cystathionine-β-synthase (CBS) has been identified. Additionally, we clarified a previously unknown role of Cryptochrome 1 (CRY1) as enzyme activity regulator.

Chapter 4

MATERIALS AND METHODS

4.1 Cell Lines and Regular Maintenance Protocols

HEK293T (human embryonic kidney), NIH 3T3:P(Bmal1)-dluc (mouse fibroblast luciferase reporter cell line), U2-OS:P(Bmal1)-dluc (human osteosarcoma luciferase reporter cell line), Neuro-2A (N2A-mouse neuronal cell line) cells were thawed from Kavakli Lab nitrogen cell stocks. As the regular surveillance protocol, these cells were maintained in high glucose DMEM with L-Glutamine (Thermo Fisher Scientific) which was supplemented with 10% fetal bovine serum (FBS (Pan Biotech)) and 100 μg/mL penicillin and streptomycin (Gibco) in a sterile cell culture incubator. The incubator was humidified and had 5% CO_2 as the optimal condition for mammalian cells. Cells were checked for mycoplasma every time they were thawed from the stock. We used ATCC universal mycoplasma detection kit (ATCC® 30-1012K™) for this purpose. Cells were used in the experiments if they are free from mycoplasma contamination.

4.2 Plasmid Constructs

Appropriate sub-cloning's were performed into pBIND and pACT vectors in order to perform Mammalian-Two-Hybrid experiment according to the instructions of Promega CheckMate™ Mammalian Two-Hybrid System. Luciferase from plasmid pG5:*luc* was used as reporter gene which was expressed by GAL4 when it was activated by VP16 activation domain. Genes sub-cloned in pBIND vector (*Bmal1, Clock, Per1, Per2, Per3, Cry1, Cry1-T1, Cry1-R602P* and *Cry2*) are expressed as a fusion protein with GAL4, on the other hand, the genes sub-cloned in pACT vector (*Cbs*, and *Per2*) are expressed as a fusion protein with VP16 activation domain. When two proteins cloned in pBIND and pACT vectors interact, GAL4 and VP16 tags come together and drives the luciferase

expression from pG5:*luc* plasmid. We used pGL4:*Renilla* vector to normalize the transfection efficiencies and cell numbers in the transfected cells.

Cbs, *Cry1*, *Cry1-T1*, *Bmal1* and *Clock* were cloned into pCMV-sport6 vector separately for Per1:*luc* reporter assay. mPer1:*luc* plasmid was used as the reporter in transfection based-Per1:*luc* reporter assay. Similar to mammalian-two hybrid assay, pGL4-*Renilla* was used for normalization purpose.

4.3 Mammalian-two-hybrid

On day zero, 2 million HEK293T cells are passaged to 10 cm plate from previously seeded confluent HEK293T cell plate [105]. On day 1, 50 ng pBIND (containing either *Cry1*, truncated versions of *Cry1*, *Cry2*, or other core clock genes), 50 ng pACT *Cbs*, 50 ng pG5-*luc* and 1 ng pGL4-*Renilla* vectors were prepared according to reverse transfection protocol by Thermo Scientific[106]. For each well of 96-well plate, total DNA concentration is equalized to 300 ng with empty pCMV-sport6 vector in total volume of 50 µl. Total DNA mixture was dissolved in DMEM without any antibiotics or serum. 0,9 µl TurboFect (Thermo Scientific)[106] cationic based transfection reagent was added onto DNA mixture and incubated for 20 minutes at room temperature. During incubation time, HEK293T cells seeded at day 0, were tyrpsinized and counted with hemocytometer. At the end of the incubation time, $4x10^4$ cells in 50 µl volume prepared in 2x medium (DMEM (Gibco) with 20% fetal bovine serum, 200 µg/µl Streptomycin and 200 µg/µl Penicillin (Gibco) and 4 mM L-Glutamine (Gibco)) are mixed with 50 µl DNA mixture and incubated for 24-36 hours at 37ºC incubator (constant 5% CO_2). After 30 hours, activity of both firefly and *Renilla* luciferase was measured using a luminometer (Thermo Fluoroskan Ascent FL) with DualGlo luciferin reagent (Promega). The firefly luciferase activity was normalized using *Renilla* luciferase for transfection efficiency. Each reaction had 3 technical and 3 biological replicates.

Table 1: Medium types used in the cell culture experiments and their compositions

Medium	**Composition**
Complete medium	DMEM (Gibco) 10% FBS (Pan Biotech) 2 mM L-Glutamine (Gibco) 100 µg/mL Penicillin and Streptomycin (Gibco)
siRNA medium	DMEM (Gibco) 10% FBS (Pan Biotech) 2 mM L-Glutamine
2X medium	DMEM (Gibco) 20% FBS (Pan Biotech) 4 mM L-Glutamine (Gibco) 200 µg/mL Penicillin and Streptomycin (Gibco)
Lumicycle Recording Medium	DMEM (Sigma, D2902) 10 mM HEPES 0.35 mg/ml sodium bicarbonate 100 µg/µl Streptomycin and Penicillin (Gibco) 2 mM L-Glutamine (Gibco) 1 mM luciferin (Promega) pH 7.2

4.4 Per1:luc Reporter Gene Assay

3 million Neuro-2-A (N2A) cells were seeded to 10-cm dish in complete DMEM medium (10% FBS, 100 µg/mL Penicillin and Streptomycin and 2 mM L-Glutamine) one day prior of reverse transfection day. Next day, cells were reverse transfected with TurboFect (Thermo Scientific) transfection reagent with the indicated plasmids: 50 ng *Bmal1* in pCMV-sport6, 125 ng *Clock* in pCMV-sport6, 50 ng *mPer1-luc*, 10 ng *Renilla*-PGL4, 5 ng *Cry1*-pcDNA (or *Cry1-R602P*-pcDNA), 20 or 30 ng *Cbs*-pCMV-sport6 or *Cbs*-I278T-pCMV-sport6 or *GAPDH*-pCMV-sport6. Total transfected DNA amount was made equal in all wells with pCMV-sport6 vector up to 300 ng. As mentioned in mammalian-two hybrid experiment, activity of both firefly and *Renilla* luciferase was measured using a luminometer (Biotek-Synergy) with DualGlo luciferin reagent (Promega). The firefly luciferase activity was normalized using *Renilla* luciferase for transfection efficiency. Each reaction had 3 technical and 3 biological replicates. In one biological replicates, 6 technical replicates were made and 3 of them were collected and used for CBS protein amount check with western blot.

4.5 Cell Based Circadian Assay

350,000 U2-OS:P(Bmal1)-dluc or NIH-3T3:P(Bmal1)-dluc cells were seeded on 35-mm dishes in siRNA medium (Table 1). Next day, cells reached to 80-90 % confluency and transfected with human or mouse Cry1 or Cbs siRNA mixes with Invitrogen Lipofectamine RNAiMAX Reagent (Cat no. 13778100). According to the manufacturer's instructions, siRNA mixes (Table 2) and RNAiMAX were diluted in opti-MEM (Gibco Cat no. 31985062) separately. Diluted siRNA and diluted RNAiMAX were mixed and incubated 5 minutes at room temperature. At the end of the incubation, transfection mix was added dropwise to 35-mm dishes.

48 hours after transfection, medium was replaced with lumicycle recording medium (Table 1) with final 0.2 µM dexamethasone to synchronize the cells. Dishes were sealed with autoclaved silicone grease to prevent evaporation from the medium and they were placed in lumicycle recorder.

Table 2: siRNA target genes, their host species and the catalog numbers of used siRNAs in the experiments.

Target gene	Host Species	Catalog Numbers
Cbs	mouse	SI00942606, SI00942620, SI00942613, SI00942599
Cry1	mouse	SI02708041, SI02686271, SI02666580, SI02732086
Cbs	human	SI03058391, SI02777159, SI00001316, SI02777166
Cry1	human	SI00059430, SI00059416, SI04434780, SI02757370
Non-Targeting	Mouse and human	1027280

4.6 Bimolecular Fluorescence Complementation Assay (Bi-FC)

In Bi-FC assay, N-terminal and C-terminal halves of Venus fluorescence protein are fused with two proteins that we want to investigate their interactions. If two proteins interact with each other, two halves of VENUS come together, and fluorescent protein is detected. (**Figure 4-1**)

250,000 HEK293T cells were seeded in in 6-well dishes in complete medium (Table 1) to have 60-70% confluency on the next day. On the transfection day, cells were transfected with venus plasmids (either wild type or mutant 200 ng CRY1-VC ((CRY1 fused with venus C-terminal) and 300 ng CBS-VN (CBS fused with venus N-terminal)) and 200 ng pmCherry-C1 by using Fugene HD (Promega). According to the manufacturer's instructions, plasmids were diluted in opti-MEM and Fugene HD was added on diluted plasmids. After 10 minutes incubation at room temperature, the transfection mixture was added dropwise on the cells. At 24 h post-transfection, the cells were visualized using YFP and mCherry filter set in fluorescence microscopy.[7]

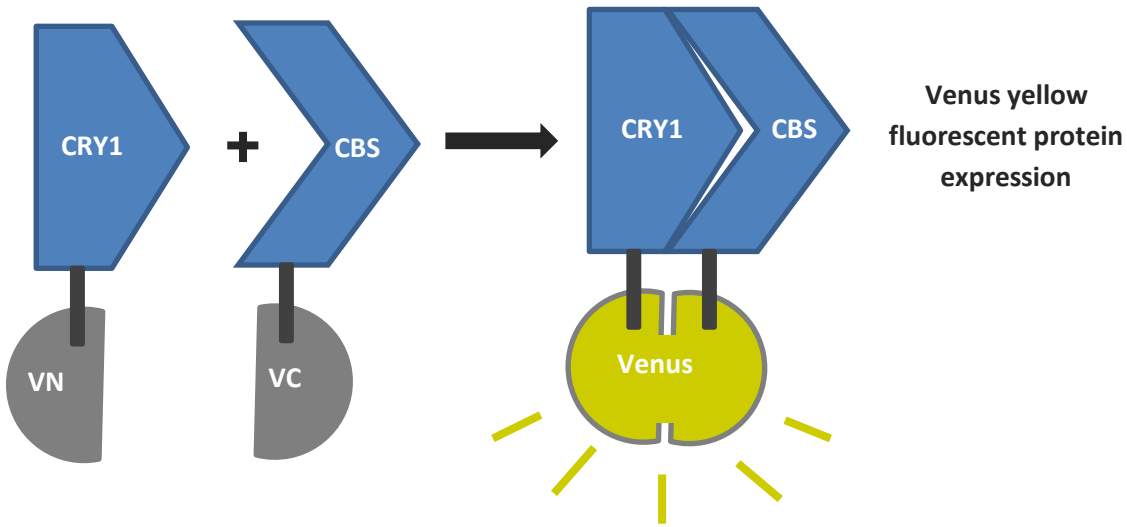


Figure 4-1: Schematic representation of bimolecular fluorescence complementation

4.7 Co-immunoprecipitation (co-IP)

HEK293T cells were seeded in complete medium to 10 cm plates in order to have 70-80 % confluency for forward transfection on the next day. Cells were transfected with mix 1 (*Cry1*-pcDNA and *Cbs*-pCMV-sport6), mix 2 (*Cry1*-T1-pcDNA and *Cbs*-pCMV-sport6), only *Cry1*-pcDNA, only *Cry1-T1*-pcDNA, and only *Cbs*-pCMV-sport6 by using PEI as a transfection reagent. 48 hours after transfection, cells were collected after aspiration of the medium in ice cold PBS. Collected cells in PBS were centrifuged at 5000 g, 4ºC for 5 minutes and supernatant was discarded. Pellets were dissolved in cold non-denaturing Co-IP lysis buffer (Table 3) and sonicated 2 times for 10 seconds with 15% power (Bandelin, Germany). Lysed and sonicated cells are centrifuged at 19000 g, 4ºC for 40 minutes, then the supernatants were saved as cell free extracts. 1/10 of supernatant was mixed with 6x protein loading dye for Western Blot to use as input samples. The cell lysate and loading dye mixture was boiled for 7 minutes. After expression check of the input samples with western blot, the rest of the pellets were processed in the same way, but instead of mixing with 6x loading dye, lysates were used for co-immunoprecipitation. In order to equilibrate either Anti-Flag M2-Flag or Ni-NTA His resin, they were washed 2 times with TBS after the removal of glycerol with centrifugation. To perform co-immunoprecipitation, lysates and beads were mixed and incubated overnight at 4 ºC with rotation. All centrifuges of resins were processed at 4 ºC, 5000 g, for 5 minutes.

Next day, beads were washed 3 times with TBS, in order to eliminate non-specific bead binding. And then beads were boiled with 1x loading dye and processed for Western blot.

Table 3: Buffers and their compositions which were used in the experiments. All buffers which were used for protein experiments were supplemented with protease inhibitors.

Buffer	Composition
Co-IP Lysis Buffer	(50 mM pH 8 Tris-Cl, 150 mM NaCl, 1 mM EDTA and 1% Triton-X supplemented freshly with Protease Inhibitor Cocktail (Sigma))
PBS	(37 mM NaCl, 2.7 mM KCl, 10 mM Na_2HPO4, 1.8 mM KH_2PO_4, pH 7.4)
6X protein loading dye	(300 mM Tris-Cl pH 6.8 12 % β-mercaptoethanol 6 % (w/v) SDS 0,003 % (w/v) bromophenol blue 12 % (v/v) glycerol
Cytosolic Lysis Buffer	10 mM HEPES pH 7,9, 10 mM KCl, 0,1 mM EDTA, 0,05 % NP40 with protease inhibitors
Nuclear Lysis Buffer	20 mM HEPES pH 7,9, 0,4 M NaCl, 1 mM EDTA, 10 % glycerol with protease inhibitors

4.8 Generating CRY1 Mutant Library

4.8.1 Construction of CRY1 Mutant Library Using Degenerate Primers

Degenerate PCR method was used for the creation of a set of CRY1 mutants. Degenerate reverse primer mix targeting single or multiple mutations within the last 20 amino acids of C-terminal tail of CRY1 were designed as shown in Table 9. CRY1 wild type-pBIND vector was used as template and amplification was achieved with Phusion DNA polymerase (Thermo). PCR protocol detailed in Table 4 was used to amplify the mutated *Cry1* plasmids. Four different PCR reactions were set up using the same forward primer and one of four reverse primers in each different PCR reaction. Reactions were set up in the presence of %5 DMSO (Thermo) to inhibit the occurrence of secondary structures of either template or primers.

Resulting PCR products and empty pBIND vector were digested by NotI and EcorV restriction enzymes (Fast Digest RE-Thermo). Agarose gel extraction was achieved with MN Gel Extraction Kit. Ligation was performed with Thermo fast DNA ligase. Ligation products were transformed to *E.Coli* DH5a strain and single colonies were picked next day for plasmid DNA isolation (MN Miniprep Kit) and restriction digestion with Sac1 enzyme (Fast Digest RE- Thermo). Finally, almost 20 different CRY1 mutants were created and sequenced by Macrogen Inc.

Table 4: PCR reaction conditions to apply degenerate PCR

Initial Denaturation	**Denaturation**	**Annealing**	**Extension**	**Final Extension**
98 C for 1 min	98 ºC for 30 seconds	55 ºC for 30 seconds	72 ºC for 2 minutes	72 ºC for 5 minutes
1 time	**30 cycles**			**1 time**

4.8.2 Site Directed Mutagenesis After the Detection of Crucial Amino Acid

Site directed mutagenesis were performed to create pcDNA CRY1-R602P mutant. For this aim, primers that create a mismatch at desired location were designed (Table 9). Then, PCR was performed using pcDNA harboring wild type CRY1 as template and mutagenic primers. Following PCR, the products were digested with DpnI for 1 hour at 37 ºC to eliminate template plasmid. Finally, they were used to transform *E.Coli* DH5a competent cells. After transformation, positive colonies were chosen and sent to be sequenced following plasmid isolation.

Table 5: PCR reaction conditions to apply site-directed PCR

Initial Denaturation	**Denaturation**	**Annealing**	**Extension**	**Final Extension**
94 C for 1 min	94 ºC for 40 seconds	55 ºC for 40 seconds	68 ºC for 11 minutes	72 ºC for 5 minutes
1 time	**12 cycles**			**1 time**

4.9 Western Blot Immunoblotting

Cell lysates were mixed with 6X western blot loading dye (Table 3) and boiled for 5-10 minutes at 95 ºC. Samples were separated based on their molecular weight by SDS-PAGE by using 10% separating and 5% stacking gels. For the Native-PAGE, samples and PAGE gel were prepared without denaturing reagents (SDS) and gradient gel from 3 % to 13 % was poured and used for PAGE. Following polyacrylamide gel electrophoresis, proteins are transferred to PVDF membrane (Milipore, Immobilon-P-Transfer Membrane) by using wet-transfer system (Bio-Rad) which is the most efficient method to transfer proteins from gel to membrane. The membrane was blocked with 5% non-fat milk (Chem Cruz SC2325) prepared in 0.15% TBS-T (Tris-buffered saline with tween) (Sigma Aldrich Tween 20 P1379). After blocking, the membrane was incubated overnight at 4 ºC with either Anti-HIS antibody (Santa Cruz SC-8036), Anti-FLAG antibody (Sigma A9469), Anti-CRY1 antibody (Bethyl), Anti-CBS antibody (Abcam ab54883), Anti-VP16 (Santa Cruz, sc-7545), Anti GAL4 DBD (Santa Cruz, sc-577), Anti ACTIN (Cell

Signaling, 8H10D10), Anti α-TUBULIN (Sigma, T9026), or Anti HISTONE-H3 (Abcam, ab1791). Following primary antibody incubation, the membrane was washed 3 times with 0.15% TBS-T for 5 minutes. Secondary antibodies were either anti-mouse (Santa Cruz SC-358920) or anti-rabbit (abcam ab97051) antibodies which were incubated for 50 minutes at room temperature. After secondary antibody incubation, membrane was washed with TBS-T again. In order to visualize the membrane with chemiluminescent detection, Advansta ECL HRP substrate was used (WesternBright Sirius Lot. No. 161212-03). Chemiluminescent signal detection was performed with BioRad Chemidoc instrument.

4.10 RNA Isolation and Real-Time PCR

4.10.1 RNA Isolation

All equipment and working area were cleaned with RNase Zap (Sigma R2020). RNA isolation was performed from both cells and livers with RNeasy Mini Kit (Qiagen Cat. No. 74106).

4.10.2 cDNA Synthesis

RevertAid First Strand cDNA Synthesis Kit (Thermo) was used for cDNA synthesis. 500 ng total RNA was used to prepare cDNA.

4.10.3 Real-Time PCR

SYBR Green real time PCR mix was used with real time PCR primers of interested genes. Real time PCR primer list is indicated in Table 8.

4.11 Cystathionine-Beta Synthase Enzymatic Activity Detection

4.11.1 Liver Lysate Preparation

Flash frozen 12 mg of mouse liver was homogenized with Dounce Homogenizer for 5 minutes in 200 µl ice cold 50 mM potassium phosphate buffer (pH 6,8) which was supplemented with protease inhibitor. After homogenization, samples were sonicated for 6 times for 8 seconds with 90 % power. Following sonication, homogenates were centrifuged at 14000 rpm, 4ºC for 45 minutes. After centrifuge, supernatant was used for CBS enzymatic activity detection. 1/10 of the lysates were saved and used for Western blotting in order to detect protein levels of CBS in the samples.

4.11.2 Determination of CBS Enzymatic Activity

Reaction mixture was prepared as 100 mM potassium phosphate buffer (pH 7.4) with 10 mM L-cysteine (CBS substrate), 2.5 mM pyridoxal-5-phosphate (CBS co-factor), 30 mM DL-proparglycine, and 2.5 mM homocysteine (CBS substrate) in total volume of 800 µl. DL-proparglycine was used to inhibit the CSE activity to specifically measure the CBS activity. A second tube was sticked to the inside wall of the main tube containing 750 µl 1 % zinc-acetate and 50 mg cotton in order to capture gaseous H_2S which was produced by the CBS in the reaction mixture. After the mixing of the liver lysate and reaction mixture, nitrogen gas was applied for 5 minutes inside of the tubes in order to replace oxygen. Tubes were kept on ice during nitrogen gas application process to prevent the enzyme activity reaction. Following 1 hour and 30 minutes incubation at 37 ºC, reaction was stopped with 50% trichloroacetic acid addition to reaction mixture. Cotton inside of the second tube was used to determine produced H_2S amount.

4.11.3 Measurement of H_2S Formation by Methylene Blue Assay

Cotton was transferred to glass tube containing 3.5 ml distilled water, and then, 400 µl 20 mM N,N-dimethyl-p-phenylenediamine sulphate prepared in 7.2 M hydrochloric acid (HCl) and 400 µl 30 mM $FeCl_3$ prepared in 1.2 M hydrochloric acid were added and color development was measured at 670 nm in microplate reader (Synergy H1 Multi-Mode Reader-Biotek).

4.12 Cytosol-Nuclear Fractionation

Wild type, *Cry1*$^{-/-}$ and *Cry2*$^{-/-}$ animal livers which were either harvested at ZT22 or ZT10 were used for fractionation analysis. 10 mg liver was suspended in 500 ul cytosolic lysis buffer (Table 3) and incubated on ice for 10 minutes. The lysate was centrifuged for 3 minutes at 4,000 g at 4 ºC. The resulting supernatant was centrifuged one more time and supernatant collected as cytosolic fraction. On the other hand, the resulting pellet from lysate centrifugation was suspended in nuclear lysis buffer (Table 3) and sonicated 2 times 10 seconds with 60% power to disrupt nuclear membrane. After centrifuge at 15,000 g for 5 minutes at 4 ºC, supernatant was collected as nuclear fraction. Collected fractions mixed with Western Blot loading dye. Fractionation efficiency was checked with western blot by using Tubulin as cytosolic marker and Histone-H3 as nuclear marker.

4.13 Generation of *Cry1*$^{-/-}$, *Cry2*$^{-/-}$ and *Cbs* $^{-/-}$ Mice

For the generation and maintenance of *Cry1*$^{-/-}$ or *Cry2*$^{-/-}$ mice, method was performed as previously mentioned by Krishnaiah et al. in 2017. Briefly, the original *Cry1*$^{-/-}$ or *Cry2*$^{-/-}$ lines of partial C57BL/6 background were backcrossed and then they were crossed again. The homozygous *Cry1*$^{-/-}$ and *Cry2*$^{-/-}$ mice were entrained by 12-hour light:dark cycle with *ad libitum* food and water. After approximately 8 weeks, mice were sacrificed by asphyxiation with CO_2 at either ZT10 or ZT22. Liver samples were frozen instantly. During the generation of *Cbs*$^{-/-}$ mice, controlled expression of mutant human cystathionine beta-synthase rescued neonatal lethality as described by Wang et al., 2005. Briefly, *Cbs*$^{-/+}$ heterozygous animals were obtained from Jackson Laboratories (Bar

Harbor, ME). The backcrossed heterozygous animals fed with 25 mol/l $ZnSO_4$ containing water for the induction of the transgene. And then, the siblings were intercrossed and fed with zinc for homozygous *Cbs*$^{-/-}$ mice generation. The generation of the transgenic mice that express human *Cbs*-I278T gene is described in [107].

4.14 Circadian Behavioral Analysis

Mice were housed with *ad libitum* food and water in individual cages containing running wheels. Temperature, humidity and light were tightly controlled. 21 wild-type and 26 *Cbs*$^{-/-}$ mice were entrained for 2 weeks with 12 hours light-dark cycles, and then they were kept in constant darkness. Cages of the animals were changed in once every two weeks. ClockLab Data Collection (Actimetrics) were used for locomotor activity detection and analysis. Fourier transform was applied for circadian power statistical analysis. The original ClockLab functions were used to analyze period, amplitude and inter-daily stability.

4.15 Metabolomics Analysis

50 mg liver tissues were thawed on ice and metabolite extraction was performed with Bligh-Dyer method [108] [109]. Briefly, tissues were dissolved in methanol:chloroform (2:1) mixture, and then they were vortexed and sonicated. Following the addition of chloroform and water, samples were vortexed and at the end of centrifugation, organic and aqueous layers were separated. The aqueous layer was dried in a speed vacuum and re-dissolved in acetonitrile:water (2:1) mixture. After the centrifugation for the removal of fine particulates, the supernatant was transferred to LC-MS certified sample vial for Ultraperformance liquid chromatography.

4.16 Mass spectroscopy data processing and enrichment analysis

Mass spectroscopy and data analysis was performed as previously mentioned [5]. Briefly, during mass spectroscopy, ion counts were obtained from TargetLynx. And the data were processed in version 3.2 R. For the LC column equilibration, QC (quality control) samples which are the mixture of all samples were injected at the beginning of every 6 injections to account instrumental drift. At the end, QC data was used to the normalize the results. Gender, time and genotype interaction was analyzed with three factor ANOVA by using 'aov' command in R. Metaboanalyst.co website was used to perform over-representation analysis [110].

Chapter 5

RESULTS

5.1 The Expression of CBS Through 24 Hour Period in Synchronized Cells

Halil Kavakli and his collaborators Ron Anafi and John Hogenesch achieved a high-throughput and genome-wide screen to detect clock component candidates with a machine learning approach. Experimental verifications of the results of machine learning approach proved that the approach was valid. Together with two other genes, *Cbs* was identified as one of the top circadian clock components candidate in their study[7]. Following the identification of CBS as a strong clock component candidate, we verified its circadian controlled expression by doing time-dependent sample collection. U2-OS-Bmal:luc cells were seeded and synchronized, then they were collected with 6 hours intervals for 36 hours.

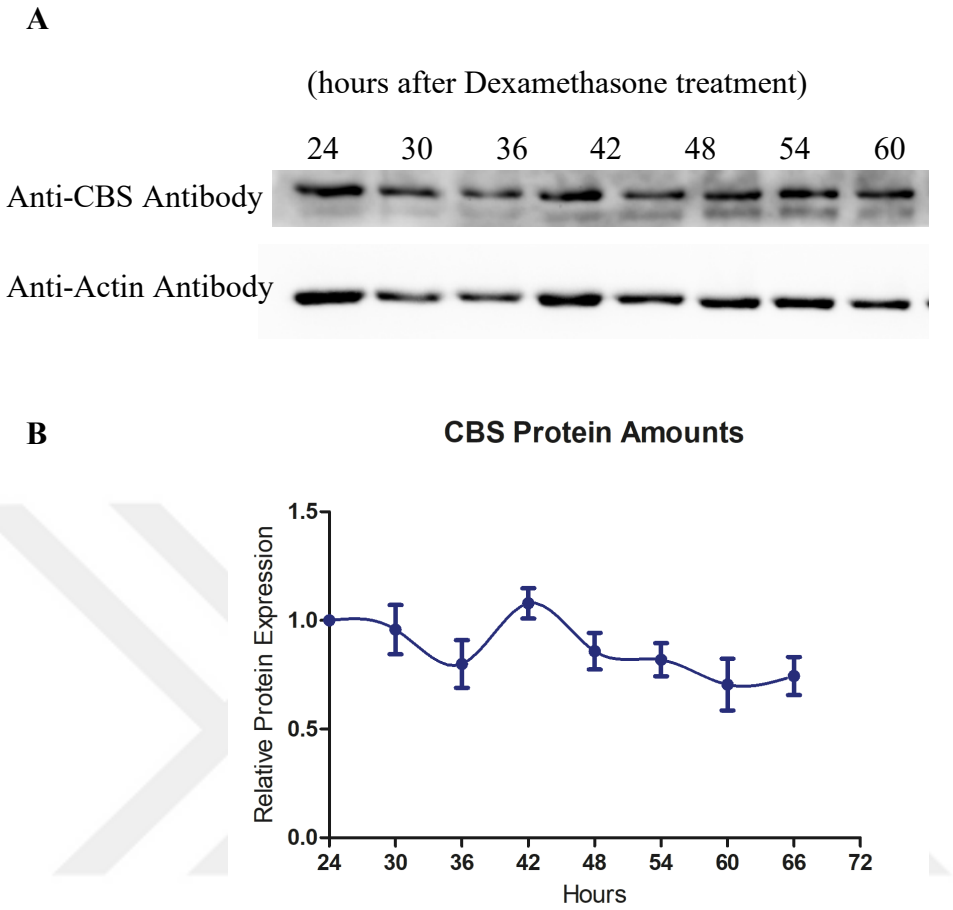


Figure 5-1: (A) Western blot detection of CBS protein amount oscillation over time after synchronization with Dexamethasone. (B) Quantification of western blot results shows the oscillation of CBS. n=3 biological replicates.

As seen from the upper figure (**Figure 5-1**), the expression of CBS is under circadian control. Additionally, our collaborator John Hogenesch and his colleagues established an online database where one can find the expression profiles of many genes throughout a day in both mouse and human tissues [111]. **Figure 5-2** shows the expressions of CBS in mouse liver and lung tissues. Which further supports our result that CBS expression profile showing circadian rhythm.

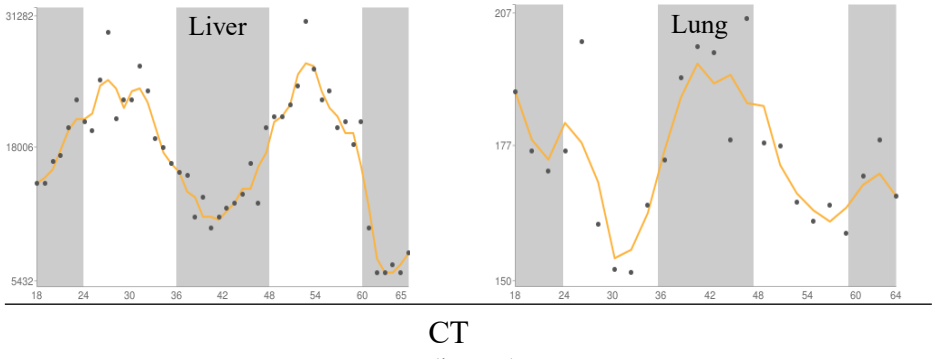
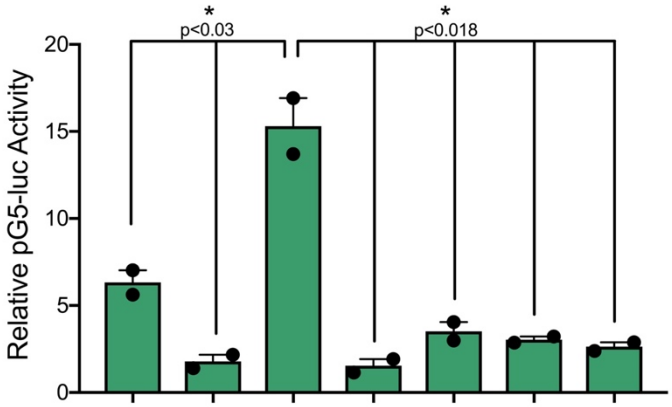


Figure 5-2: Circadian expression profile of CBS in mouse liver and lung tissues. Adopted from CircaDB online database.

5.2 Interaction Analysis of CBS with Known Clock Components

Until this point, we verified that the expression of CBS is controlled in circadian manner, and Anafi et al showed that CBS knock down significantly affected the circadian phenotypes of the cells [7]. In order to understand how CBS affects the circadian rhythm in the cells, we employed mammalian-two hybrid interaction analysis method to check the interaction of CBS and known circadian clock components. Mammalian-two hybrid system is adopted from yeast-two hybrid and it is a better platform to work on mammalian proteins, because it allows occurrence of natural post-translational modifications. Mammalian-two hybrid system is based on the expression of luminescence signal from GAL4 binding site as a result of interaction of two proteins. When two proteins interact with each other, VP16 activation domain and GAL4 DNA binding domains come together, and they drive firefly-luciferase expression [112]. In our experiment, CBS was cloned in pACT vector and fused with VP16 activation domain, on the other hand, clock components were cloned in pBIND vector and fused with GAL4 DNA binding protein. Cells were also transfected with renilla-luciferase to normalize the transfection efficiency and cell number in each technical replicate. Relative pG5-luc luciferase activity was calculated by normalizing the firefly-luciferase to renilla-luciferase. The fold was relative to negative control which contains pG5-luc and renilla only.



pG5-*luc*	:	+	+	+	+	+	+	+
pACT-CBS	:	+	+	+	+	+	+	+
pBIND-BMAL1	:	+	-	-	-	-	-	-
pBIND- CLOCK	:	-	+	-	-	-	-	-
pBIND- CRY1	:	-	-	+	-	-	-	-
pBIND- CRY2	:	-	-	-	+	-	-	-
pBIND- PER1	:	-	-	-	-	+	-	-
pBIND- PER2	:	-	-	-	-	-	+	-
pBIND- PER3	:	-	-	-	-	-	-	+

Figure 5-3: Mammalian two hybrid interaction analysis of CBS and known core clock components. Bars indicate the mean luciferase activity± SEM which was normalized by renilla-luciferase expression. n=2 * p<0.03, *p<0.018.

As clearly seen from the mammalian-two hybrid result in **Figure 5-3**, CBS interacts with CRY1. CRY1 works in the negative arm of the core clock machinery. Since CBS interacts with CRY1, its effect on circadian rhythm could be an effect of changed repression activity of CRY1. Any increasing or decreasing effect on CRY1 repression activity will change the circadian regulation of many genes and pathways throughout the body.

Before further analyzing the effect of CBS on the molecular mechanism of the circadian clock, we wanted to verify the effect of CBS on circadian rhythms of the cells by knocking it down by using small-interfering RNA (siRNA) based gene silencing approach.

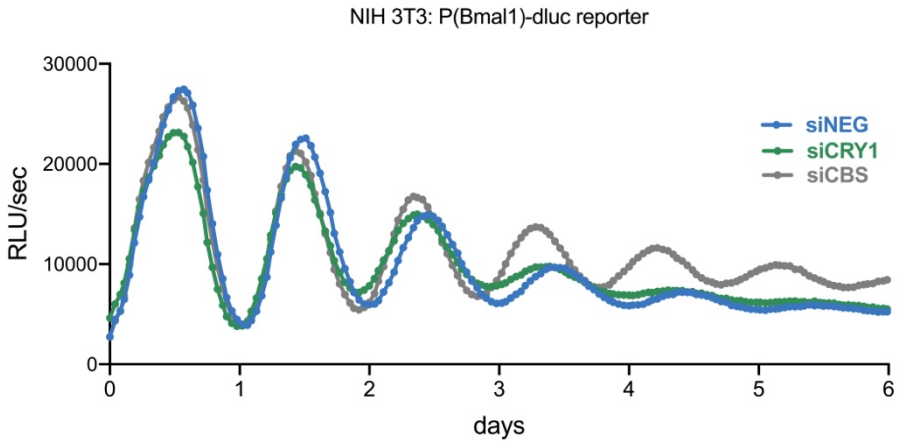
5.3 Effect of CBS siRNA Knock-Down on Circadian Rhythms of Cells

siRNAs are small interfering RNAs which induces the RNA-induced silencing complex (RISC) to target specific mRNA transcript and prevents the protein production from that gene. Either the RNA is delivered to the cell from intracellular or exogenous sources, the RNA is recognized as foreign and introduced in RISC complex. Following the formation of RISC complex, the expression of the target gene is terminated by either inhibition of the translation, mRNA degradation, or heterochromatin formation which blocks the transcription [113]. Artificially produced double stranded RNAs (dsRNAs) are used for a strong molecular tool to silence the target gene because they work more efficiently to induce RISC formation and gene silencing [114].

We purchased double stranded siRNAs from Qiagen which target mouse and human CBS and CRY1 to silence CBS and CRY1 expression in human and mouse cell lines. Catalog Numbers of used siRNAs are listed in Table 2. We used non-targeting siRNA which doesn't silence any genes in both mouse and human targets as our negative control which is abbreviated as siNEG throughout the thesis. siRNAs were transfected to U2-OS:P(Bmal1)-dluc (human osteosarcoma) NIH 3T3:P(Bmal1)-dluc (mouse fibroblast) cells with Invitrogen Lipofectamine RNAiMAX transfection reagent. Following the synchronization of the cells with dexamethasone, cells were placed in the lumicycle instrument which records luminescence signals from the dishes in every 10 minutes [115]. When there is a change in the molecular circadian rhythm of the cells, we can detect this with lumicycle as period length, amplitude, or phase change.

Real-time luminescence signals were recorded for 7 days in both cell lines as shown in **Figure 5-4A** and **Figure 5-5A**. Period length analyses of the real-time luminescence recordings were performed with R, using 'waveclock' package. Period length shortening effect of Cry1 knock-down is known in the literature [116]. We verified the period shortening effect of Cbs knock-down which was shown by Anafi and his colleagues [7]. After two days, cells in the 4^{th} technical replicate dishes were collected with Trizol and they were used for RNA isolation. First 3 technical replicates were used for lumicycle recording.

A



B

NIH 3T3:P(Bmal1)-dluc cells	
siRNA	Period Length Change
Cbs	-1.62 hour
Cry1	-0.22 hour

C

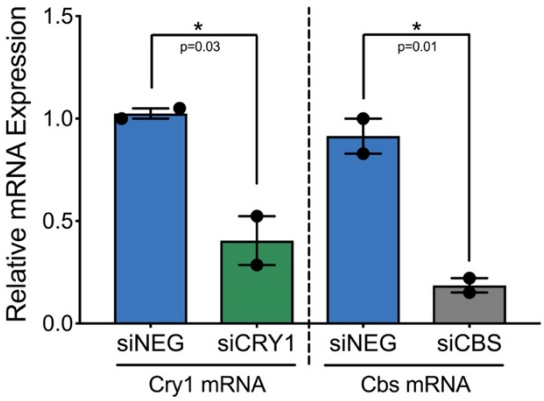
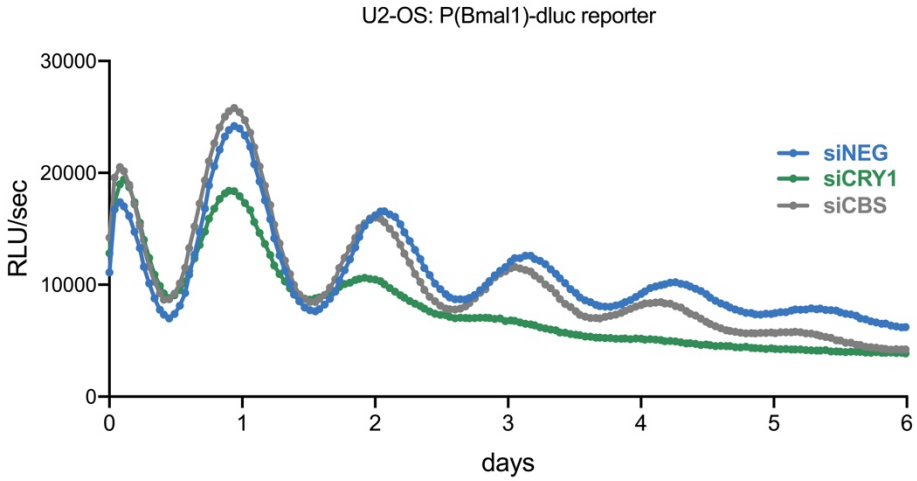


Figure 5-4: (A) Circadian phenotypes of NIH 3T3:P(Bmal1)dluc cells when Cbs and Cry1 were separately knocked-down with siRNAs. (B) Effects of Cbs and Cry1 silencing on period lenght of the cells. (C) siRNA knock-down efficiencies of the genes.

A



B

U2OS:P(Bmal1)-dluc cells	
siRNA	Period Length Change
Cbs	-0.69 hour
Cry1	-0.62 hour

C

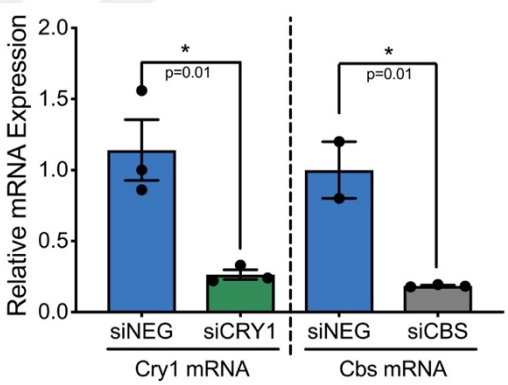


Figure 5-5: (A) Circadian phenotypes of U2-OS:P(Bmal1)dluc cells when Cbs and Cry1 were separately knocked-down with siRNAs. (B) Effects of Cbs and Cry1 silencing on period length of the cells. (C) siRNA knock-down efficiencies of the genes.

Following RNA isolation and cDNA synthesis, siRNA knock-down efficiencies were detected with quantitative PCR (Q-PCR). Unlike traditional PCR, Q-PCR is used to determine both starting amount of the template and real-time amplification of the product in the PCR reaction. Based on the amplification of PCR product, change in fluorescent signal intensity is measured by the instrument. Fluorescent signal may either come from TaqMan probe amplification or Sybr green dye. TaqMan-based Q-PCR is specific, easy to optimize, but highly expensive. Each TaqMan probe is designed specifically to each target template, and it has two fluorescent dyes which are conjugated to 5' and 3' ends of the probe. In the TaqMan probe mix, there is another primer whose binding site is close to TaqMan probe binding site. When amplification starts from the primer, it meets with 5' end of the TaqMan probe and leads its cleavage. Cleaved 5' end fluorescent dye is released from the probe and emits fluorescent signal which was previously quenched by the 3' fluorescent dye [117]. On the other hand, sybr green dye emits fluorescent signal when it binds to amplified double stranded product. Unlike TaqMan probe-based method, one can use sybr green dye with any primer in any PCR reaction. The fluorescent signal is weak before 15^{th} cycle and it reaches to plateau after 35^{th} cycle. Even though it is not as specific as TaqMan probe-based method, it is easy to apply and cheaper [118]. In both methods, primer dimers and primer designs to exon-exon junctions are crucial to prevent non-specific bindings. Q-PCR primers used in our experiments were listed in Table 8. In order to quantify mRNA expression levels in samples, we utilized sybr green based Q-PCR method [119]. siRNA knock-down efficiencies of mouse and human Cbs and Cry1 siRNAs were represented in **Figure 5-4C** and **Figure 5-5C**. In all samples, our siRNAs were worked and reduced their target mRNA levels significantly.

CBS is an important enzyme in one carbon metabolism pathways. It works in transsulfuration pathway which is interlocked with methyl, folate, urea glutathione pathways [120]. Any effect on expression or activity fluctuation in CBS will affect the harmony in one carbon metabolism pathway. In order to show that the effect of CBS knock down on period length is not caused by metabolite level changes, we measured the real-time luminescence responses of the cells by manipulating methionine and glutathione concentrations (**Figure 5-6**).

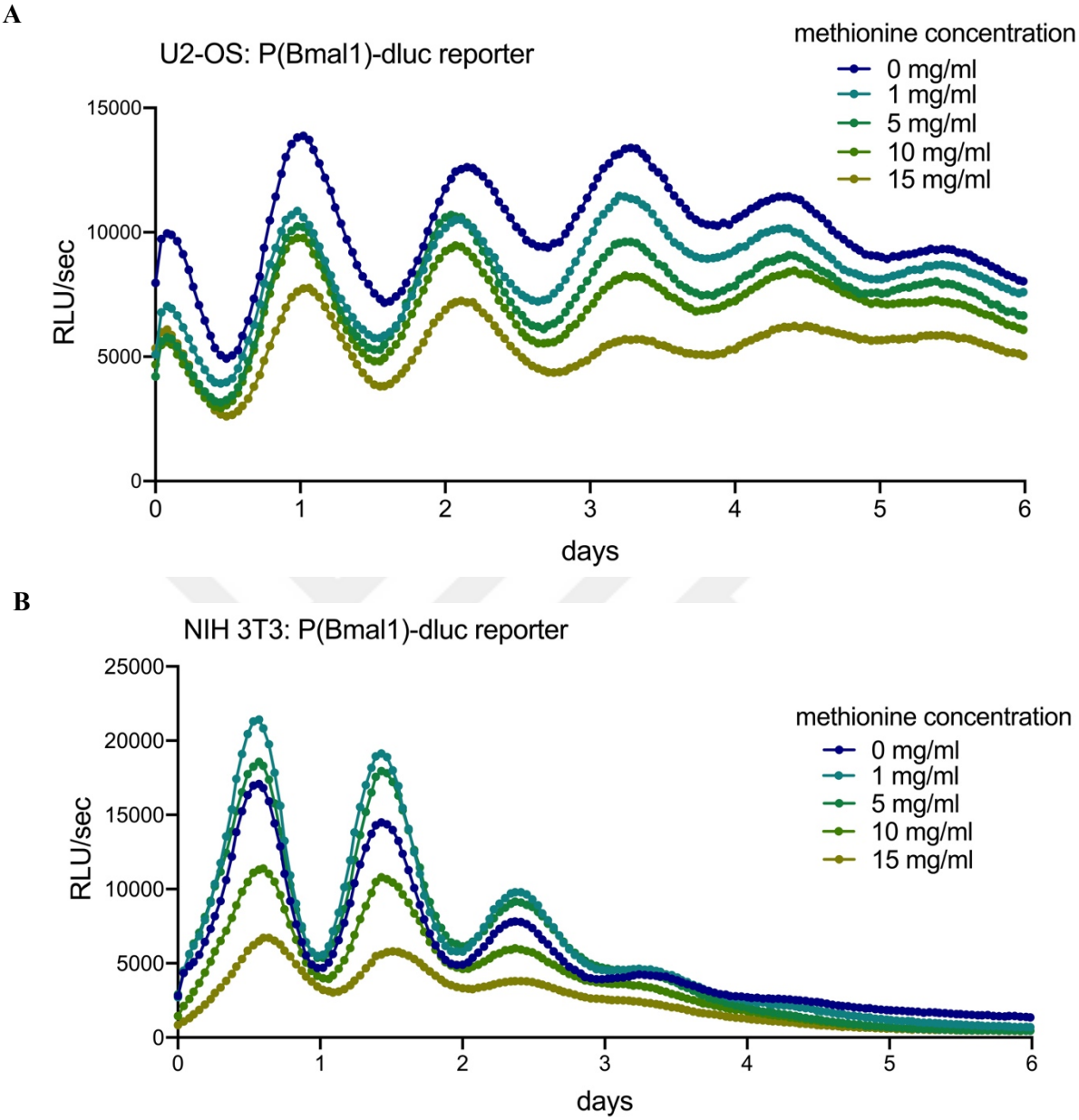
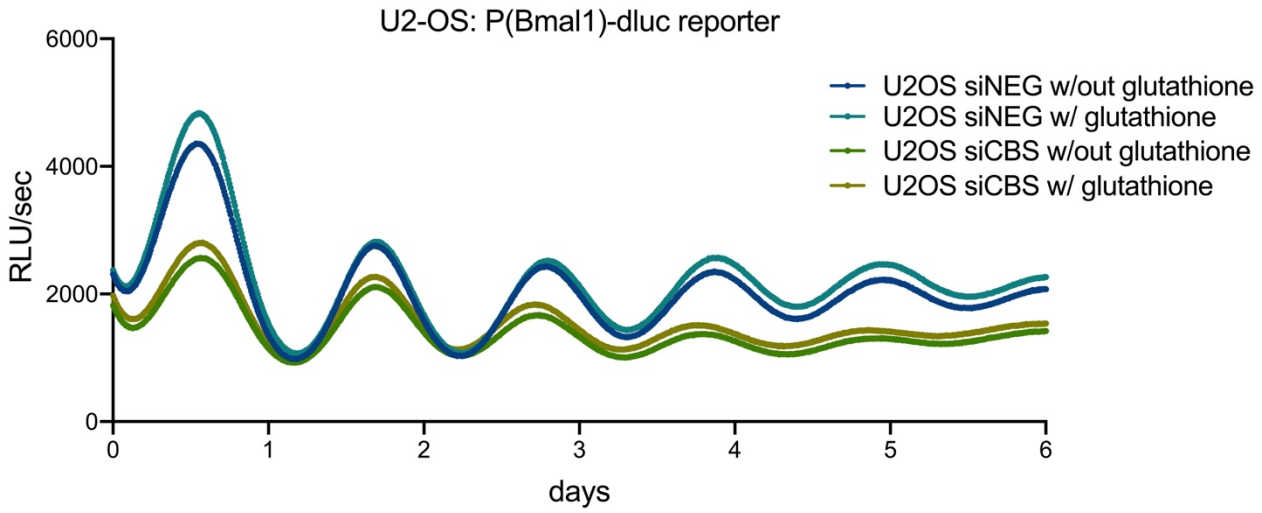


Figure 5-6: Effect of different methionine concentrations on circadian phenotypes of cells. (A) (B) Circadian responses of U2-OS: P(Bmal1)-dluc and NIH 3T3: P(Bmal1)-dluc cells to 0, 1, 5, 10 and 15 mg/mL methionine concentrations.

As **Figure 5-6** shows, concentration change in methionine doesn't affect circadian periods of both U2-OS: P(Bmal1)-dluc and NIH 3T3: P(Bmal1)-dluc cells. Since methionine is at the upstream of the CBS in one carbon metabolism, we also detected the

effect of glutathione, because it is the key component of anti-oxidant regulation and at the downstream of CBS in the one carbon metabolism pathway.

A



B

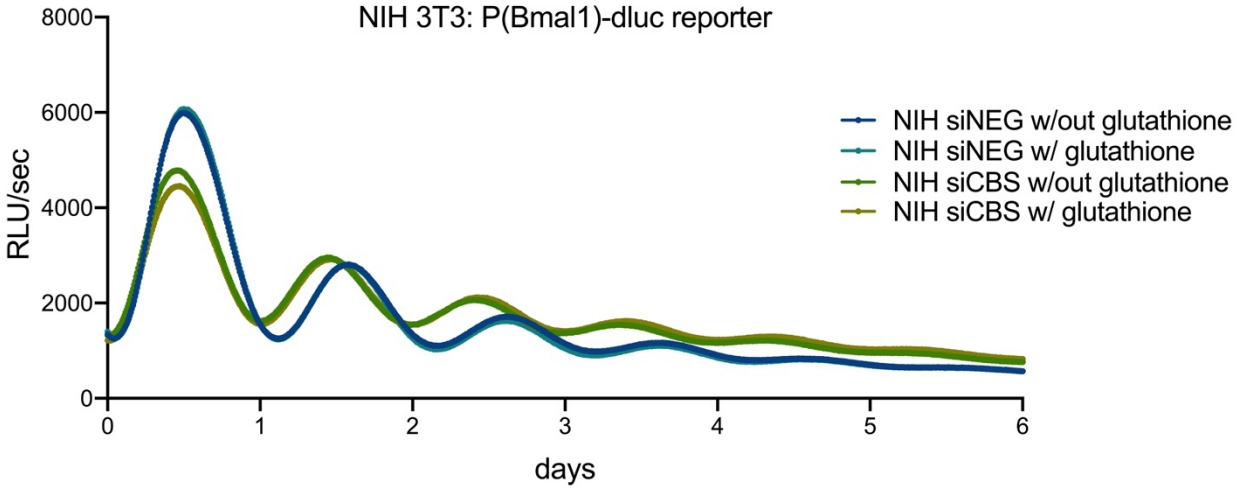


Figure 5-7: Effect of different glutathione on circadian phenotypes of cells in the wild type and CBS knock-down cells. (A) (B) Circadian responses of U2OS: P(Bmal1)-dluc and NIH 3T3: P(Bmal1)-dluc cells glutathione addition to the cells. Addition of glutathione doesn't affect period lengths of the cells.

As parallel with what we saw with the methionine concentration, glutathione concentration change didn't affect the circadian periods of cells in both wild type and CBS knocked-down cells.

Figure 5-6 and **Figure 5-7** shows that the period shortening effect of CBS gene silencing is not a result of metabolite level fluctuations. Instead, the period change might be the result of direct or indirect effect of CBS on molecular circadian clock machinery. In order to further address this hypothesis, we started to analyze the physical and functional details of CBS and CRY1 interaction.

5.4 Circadian Behavioral Analysis of *Cbs*$^{-/-}$ Mice

Cbs$^{+/-}$ animals were obtained from Warren Kruger's lab and they were maintained in animal facility of University of Pennsylvania (UPENN). *Cbs*$^{+/-}$ mice were crossed with their siblings to generate *Cbs*$^{-/-}$. Since the direct Cbs knock out is lethal. These mice expressed Cbs-I278T gene under the control of Zinc-inducible promoter. The detailed generation and maintenance were described by Wang L. et al [107]. 25 mol/L Zinc containing water was given to these mice after they passed their developmental stages. We abbreviate these mice as *Cbs*$^{-/-}$. In order to perform behavioral analysis, *Cbs*$^{-/-}$ and their littermate wild type control mice were entrained with 12 hours light-dark cycles for two weeks with ad libitum food and water. Mice have to be housed in individual cages to measure their locomotor activities in the wheel cages. Every wheel turn by the mouse is represented as black bars in the actogram plots. Light-dark and dark-dark periods are represented in the actogram (**Figure 5-8A**). When mice kept under constant darkness, we are able to measure their free running activity which is the representative of their central clock without external time cues control.

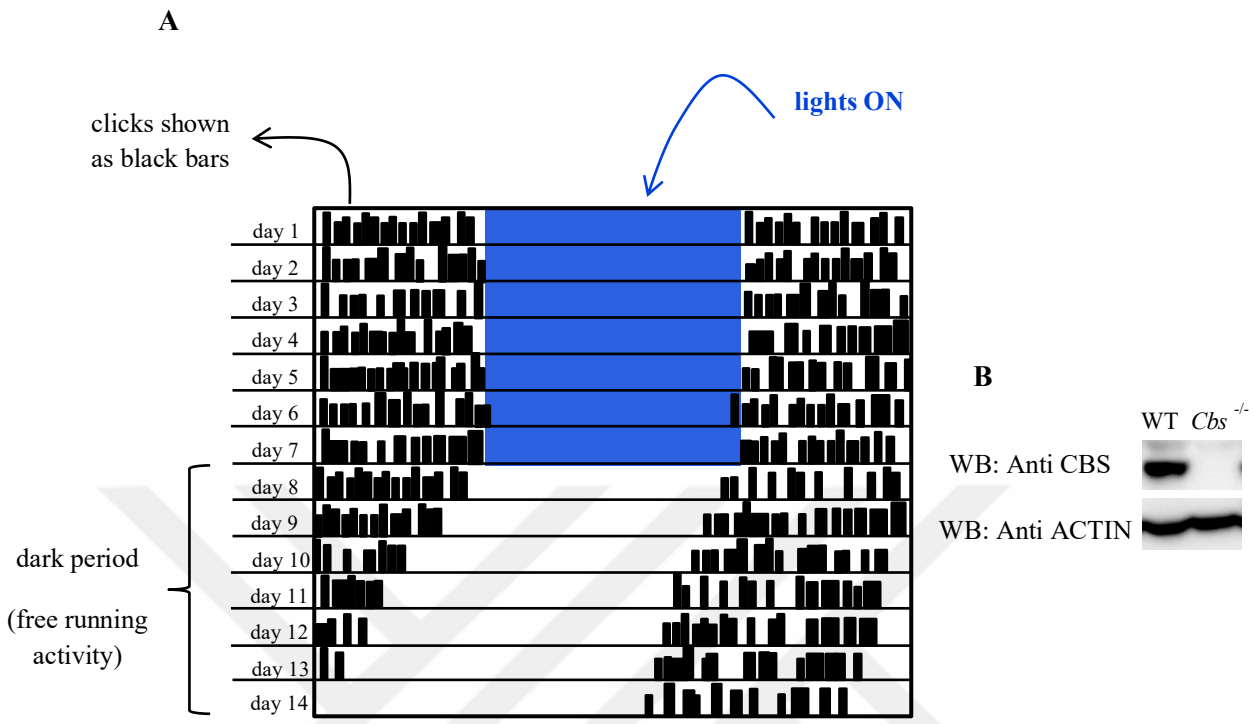


Figure 5-8: Representative actogram and *Cbs*$^{-/-}$ genotype verification at protein level. Protein samples prepared from *Cbs*$^{-/-}$ mouse liver.

After the completion of the circadian behavioral assay, we collected liver tissues from *Cbs*$^{-/-}$ mice at ZT12 and checked the CBS wild type protein expression to verify the knock-out genotype. Western blot data is represented in **Figure 5-8B**.

Figure 5-9 and **Figure 5-10** show wild type and *Cbs*$^{-/-}$ female mice actograms, while **Figure 5-11** and **Figure 5-12** will show male results. We represented 4 mice actograms for each genotype and gender for clarification. We used total 47 mice data whose raw results represented in Table 7.

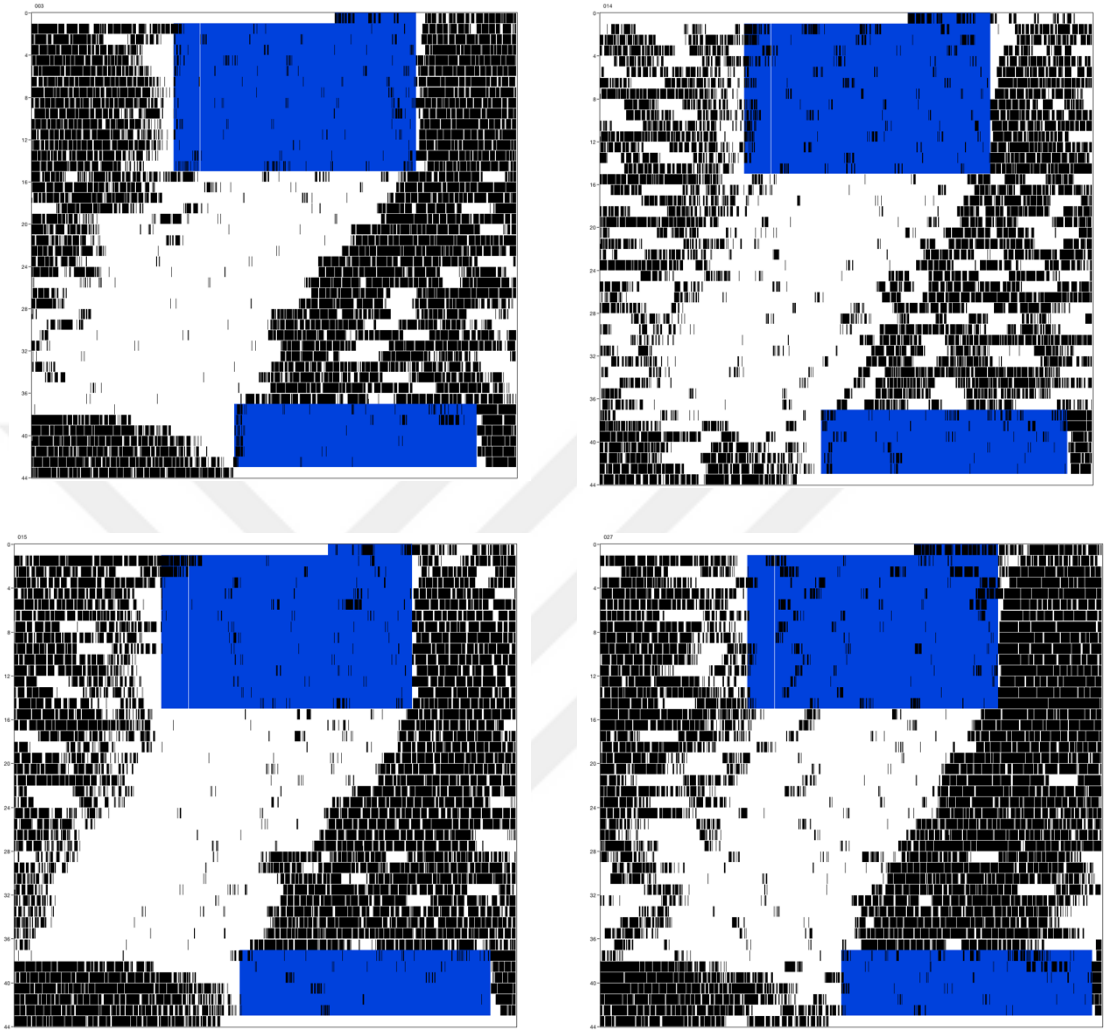


Figure 5-9: Wild type female actogram results.

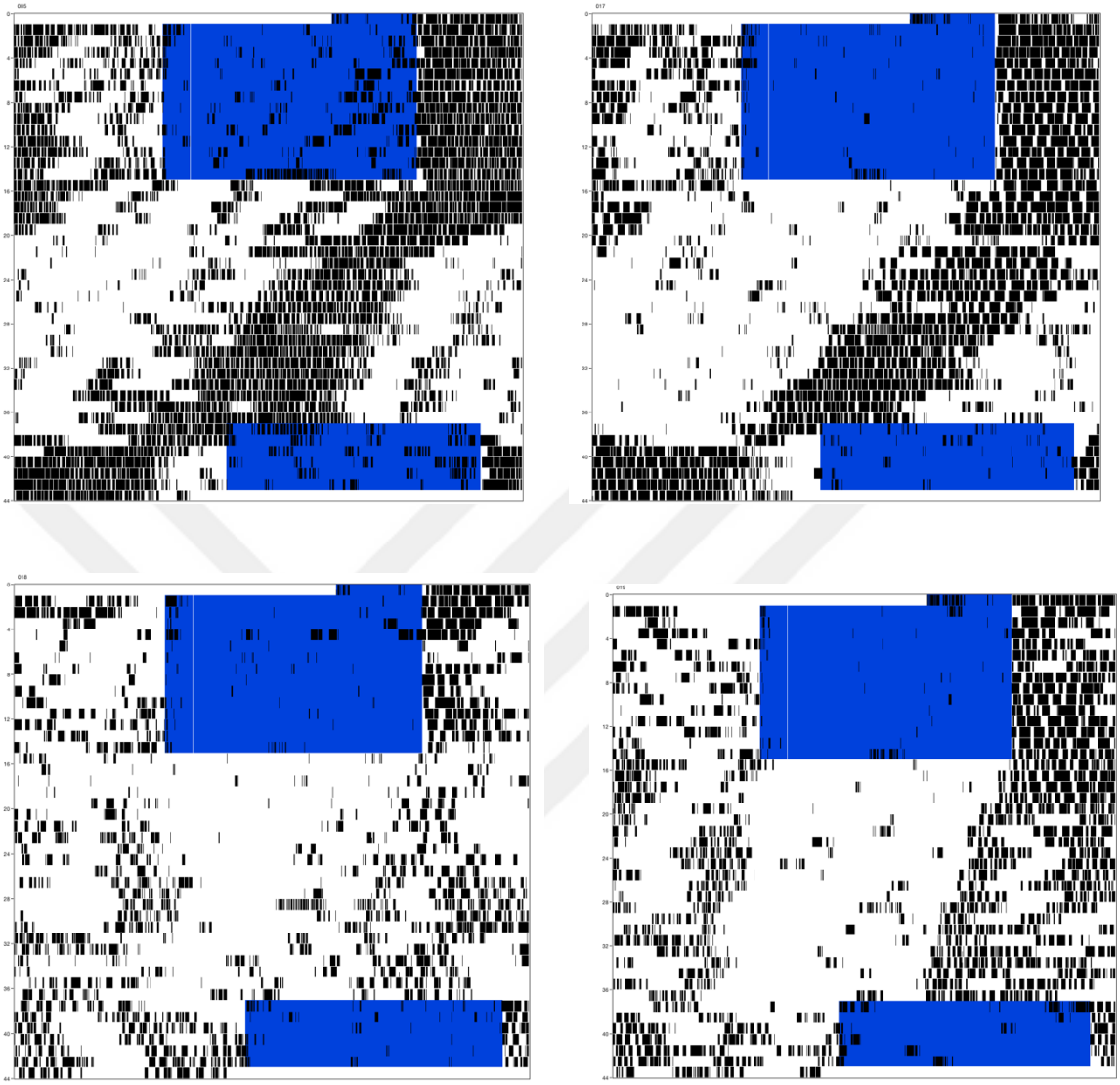


Figure 5-10: CBS knock-out female actogram results.

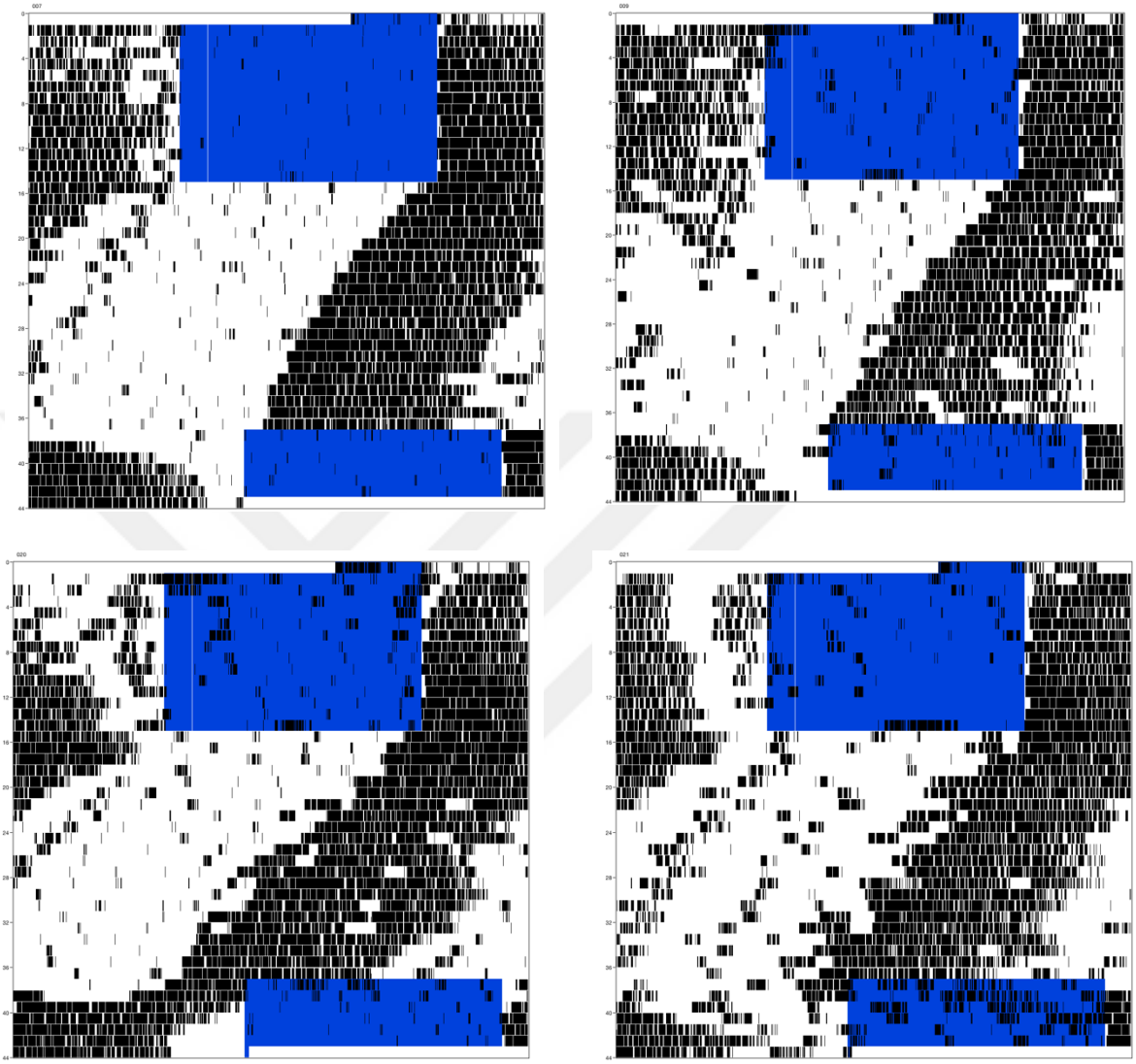


Figure 5-11: Wild type male actogram results.

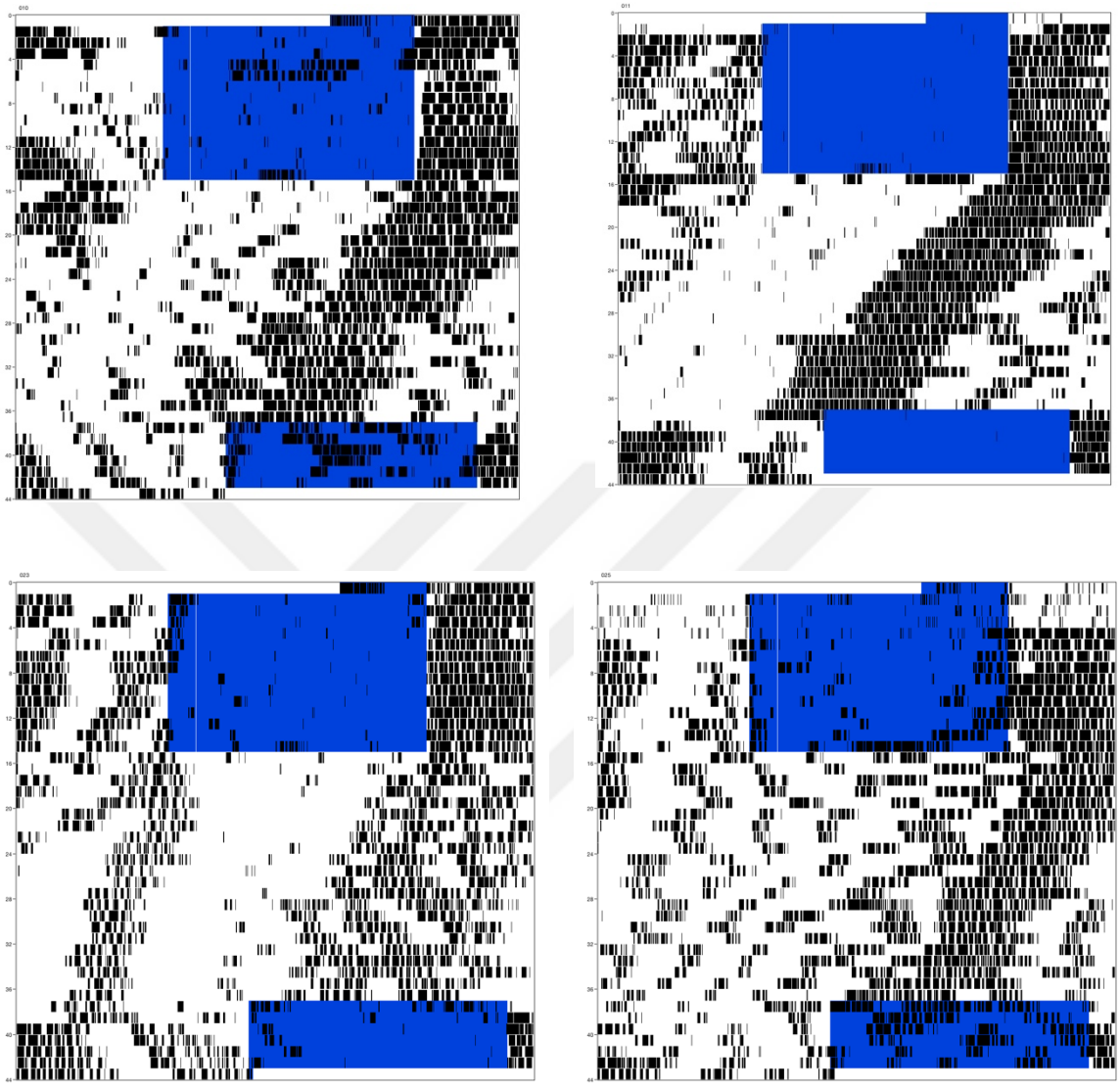


Figure 5-12: CBS knock-out male actogram results.

Actogram results above show that CBS absence induces mice to be active in the resting phase -when lights are on- and it reduces entrainment efficiency. In wild type mice, (**Figure 5-9** and **Figure 5-11**) wheel running activity is clustered in active phase, while it is dispensed through active and resting phase in *Cbs*$^{-/-}$ mice (**Figure 5-10** and **Figure 5-12**). In order to make quantitative comparisons, we calculated period, amplitude and circadian power of this mice by using ClockLab Software.

Even though there is no difference between circadian period of female and male wild type and *Cbs*$^{-/-}$ mice, relative amplitude of female *Cbs*$^{-/-}$ mice is slightly reduced. The most significant difference between wild type and *Cbs*$^{-/-}$ mice is detected in circadian power behavior (**Figure 5-13**). Circadian power indicates the ability to show consistent circadian phenotype between days. Thus, *Cbs*$^{-/-}$ mice lacks the ability to keep their circadian clock intact.

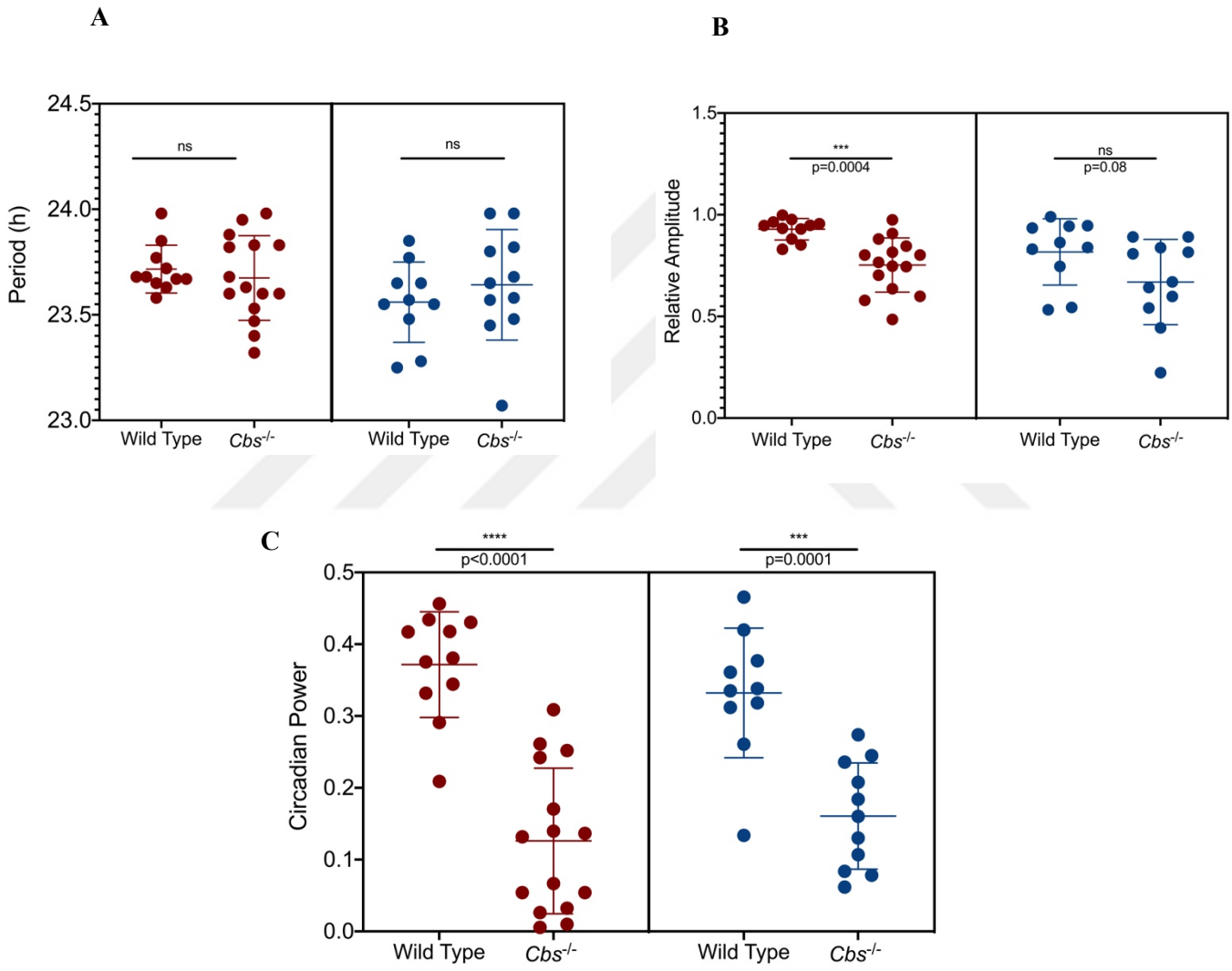


Figure 5-13: (A) (B) (C) Respectively, circadian period, relative amplitude and circadian power analysis results of *Cbs*$^{-/-}$ mice circadian locomotor activities. Closed red circles represent female samples, closed blue circles represent male samples.

5.5 Further Analysis of The Interaction of CRY1 and CBS

In this section of the experiments, first, we identified two non-CBS-binding CRY1 and used them as controls in further studies. With different interaction analyses methods, we proved that CRY1-CBS interaction is physical, and this interaction takes place in both cytosol and nucleus. After these experiments, we continued our project to investigate the effects of these two proteins to each other's roles in the cells.

5.5.1 Identification of the Crucial Binding Site on CRY1 for Its Interaction with CBS

C-terminal region of mammalian CRY1 protein is important for its repression function [121]. That region doesn't have a proper structure, it changes structure depend on binding partner of CRY1. In order to detect the effect of CRY1 C-terminal region on CBS-CRY1 interaction, we constructed CRY1 proteins which lack 20 amino acids from their C-terminals. As the first step, we checked the expressions of these constructs with western blot by using GAL4 antibody (**Figure 5-14 A and B**).

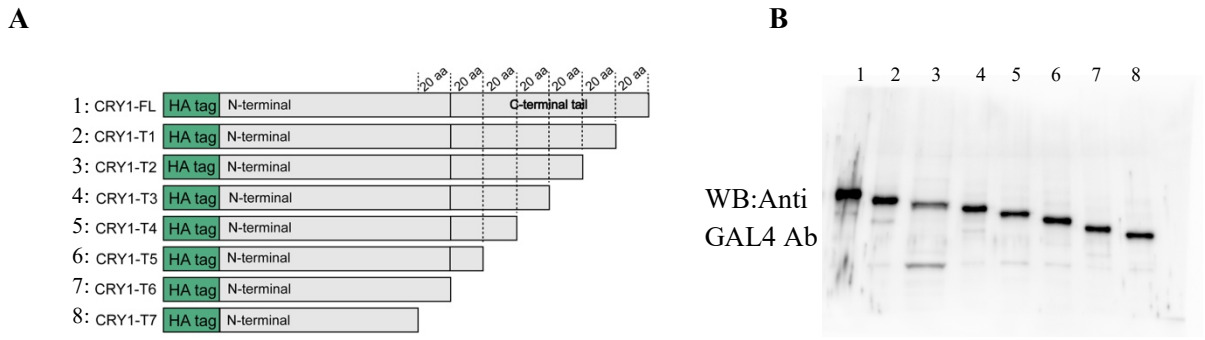
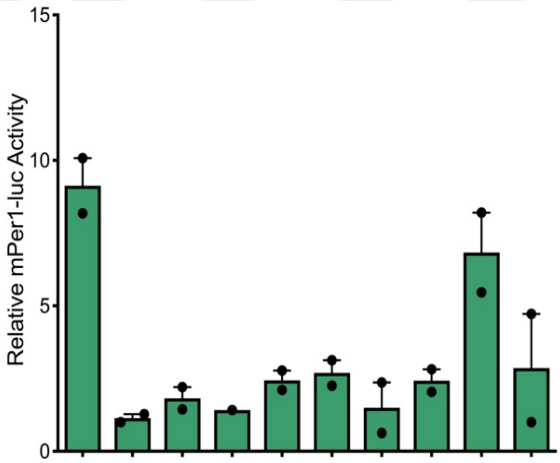


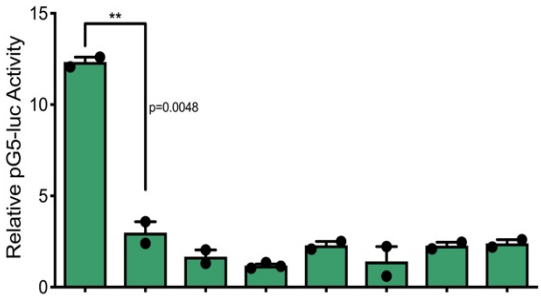
Figure 5-14: (A) C-terminal Truncated CRY1 constructs in pBIND vector. (B) Expression of all of the constructs which were detected by anti-GAL4 western blot antibody.

The C-terminal tail region of CRY1 is important for its function to modulate period [122]. Following the expression check of the constructs, we detected their repression activities on BMAL1-CLOCK complex with *Per1:luc* reporter assay. All constructs until CRY1-T6 have repression activity (**Figure 5-15**). Means that, C-terminal truncated CRY1 constructs produce functioning proteins. Then, we applied mammalian-two hybrid assay to check their interaction with CBS. The last 20 amino acids of CRY1 protein is important for its interaction with CBS (**Figure 5-16**). To find the prominent amino acid or amino acids in this 20 amino acid long region, we used random mutagenesis approach to make random mutations in this area.



mPer1-*luc*	:	+	+	+	+	+	+	+	+	+	+
sport6-BMAL1	:	+	+	+	+	+	+	+	+	-	-
sport6-CLOCK	:	+	+	+	+	+	+	+	+	-	-
pcDNA-CRY1-FL	:	-	+	-	-	-	-	-	-	-	-
pcDNA- CRY1-T1	:	-	-	+	-	-	-	-	-	-	-
pcDNA- CRY1-T2	:	-	-	-	+	-	-	-	-	-	-
pcDNA- CRY1-T3	:	-	-	-	-	+	-	-	-	-	-
pcDNA- CRY1-T4	:	-	-	-	-	-	+	-	-	-	-
pcDNA- CRY1-T5	:	-	-	-	-	-	-	+	-	-	-
pcDNA- CRY1-T6	:	-	-	-	-	-	-	-	+	-	-
pcDNA- CRY1-T7	:	-	-	-	-	-	-	-	-	+	-

Figure 5-15: Repression activity of truncated CRY1 proteins on BMAL1-CLOCK transactivation.



pG5-*luc*	:	+	+	+	+	+	+	+	+
pACT-CBS	:	+	+	+	+	+	+	+	-
pBIND-CRY1-FL	:	+	-	-	-	-	-	-	-
pBIND-CRY1-T1	:	-	+	-	-	-	-	-	-
pBIND-CRY1-T2	:	-	-	+	-	-	-	-	-
pBIND-CRY1-T3	:	-	-	-	+	-	-	-	-
pBIND- CRY1-T4	:	-	-	-	-	+	-	-	-
pBIND- CRY1-T5	:	-	-	-	-	-	+	-	-
pBIND- CRY1-T6	:	-	-	-	-	-	-	+	-
pBIND- CRY1-T7	:	-	-	-	-	-	-	-	+

Figure 5-16: Mammalian-two hybrid interaction analysis of CBS and truncated CRY1 proteins.

Degenerate primers were designed to make random mutations with degenerate-PCR. In this method, one can design primers having different bases at the desired points [123]. Our degenerate PCR primers to make random mutations on the last 20 amino acids in the C-terminal tail region of CRY1 are listed in Table 9. The IUPAC meanings of the unusual codes in the primer sequences were listed in Table 10. After the PCR reaction, we digested the wild-type plasmid template with Dpn1 enzyme digestion. Dpn1 enzyme digests methylated DNA [124]. Our common lab *E. Coli* strain Dh5α has dam, dcm and EcoKI methylases which add methyl groups to different sites of DNA. Based on this knowledge, in modern molecular biology, we generally use this enzyme to digest DNA which is methylated by methylases during bacterial DNA synthesis. After the elimination of wild-type plasmid template, we transformed mutation containing plasmids into competent Dh5α bacteria and selected as much as colonies we can. We sequenced plasmid DNA from these colonies and checked their interaction with CBS. These CRY1 constructs have random mutations on their last 20 amino acids. The table below assembled from mammalian-two hybrid and DNA sequencing data. It is clear that when arginine at 602nd position turns into proline, the interaction of CRY1 and CBS significantly reduces. Then, we introduced R602P mutation into wild type CRY1 construct with the same protocol by using site-directed mutagenesis PCR primers.

Table 6: Different mutations detected after degenerate PCR and their interaction with CBS based on mammalian-two hybrid signals.

WT amino acid sequence (586-606 aa)	P	S	Q	E	E	D	A	Q	S	V	G	P	K	V	Q	R	Q	S	S	N	Luciferase activity detected from CBS-CRY1 interaction
Wild Type	P	S	Q	E	E	D	A	Q	S	V	G	P	K	V	Q	R	Q	S	S	N	+++++
Mutant 2	P	S	Q	E	E	D	A	Q	S	V	G	P	K	V	Q	P	Q	I	S	K	+
Mutant 3	P	S	Q	E	E	D	A	Q	S	V	G	P	K	V	Q	L	Q	S	S	K	++
Mutant 7	P	S	Q	E	E	D	A	Q	S	V	G	P	K	V	Q	P	Q	S	S	K	++
Mutant 9	P	S	Q	E	E	D	A	Q	S	V	G	P	K	V	Q	R	Q	S	S	K	+++++
Mutant 28	P	S	Q	E	E	D	A	Q	S	V	G	P	K	V	P	A	A	E	Q	Q	+++
Mutant 48	P	S	Q	E	E	D	A	Q	S	V	G	P	N	V	Q	R	Q	S	S	N	++
Mutant 60	P	S	Q	D	E	A	A	H	S	G	G	P	K	V	Q	R	Q	S	S	N	++

After sequence verification of CRY1-R602P mutation, we checked its expression with anti-HIS western blot antibody. Plasmids were transfected to HEK293T cells with PEI. CRY1-R602P is expressed as much as wild-type and truncated CRY1 constructs (**Figure 5-17A**). Additionally, Arginine-602 point is highly conserved according to NCBI Homologene Database across 9 different organisms (**Figure 5-17B**). Up to this point, we verified the sequence and expression of CRY1-R602P. Then, we aimed to show the functionality of the constructs by detecting their interaction and repression abilities. We applied mammalian-two hybrid system to check the interaction of CRY1-WT, CRY1-T1 and CRY1-R602P with PER2, as can be seen from the **Figure 5-17C**, both CRY1-T1 and CRY1-R602P interact with PER2.

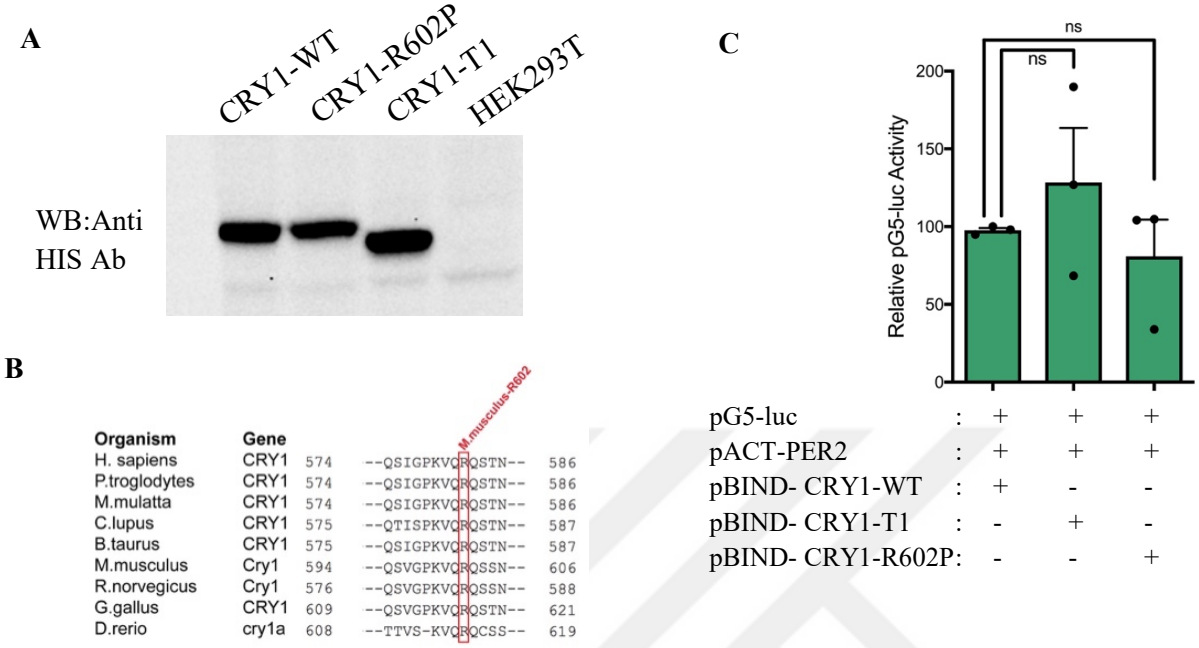


Figure 5-17: Even though the new constructs are functionally active, they do not interact with CBS. (A) Expression of wild-type, mutant, and truncated CRY1 constructs which were transfected to HEK293T cell line with PEI. (B) Clustal Omega conservation analysis of R R602 point across different organisms. (C) Mammalian two hybrid interaction analysis of CRY1-WT, CRY1-R602P and CRY1-T1 with PER2. All constructs interact with PER2.

In addition to functionality analyses, we detected their repression activities on BMAL1-CLOCK transactivation on *Per1-luc* promoter. As the result of three independent experiments, **Figure 5-18A** shows that CRY1-T1 and CRY1-R602P repress the transactivation as better as wild-type CRY1.

As the last step of this part of the experiments, we did mammalian-two hybrid experiment with CRY2, CRY1-WT, CRY1-T1, and CRY1-R602P (**Figure 5-18B**). Unlike wild-type CRY1; CRY2, CRY1-T1, and CRY1-R602P do not interact with CBS.

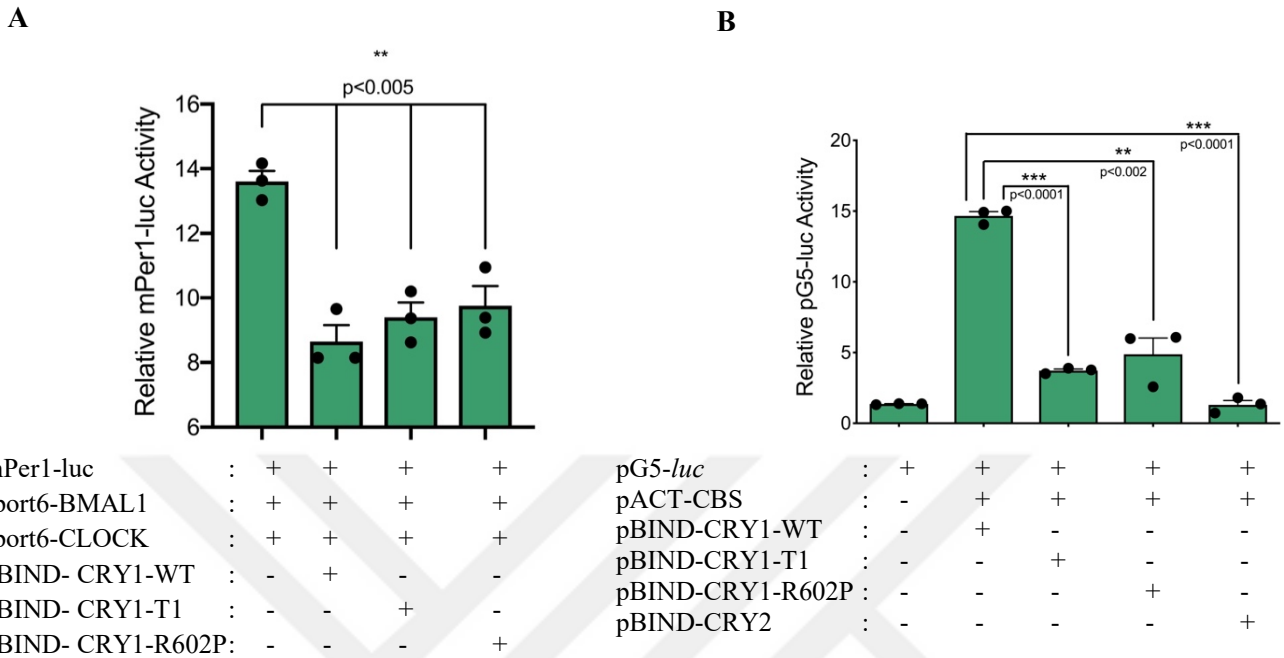


Figure 5-18: (A) Repression activities of CRY1-WT, CRY1-R602P and CRY1-T1 on BMAL1-CLOCK transactivation. CRY1-T1 and CRY1-R602P are able to repress the BMAL1-CLOCK transactivation as much as wild type CRY1. (B) Mammalian two hybrid interaction analysis of CRY1-WT,

In the further experiments, we either used CRY1-T1 or CRY1-R602P as our non-CBS binding control. The importance of using non-CBS binding control is valuable for many of the following steps to determine the importance of either CBS in the circadian clock or CRY1 in the metabolism.

5.5.2 Co-Immunoprecipitation Verified the Physical Interaction Between CRY1 and CBS

Although mammalian-two hybrid is an *in vitro* interaction analysis method, it is not solely enough to prove the physical interaction between two proteins. In order to address whether CRY1 and CBS physically interact with each other, we used co-immunoprecipitation method. Co-immunoprecipitation is based on pulling down a protein with antibody specific to protein or its tag, and detection of its binding partner with western blot. To perform this method, we co-expressed CRY1 and CBS in HEK293T cells by using CRY1-T1 and CBS co-expression as negative control. As additional controls, only CRY1 and only CBS were expressed and used in the assay, too.

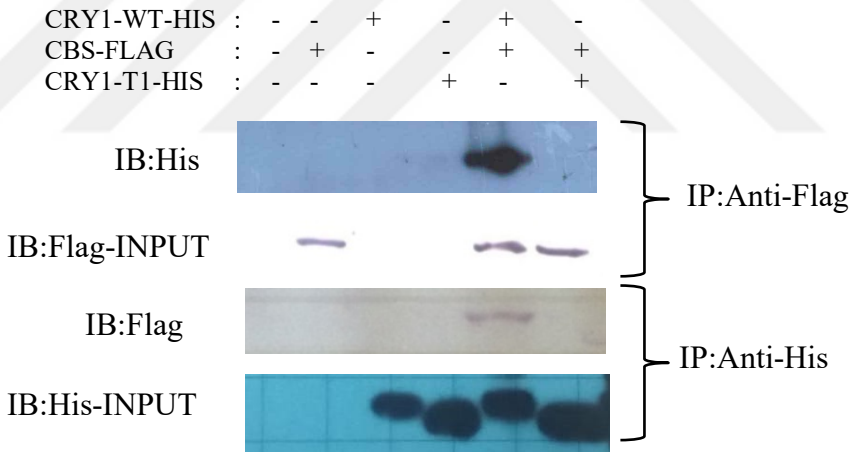


Figure 5-19: Proof of physical interaction between CRY1 and CBS by co-immunoprecipitation. The upper panel shows the result of CBS pull down with Flag tag. 2nd panel is the western blot of the input samples used for Flag-tagged pull down. 3rd and 4th panels are the pull down and input blots of His-tagged CRY1 immunoprecipitation.

After cell collection, cells were lysed in proper buffers as indicated in materials and methods section. Lysed cells were centrifuged, and cell free extracts were obtained. Cell free extracts were either incubated with Anti-His resin to pull down His-tagged CRY-WT and CRY1-T1 proteins or they were incubated with Anti-Flag resin to pull down Flag-tagged CBS protein. Following the washes with TBS to eliminate non-specific bindings, we eluted bead-bound complexes by boiling the samples. After that, all samples were run on western blot to detect the results (**Figure 5-19**). When CBS was pulled down with Flag tag specific resin, CRY1-WT was detected as its interacting partner. On the other hand, CRY1-T1 was not pulled down CBS, because they do not physically interact. The very same experiment was repeated as reverse, by pulling down CRY1-WT and CRY1-T1. CBS was pulled down only with CRY1-WT, not with CRY1-T1. As a result of co-immunoprecipitation experiment, we can conclude that CRY1 and CBS physically interacts with each other.

5.5.3 Bi-Molecular Fluorescence Complementation (Bi-FC) Assay Showed CBS-CRY1 interaction *in vitro*

Bi-molecular fluorescence complementation (Bi-FC) analysis is used to detect the interaction of two proteins in the living cells. It based also allows us to detect the localization of the interaction. In Bi-FC assay, two proteins were fused to two halves of fluorescent protein. When those two proteins come together and interact, fluorescent protein is complemented and detected under microscope. By addition of cytosol, nucleus or organelle specific dyes, one can clearly detect the interaction region. In our experiment, C-terminal half of Venus protein is conjugated with CRY1 (CRY1-R602P-VC/CRY1-WT-VC), and N-terminal half of it is fused with CBS (CBS-VN). Even though Bi-FC assay might give non-specific fluorescent signals, by using proper controls and by optimizing the amounts of transfected plasmids, this odd can be eliminated [125]. In our Bi-FC assay, we used CRY1-R602P mutant as our interaction specificity control. Additionally, we expressed mCherry protein in the cells to see cytosols and to check transfection efficiencies between samples. **Figure 5-20B** shows the expressions of CRY1 and CBS in the “CBS-VN and CRY1-R602P” and “CBS-VN and CRY1-WT” samples.

In the first channel of **Figure 5-20**, we see mCherry expression in both upper (CBS and CRY1-R602P) and lower (CBS and CRY1-WT) panels, which means the transfection efficiencies in both samples are good. The second channel is YFP (yellow fluorescent protein channel) which allows us to detect Venus protein. We do not see yellow in the upper panel of Venus channel which shows that mutant CRY1 and CBS do not interact. Whereas, we see yellow in the lower part because wild type CRY1 and CBS interact with each other. In the merge image, we see that this interaction is both in cytosol and nucleus. We know that CRY1 is a transcription factor which mainly works in the nucleus, but we do not know whether it has function in the cytosol by interacting with CBS or not. On the other site, CBS is an enzyme, and it works in the cytosol. It has been detected in the nucleus before [126], but no one hasn't explained what the purpose is carrying CBS into the nucleus.

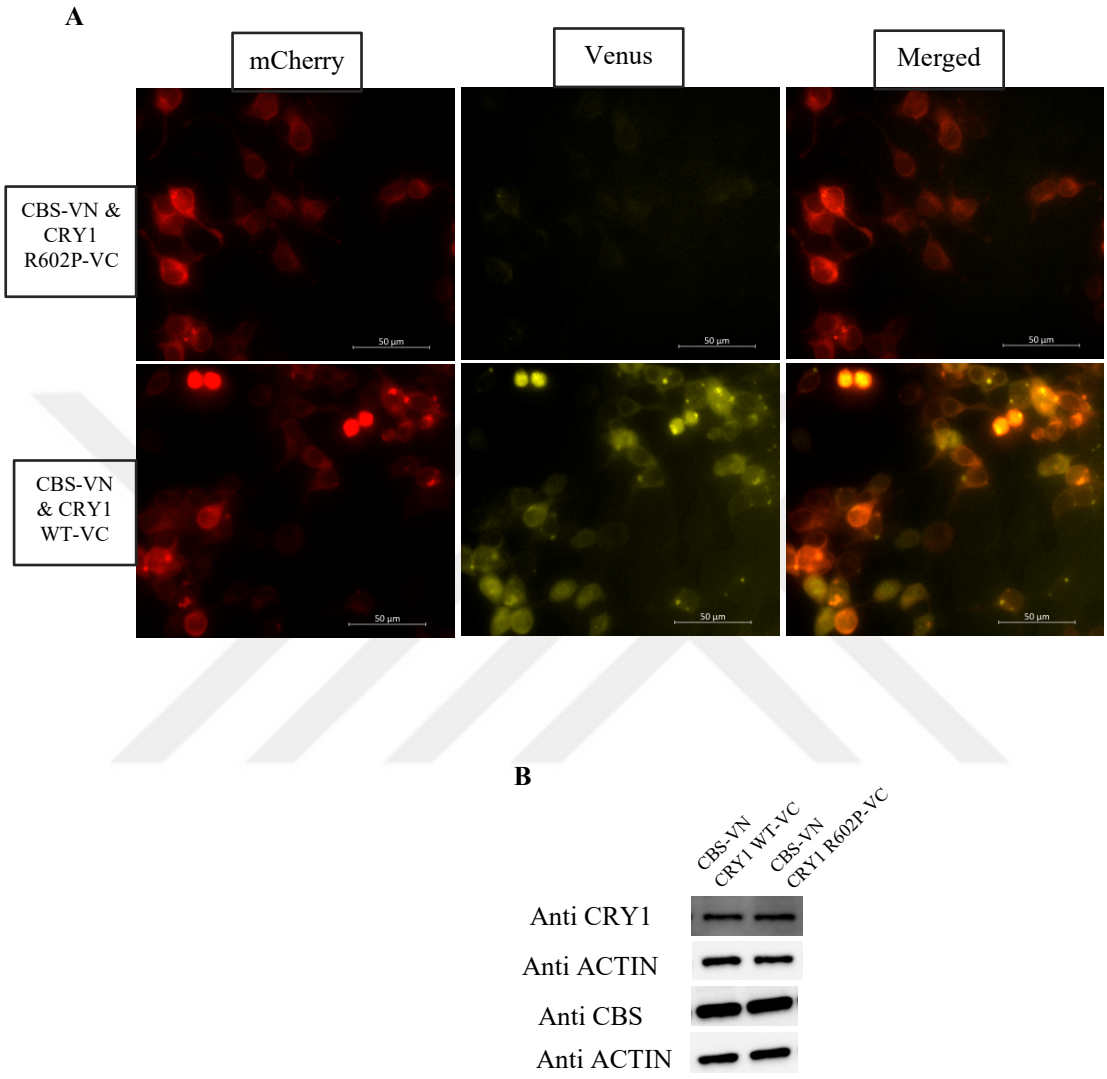


Figure 5-20: Bi-FC result of CBS and CRY1. (A) Upper photos show that CRY1-R602P and CBS do not interact. The lower photos show that CRY1 and CBS interact. We can see from the merged image that this interaction is both in cytosol (orange areas-overlapping of yellow and red) and in nucleus (yellow areas-no overlap with red). (B) Expressions of CBS and CRY1 in upper and lower panels where mutant CRY1 and CBS and wild type CRY1 and CBS co-expressed for Bi-FC visualizations.

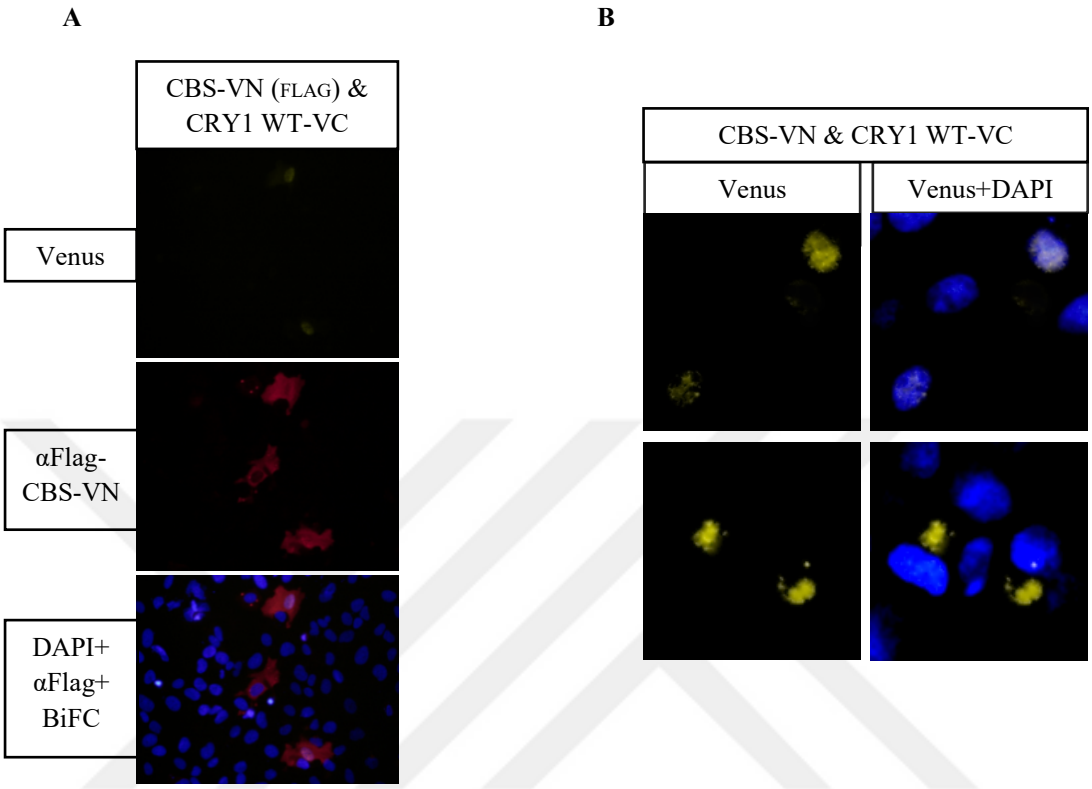
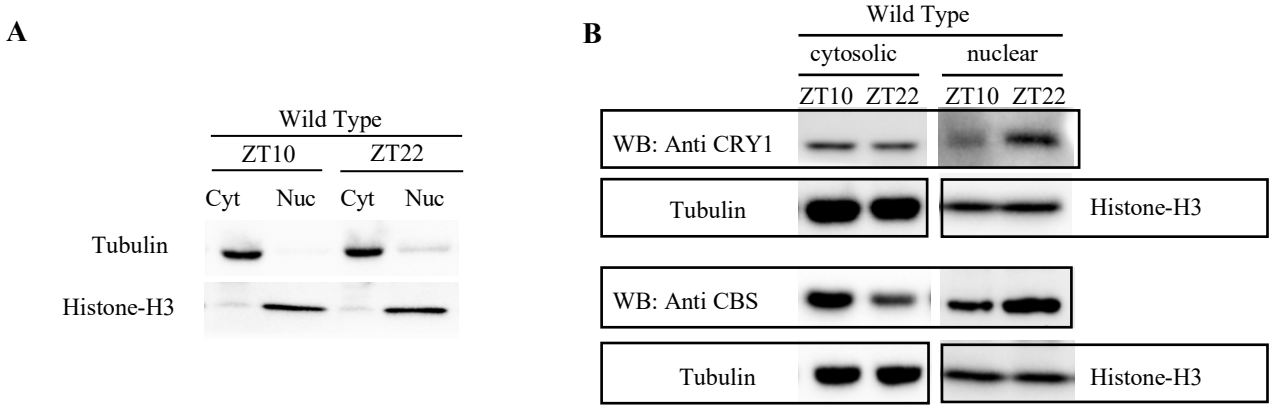


Figure 5-21: Detection of the interaction localization of CBS and CRY1. (A) Together with Bi-FC detection, co-localization of CBS at the interaction site was determined with Anti-Flag antibody detection. (B) Both cytosolic and nuclear localization of the interaction of CBS and CRY1 were verified with DAPI staining.

Figure 5-21 further verifies both localization of CBS at the interaction site (Flag overlaps with Bi-FC in **Figure 5-21A**) and nuclear and cytoplasmic localization of the interaction (**Figure 5-21B**). DAPI dye labels DNA which allows us to visualize nucleus under microscope [127]. In order to reproduce the literature and prove the localization of both proteins in both cell fractions, we fractionated mouse liver samples in the following section.

5.5.4 Nucleo-cytoplasmic Fractionation of Liver Proved the Localization of CBS and CRY1 at both Cytosol and Nucleus *in vivo*

After we detected CBS and CRY1 interaction in both cytosol and nucleus with Bi-FC (**Figure 5-20**), we aimed to show the localizations of both proteins in both cell compartments *in vivo*. Since both CBS and CRY1 are highly abundant in liver, we did fractionation assay in wild type mice livers. Mice livers were sent to us from our collaborators at University of Pennsylvania (UPENN) at -80 °C. Our collaborators entrained those wild type mice at 12:12 LD and sacrificed them at ZT10 and ZT22 time points which are through and peak points of CRY1 oscillation. We weighted the necessary amounts without melting the rest of the organ when needed. In the first step of the cell lysis, only cytosolic membranes should be disrupted, while the nuclear membranes need to stay intact. In order to achieve that, we used specific buffer and we optimized homogenization procedure. After centrifuge, we obtained supernatant as cytosolic fraction, and we further lysed the pellet which contains nucleus. At the end of the last centrifuge, we obtained the supernatant as the nuclear fraction.



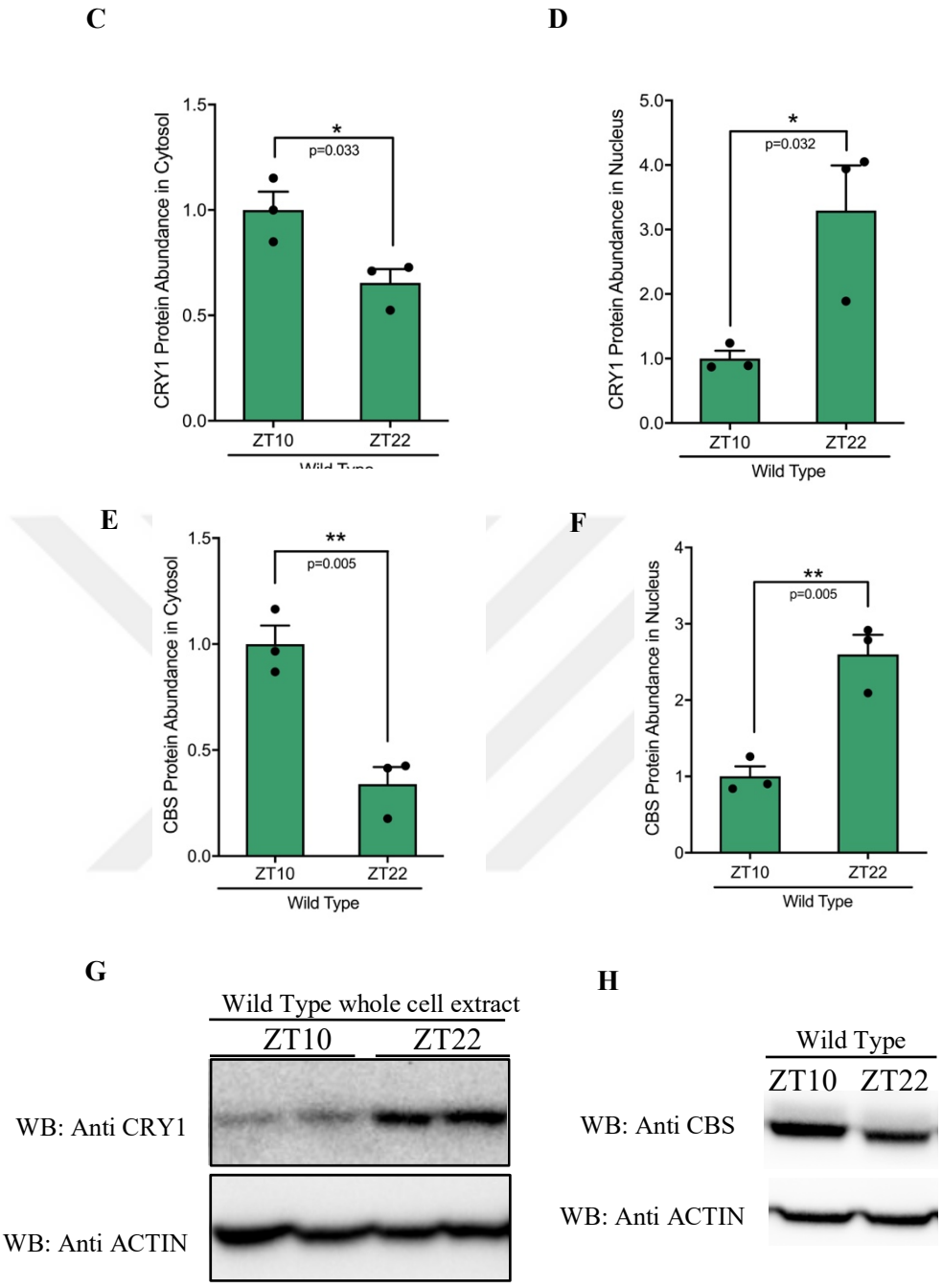


Figure 5-22: Cytosolic and nuclear fractions of mouse liver samples which were obtained at ZT10 and ZT22. Tubulin was used as cytosolic loading control, Histone-H3 was used as nuclear loading control. (A) Control of the success of fractionation experiment. Both tubulin and Histone-H3 was detected in both fractions. (B) Both CBS and CRY1 were detected in both fractions. (C) (D) Cytosolic and nuclear abundances of CRY1. (E) (F) Cytosolic and nuclear abundances of CBS. (G) CRY1 protein amounts at ZT10 and ZT22 in whole cell lysates. (H) CBS protein amounts at ZT10 and ZT22 in whole cell lysates.

We checked the success of our fractionation experiment by detecting both Tubulin and Histone-H3 in both fractions. As seen from **Figure 5-22A**, we successfully separated cytosolic and nuclear fractions. Then, we detected CBS and CRY1 in both fractions of samples from both time points (**Figure 5-22B**). Since the total CRY1 amount peaks at ZT22 (**Figure 5-22G**), that peak comes from its excess amount in nucleus at ZT22 (**Figure 5-22D**). Whereas in the cytosol, it peaks at the same time with CBS. If we focus on nucleus, even though total CBS peaks at ZT10, nuclear CBS peaks at ZT22 which is the nuclear and total CRY1 peak time.

Since CBS is an enzyme which converts cystathionine into cysteine in the cytosol and CRY1 is a transcription factor which works in the nucleus, these results leaded us to hypothesize that these two proteins might be affecting each other's activities. To test this hypothesis, we first analyzed the effect of CBS on the repression activity of CRY1 on BMAL1-CLOCK transactivation.

5.5.5 Disease causing CBS Mutation (I278T) Blocks CBS-CRY1 Interaction

Homocystinuria is a multi-system affecting syndrome which is caused by CBS deficiency. Mutations on CBS are inherited as autosomal recessive and reduces or inhibits the enzyme activity and causes defects at THF (tetra-hydro folate) and methyl cycles. These defects cause skeletal, muscular and vascular system problems, vision and mental retardations [128]. The most common mutation (25% of all mutations) which causes homocystinuria is Isoleucine-278 to Threonine mutation in humans [96]. Homo-oligomerization is important for CBS to bind its activator SAM (S-adenosyl-L-methionine) [129]. This mutation causes CBS loss of function by inhibiting its homo-tetramerization [130]. In order to investigate the relation of circadian clock and disease related effect of CBS on circadian clock, we first checked the interaction of CBS-I278T and CRY1 with mammalian-two hybrid assay (**Figure 5-23A**). Since mammalian-two hybrid is a method to screen interactions *in vitro*, we also applied co-immunoprecipitation to check the physical interaction. As seen from **Figure 5-23B**, while wild type CBS physically interacts with CRY1, disease causing mutant CBS doesn't interact with it. Bottom two panels shows the expressions of proteins in input samples. Anti-His blotting in input samples allows us to detect CRY1-His expression in the samples used for immunoprecipitation, while Anti-Flag in input samples shows the expressions of either wild type or mutant CBS in the same samples.

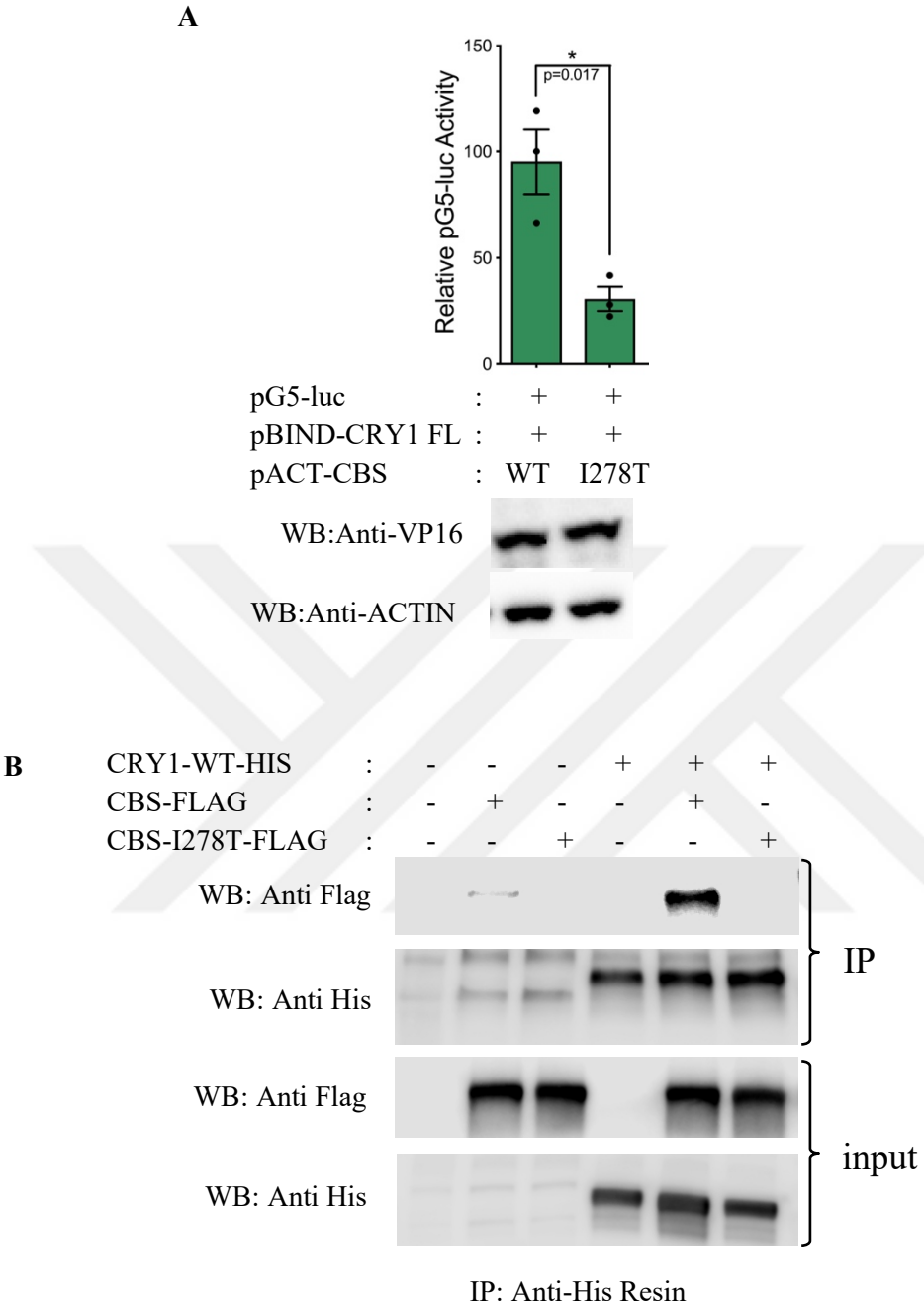


Figure 5-23: Disease causing mutation inhibits the interaction of CRY1 and CBS (A) Mammalian-two hybrid experiment showing significantly less interaction between CBS-I278T and CRY1. (B) Co-immunoprecipitation results showing the interaction between wild type CBS and CRY1 and disruption of the interaction between CBS-I278T and CRY1. Top two panels show the western blot of immunoprecipitation samples and bottom two panels show the western blot of the input samples.

Top two panels in **Figure 5-23B** shows the presence of either CBS (blotted with Anti-Flag) or CRY1 (blotted with Anti-His) in immunoprecipitation samples. Since the immunoprecipitation was achieved with Anti-His Resin, which allows us to pull down CRY1 in our case, all samples having CRY1 were detected with Anti-His antibody. In the top panel, Flag was detected only in the sample containing CRY1 and wild type CBS, but not in the samples containing CRY1 and CBS-I278T. Second and third rows contain only wild type CBS and CBS-I278T respectively, to show that flag tagged proteins cannot bind to His-resin themselves. As a result, disease causing CBS mutation inhibits the interaction between CRY1 and CBS.

5.6 Wild Type but Not Mutant CBS Enhances CRY1 Repression

In order to detect the dose dependent of CBS, we used Neuro-2A cell line which has significantly less amount of CBS endogenously (**Figure 5-24B**). The Per1:luc reporter assay is based on the luciferase production from Per1 promoter by BMAL1-CLOCK transactivation. Renilla-luciferase was used for transfection and cell number normalization as we did in mammalian two hybrid assay.

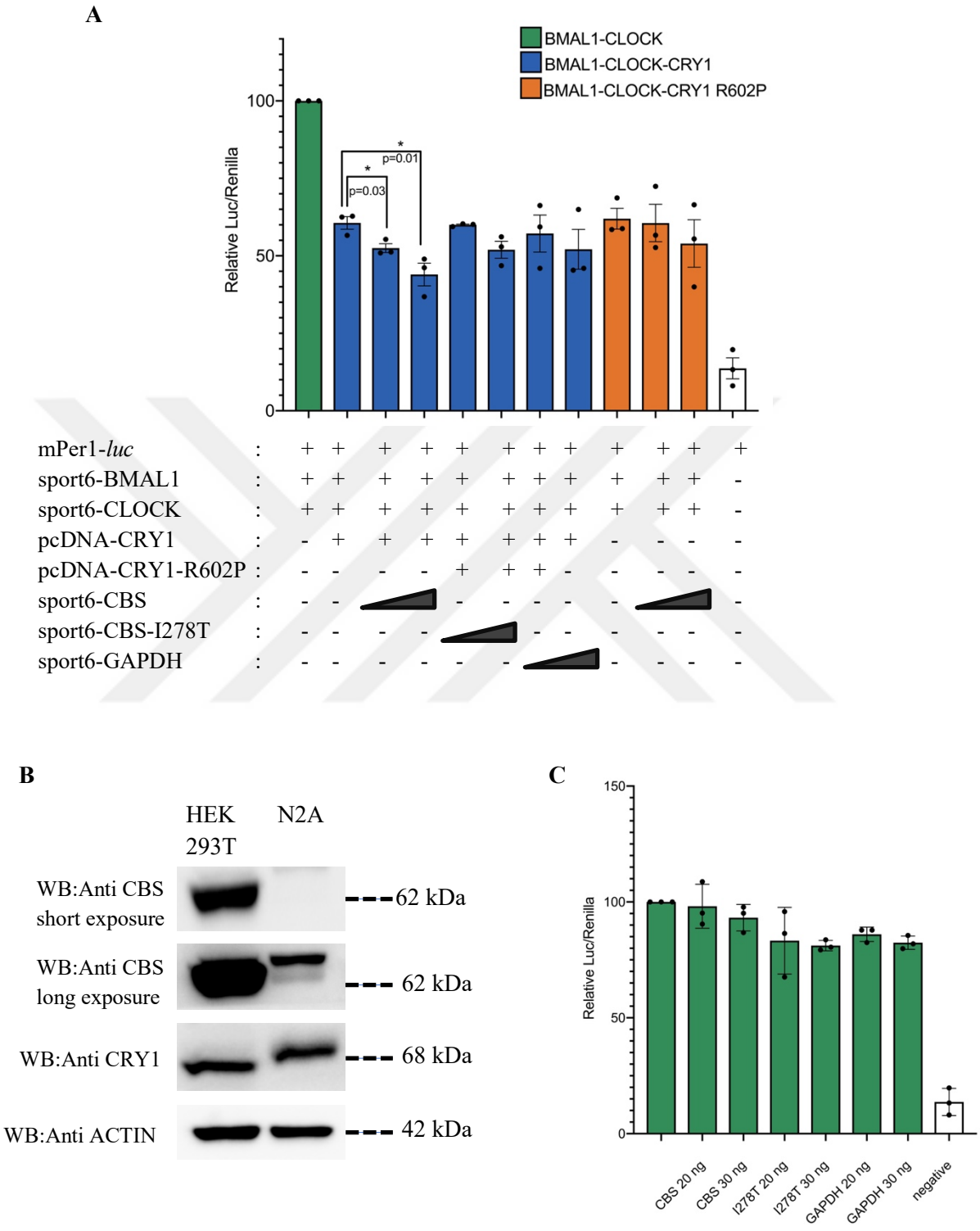


Figure 5-24: Analysis of the effect of CBS on the repression activity of CRY1. (A) Per1:luc reporter assay analyzing the effect of CBS on CRY1's repression activity on BMAL1-CLOCK transactivation. (B) CBS and CRY1 protein amounts in HEK293T and Neuro-2A cell lines. (C) The effects of CBS-WT, CBS-I278T and GAPDH on BMAL1-CLOCK transactivation, in the absence of CRYs.

Renilla normalized luciferase activity by BMAL1-CLOCK transactivation on Per1 promoter is shown as 100 folds in **Figure 5-24A.** We added 3 ng of CRY1 plasmid which represses BMAL1-CLOCK transactivation around 40 percent. Only wild type CBS, but not CBS-I278T, is able to increase the repression activity of CRY1. This effect is clearly seen as a dose dependent manner since we used 20 and 30 ng of CBS. We used GAPDH in the same vector backbone and proved that this effect is not an artifact of the assay because GAPDH cannot increase the CRY1 repression activity.

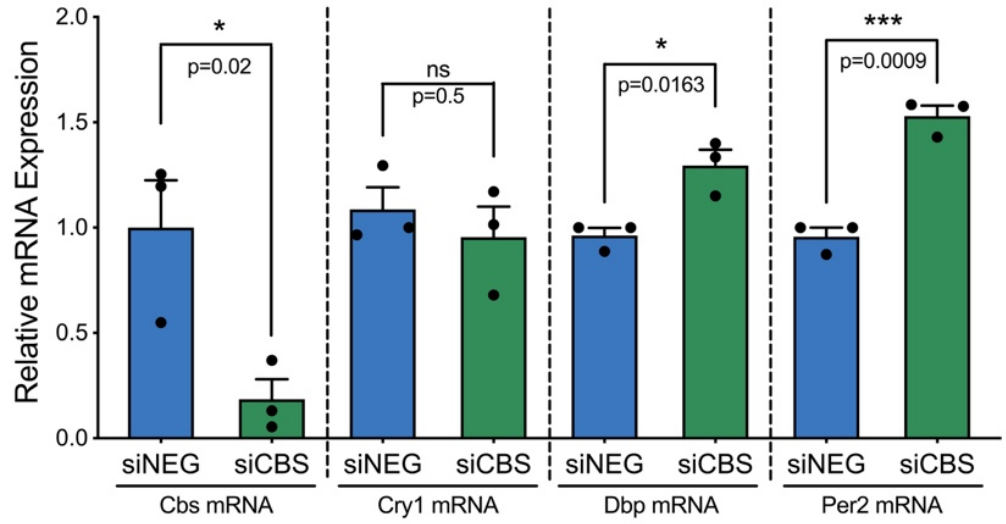


Figure 5-25: mRNA levels of Dbp and Per2 in Cbs knocked-down samples.

Since CBS increases the repression activity of CRY1, we aimed to show the effect of CBS absence on the expression of E-Box output genes. In order to do that, we knocked-down CBS in U2-OS cells and checked the mRNA levels of *Cry1*, *Dbp*, and *Per2*. As seen from **Figure 5-25**, even though the mRNA expression of *Cry1* doesn't change, *Dbp* and *Per2* mRNA levels increases in the absence of *Cbs*. Reduced CBS in the cells caused reduction in the repression activity of CRY1 which leaded the increase in E-Box output genes *Dbp* and *Per2*. We also verified this result *in vivo*. $Cbs^{+/-}$ animals were obtained from Warren Kruger's lab and they were crossed with their siblings to generate $Cbs^{-/-}$. We abbreviate these mice as $Cbs^{-/-}$. We extracted protein lysate from their liver and verified that CRY1 protein level doesn't change (**Figure 5-26A and B**). Even though CRY1 protein level remains same, mRNA of *Dbp* and *Per2* were increased as the result of decreased repression activity of CRY1 (**Figure 5-26C**).

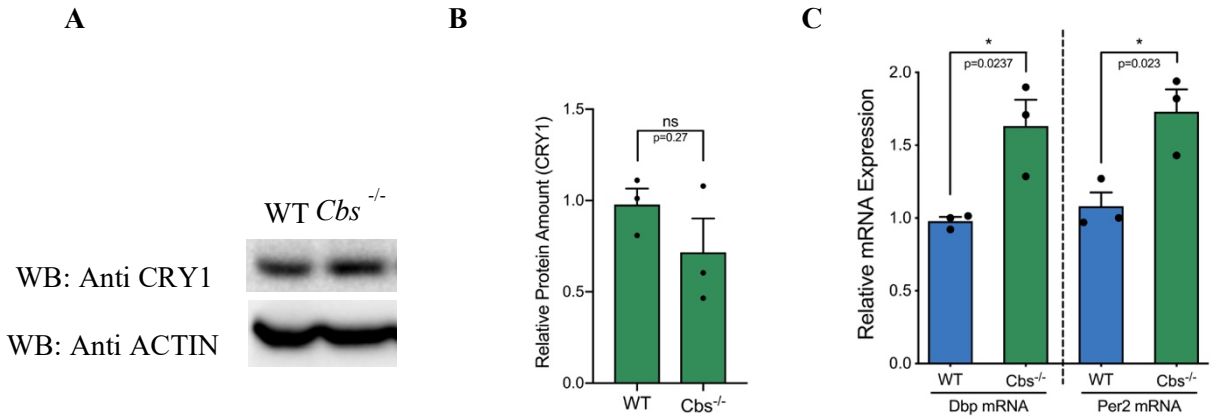


Figure 5-26: Change in the output of E-box promoters in Cbs knock out liver samples. (A) (B) CRY1 protein amount in *Cbs*$^{-/-}$ liver samples and their quantifications. (C) Dbp and Per2 mRNA levels in CBS knock out liver samples.

As a result, we showed that CBS increases the repression activity of CRY1, and absence of CBS increases the E-box output gene expression *in vitro* and *in vivo*. These results prove that; wild type CBS enhances the CRY1 repression activity, while disease-causing mutation on CBS cannot do the same. We verified this effect by showing the increased expression of *Dbp* and *Per2* in the absence of CBS.

5.7 CRY1 is Increasing the Enzymatic Activity of CBS in Liver

Up to this point; we have showed that CBS and CRY1 interact, CBS increases the repression activity of CRY1. Since these two proteins interact, we claimed that CRY1 might regulate the CBS enzyme activity as a reciprocal regulatory mechanism. In order to understand that, we checked the CBS enzyme activity in CRY1 knock-out mouse livers. In order to measure the CBS enzyme activity, we utilized a colorimetric assay which measures the production of H_2S. There are three different enzymes in liver which regulates H_2S production in liver. Cystathionine-γ-lyase (CSE) and 3-mercaptopyruvate sulfurtransferase (MST) are other two enzymes which regulate liver metabolism by contributing to H_2S production. However, substrate of MST is different than CBS and CSE substrate and it is not the main contributor for H_2S production [131]. Since CSE produces H2S by using the same substrate, we used CSE-specific pharmacological inhibitor to measure CBS-produced H_2S in our colorimetric assay [132]. The dose of CSE-inhibitor PAG (DL-propargylglycine) was determined by detecting H_2S production in *Cbs*$^{-/-}$ mouse liver. As **Figure 5-27C** indicates, when we add 30 mM PAG, we inhibit more than 70% of CSE activity in the sample.

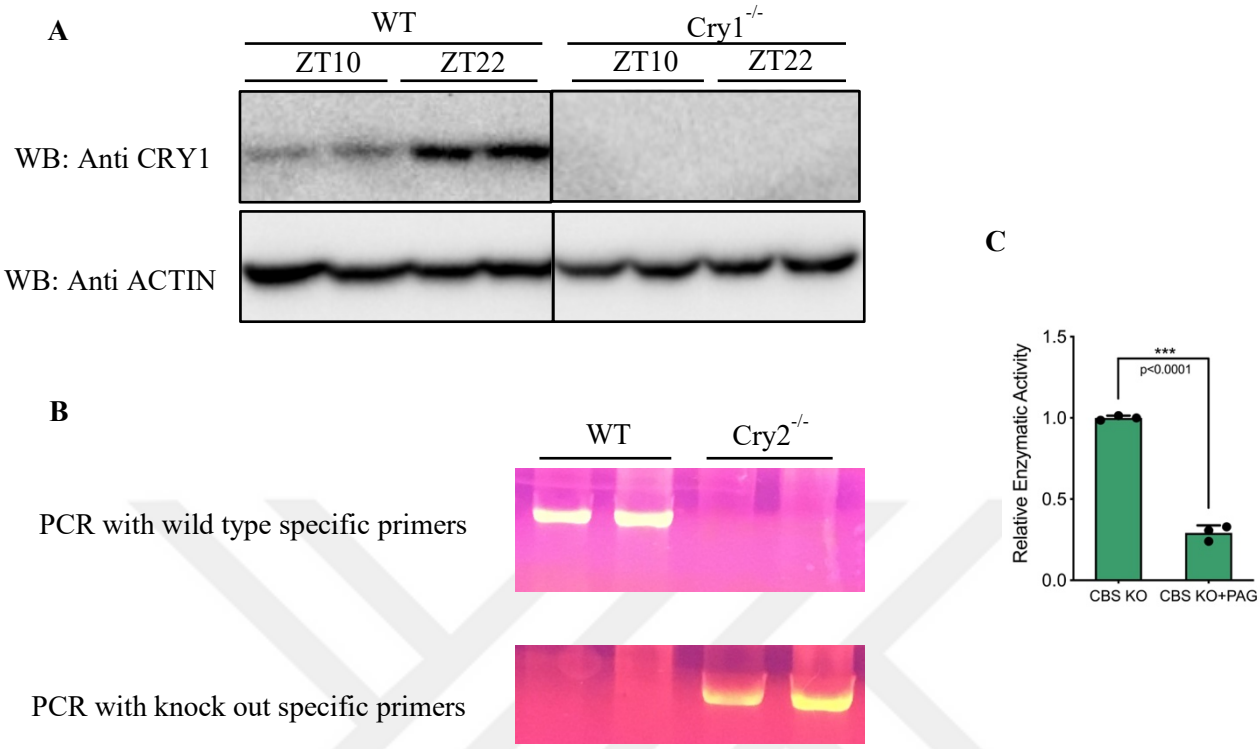


Figure 5-27: (A) Cry1$^{-/-}$ genotype verification by western blot and CRY1 total abundance verification at ZT10 and ZT22. (B) Cry2$^{-/-}$ genotype verification by PCR. (C) Inhibition of CSE activity in Cbs-/- liver samples by 30 mM PAG.

Cry1$^{-/-}$, *Cry2*$^{-/-}$ and wild type mice were entrained with 12:12 light:dark cycle and sacrificed and liver samples were collected at ZT10 and ZT22 where total CRY1 protein amount is at its peak and through respectively (**Figure 5-27A**). Mouse experiment and organ collections were performed by our collaborators at University of Pennsylvania (UPENN) and they sent us the liver samples for further assays. We firstly verified the genotypes with either western blot or PCR. *Cry1*$^{-/-}$ genotype verification was performed by western blot at both ZT10 and ZT22. Total protein lysates were prepared from liver samples by using RIPA buffer and 4x SDS-PAGE loading dye. Gel was blotted with CRY1 and Actin antibodies. On the other hand, *Cry2*$^{-/-}$ genotype was verified with PCR by using wild type and mutant specific PCR primers (**Figure 5-27A and B**).

After mouse genotype verifications, we prepared total cell lysate under native conditions for CBS activity detection. In our system, we placed an inner tube inside of a bigger tube as our closed system. H_2S is a gaseous molecule which leads sulfide oxidation when there is oxygen around [133]. Because of that, we replaced O_2 by sending N_2 into the system, then we blocked the gas traffic by sealing the system. **Figure 5-28** represents the enzyme activity detection system setup. Reaction mix contains the soluble protein lysate from mouse liver, CBS substrate (L-cysteine), CBS co-factor PLP (pyridoxal 5-phosphate) [134], and PAG [132]. The inner tube was isolated from the reaction mix, which contained cotton with zinc acetate (ZnAc) to capture H_2S. At the end of 1.5-hour incubation at 37 °C, we added 50% trichloroacetic acid into the reaction mix to degrade the proteins and stop the reaction. As the last step, we took out the cotton and used the trapped H_2S to perform methylene blue production.

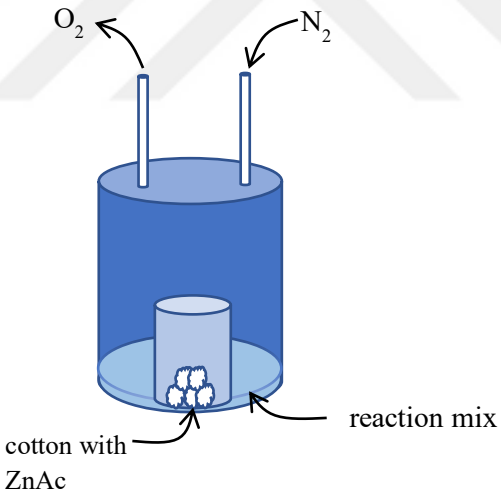


Figure 5-28: CBS activity detection system setup.

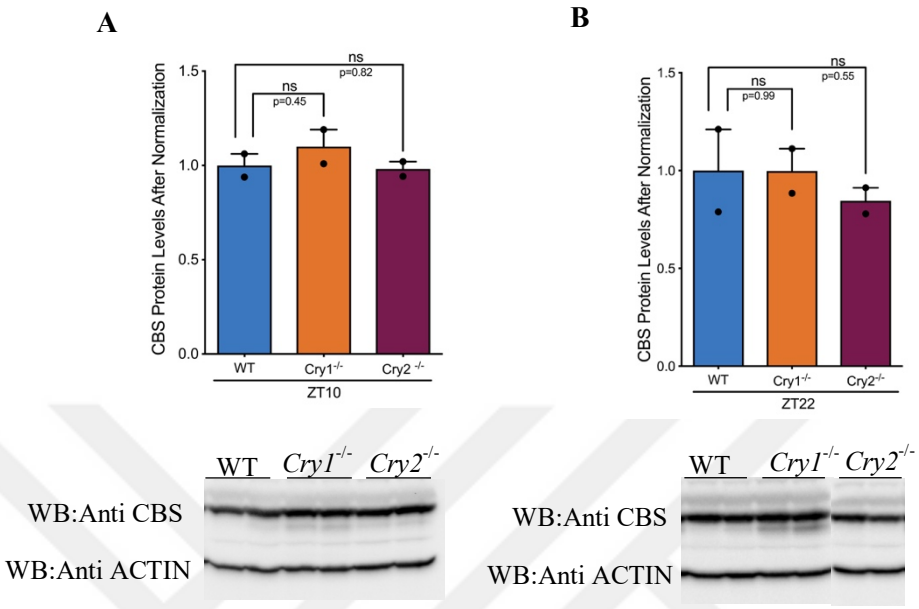


Figure 5-29: CBS protein levels in the samples used in enzyme activity detection experiments at ZT10 and ZT22.

As seen from **Figure 5-30A and C**, CBS activity is reduced in *Cry1*$^{-/-}$ samples while the activity increases in *Cry2*$^{-/-}$ samples which has more CRY1 protein than wild type samples (**Figure 5-30B and D**). After lysate preparation, we checked the CBS protein levels with western blot and diluted the samples to have equal CBS amounts in each sample. Right before starting the activity assay, we saved some protein samples to verify their CBS protein content. **Figure 5-29A and B** shows the western blot quantification results of the equal CBS amounts in the assay samples at ZT10 and ZT22, respectively.

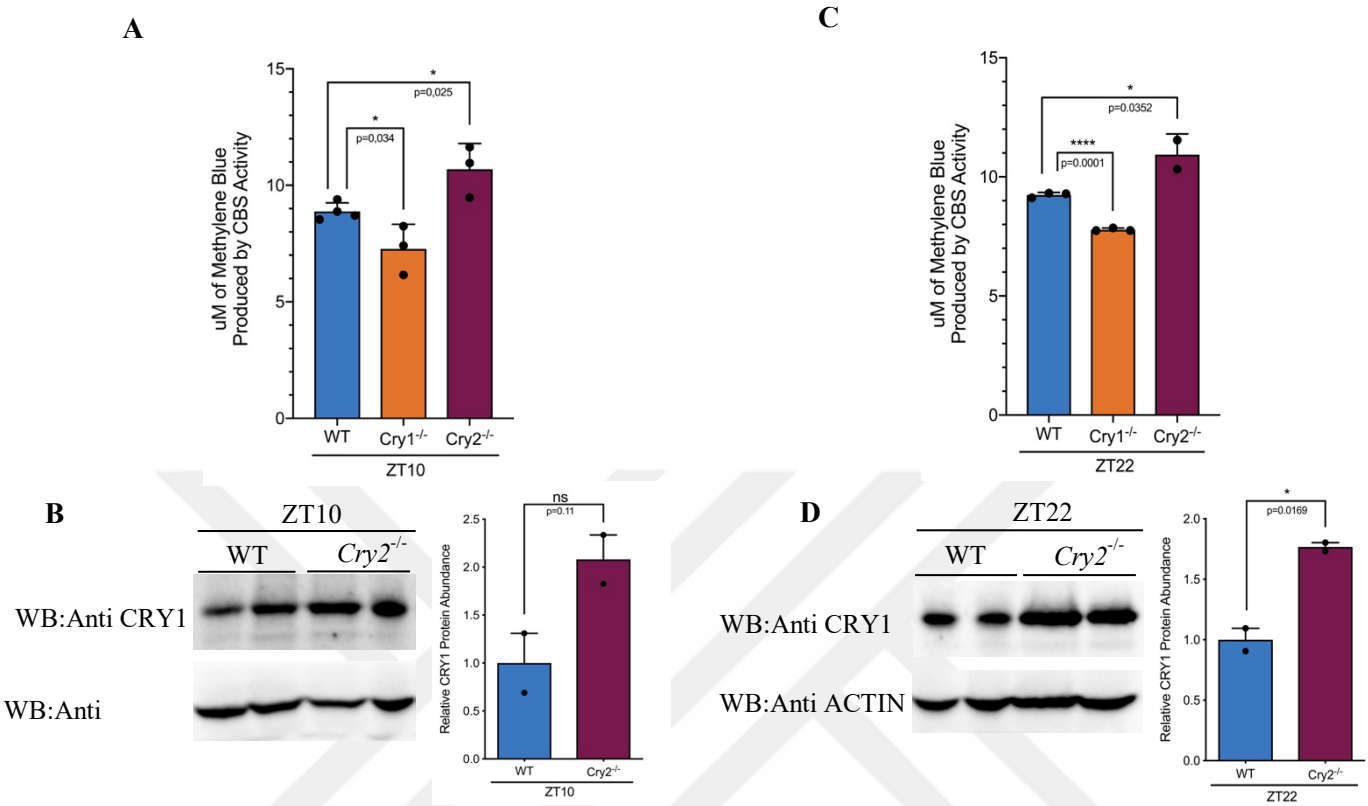


Figure 5-30: Analysis of the effect of CRY1 and CRY2 absence on the enzyme activity of CBS. (A) (C) CBS enzyme activity change in CRY1 knock out and CRY2 knock out mouse liver samples at ZT10 and ZT22. (B) (D) CRY1 protein amounts in CRY2 knock out samples at ZT10 and ZT22 with their quantifications.

To verify that the real reason behind the decreased CBS activity in *Cry1*$^{-/-}$ liver samples, we applied complementation assay by supplementing the *Cry1*$^{-/-}$ liver extracts with *in vitro* over expressed CRY1. In this assay, we extracted protein samples from *Cry1*$^{-/-}$ liver samples as performed in the enzyme activity detection assay as performed in **Figure 5-28**. In order to complement the reduced enzyme activity in *Cry1*$^{-/-}$ liver samples we added wild type CRY1, R602P mutant CRY1 and T1 truncated CRY1 which we overexpressed in HEK293T cells.

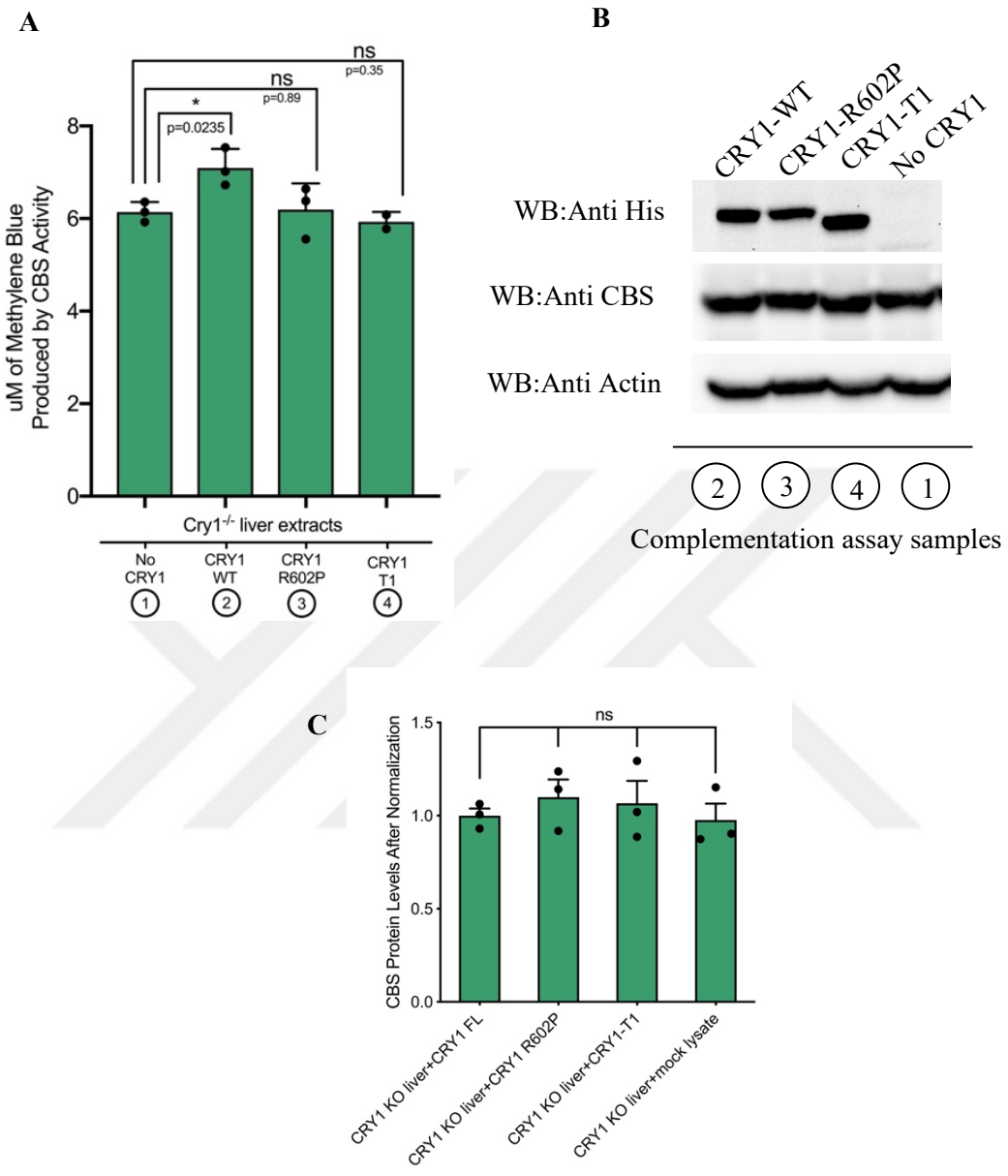


Figure 5-31: (A) Complementation assay showing the increase in the CBS enzyme activity in the presence of CRY1-WT in Cry1-/- liver samples. (B) CBS and CRY1 protein amounts in the assay samples. (C) CBS protein level quantification in complementation assay samples.

Figure 5-31A shows that only the wild type CRY1 was able to complement the decreased CBS activity in in *Cry1*$^{-/-}$ liver samples. The comparable expressions of different CRY1 versions and equal CBS amounts in the assay samples were shown in **Figure 5-29**.
Thus, these results show that the absence of CRY1 reduces the CBS activity and this reduction is only complemented by wild-type CRY1. The activity of CBS is highly correlated with its homo-tetramerization [129]. To further analyze the CBS activity regulation mechanism of CRY1, we analyzed the effect of CRY1 on homo-tetramerization of CBS in the following experiments.

5.8 CRY1 Favors the Homo-Tetramerization of CBS by Enhancing Its Enzyme Activity

Homo-tetramerization of CBS is one of the key factors of its enzyme activity. Loss of oligomerization directly causes loss-of activity. We see this in disease-causing mutations. If the mutation reduces homo-tetramerization or causes no homo-tetramerization, that mutation either reduces the enzyme activity, or causes total loss-of-function [130]. In order to further investigate the mechanism of the enzyme activity increasing effect of CRY1, we detected the oligomerization pattern of CBS in the presence of either CRY1-WT or CRY1-R602P. We overexpressed either GFP, CRY1-WT or CRY1-R602P in HEK293T cells and prepared the total protein samples under non-reducing conditions. We used the samples to run in native-PAGE to separate them based on their secondary structures. We used BSA which forms oligomers as our ladder.

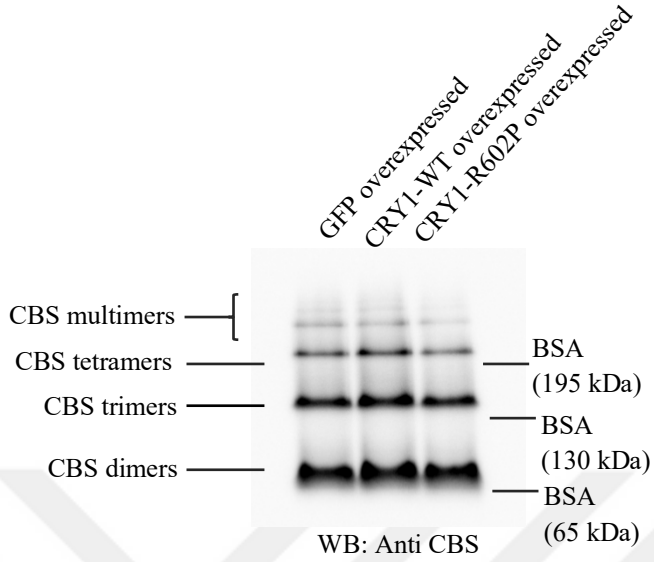


Figure 5-32: Native-PAGE showing homo-oligomers of CBS when either GFP, CRY1-WT or CRY1-R602P was overexpressed in HEK293T cells.

We quantified each band by dividing them to total protein amounts in each well. When we quantify the native-PAGE result in **Figure 5-32**, we showed that CBS tetramer amount significantly increases in the presence of CRY1-WT, not by CRY1-R602P. When CRY1 favoring the tetramer formation, we can clearly see that dimers are reduced at the same time. Since tetramer is the more active form of CBS, we conclude that CRY1 binds to CBS dimers and favors them to form tetramers and results in more active CBS *in vitro* (**Figure 5-33**). Blue-native PAGE assay allowed us to determine the mechanism how CRY1 increases the enzyme activity of CBS which is homo-tetramer form increase. CRY1-R602P used as non-CBS binding control and it cannot increase the homo-tetramer form of CBS.

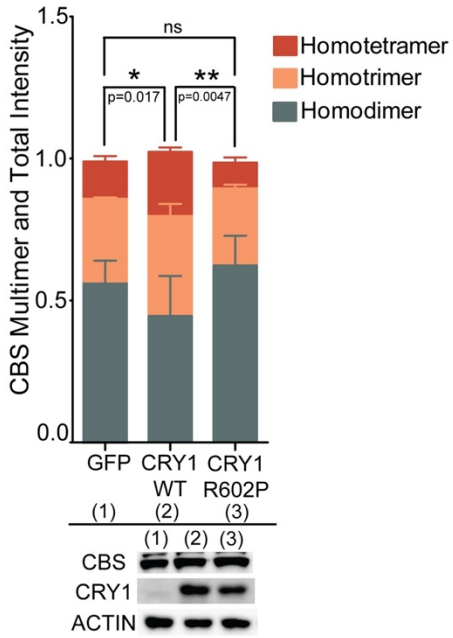


Figure 5-33: Quantification of Native-PAGE showing increased tetramer amount of CBS by only CRY1-WT. The below SDS-PAGE followed by western blot shows comparable expressions of CBS, CRY1 and ACTIN under reducing conditions.

5.9 Absences of CBS and CRY1 Affects the Same Pathways in Mouse Liver

CBS utilizes serine and homocysteine and produces cystathionine as a part of transsulfuration pathway [135]. Transsulfuration pathway is directly connected to oxidative stress response pathway and methyl cycle. Reduced CBS protein expression or enzyme activity decreases SAM/SAH and increases homocysteine levels in serum samples [136]. In order to have better understanding about the effect of CBS deficiency on metabolism, we applied untargeted metabolomics screen in *Cbs*$^{-/-}$ mouse liver samples. In order to compare the effects of CBS deficiency and CRY1 deficiency/increase, we also applied untargeted metabolomics screen in *Cry1*$^{-/-}$ and *Cry2*$^{-/-}$ mouse liver samples. We aimed to detect the affected metabolites and pathways to be similar in the cases of CBS and CRY1 deficiencies, since we hypothesized that CRY1 regulates the metabolism through its interaction with CBS. Affected metabolites in *Cry1*$^{-/-}$ and *Cry2*$^{-/-}$ samples were compared with their wild type littermate controls. Individual metabolite change results were shown in **Figure 5-34** to **Figure 5-36**.

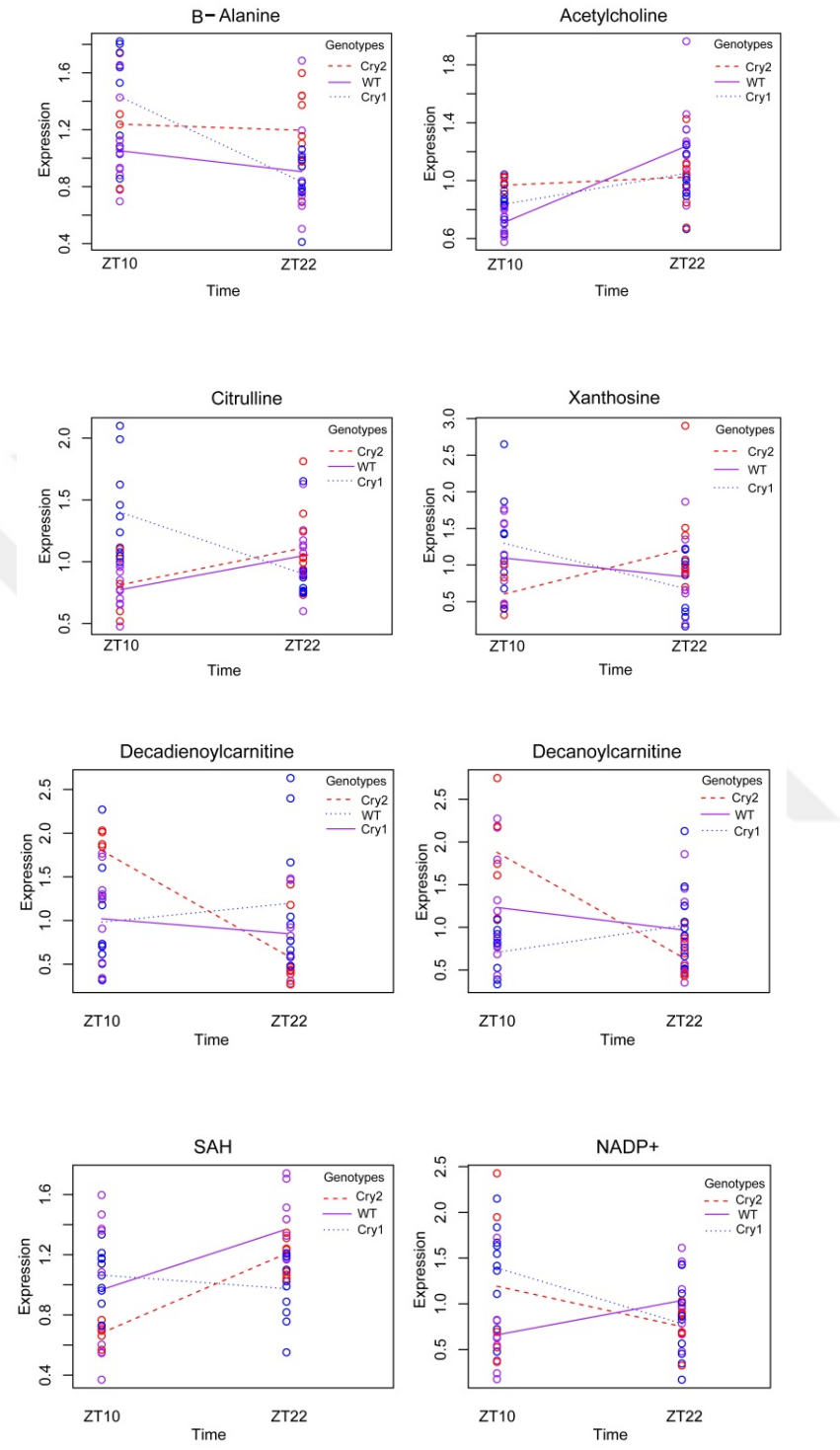


Figure 5-34: Metabolites significantly affected by the absence of either CRY1 or CRY2, compared by their wild type littermate controls.

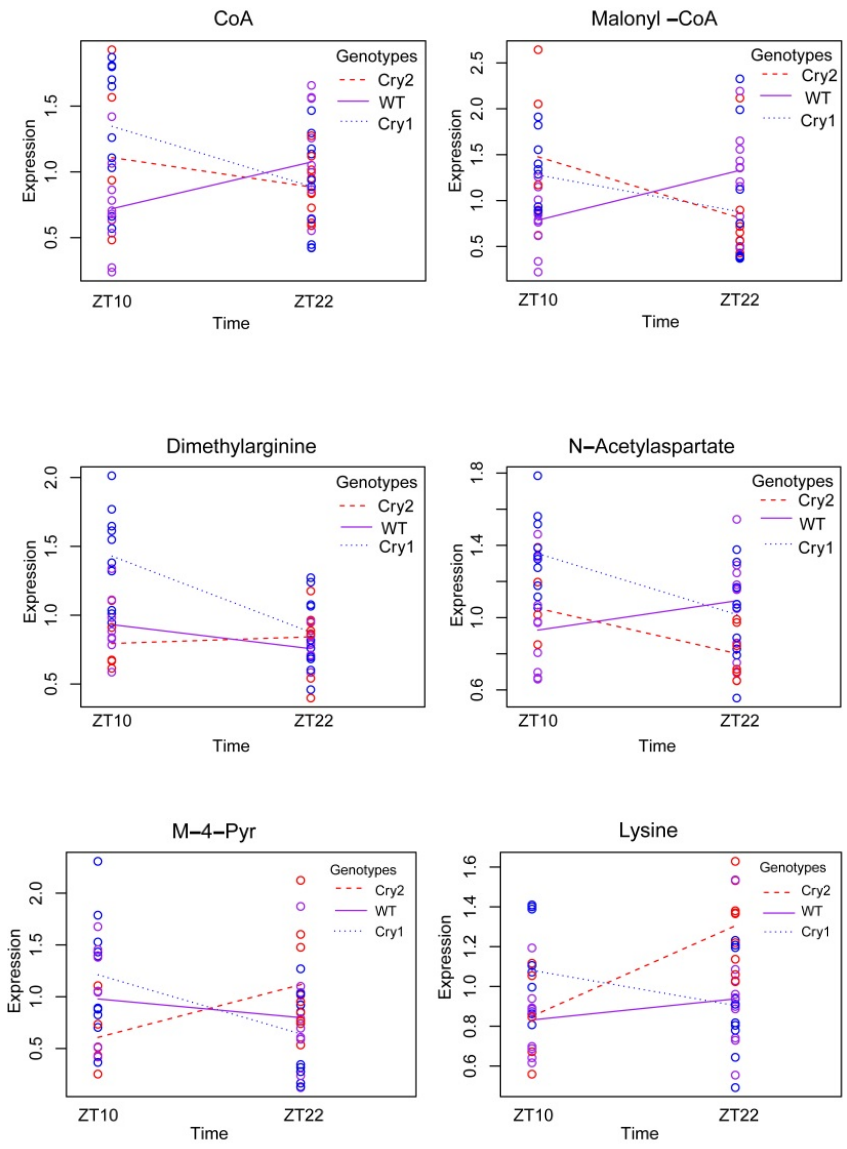


Figure 5-35: Metabolites significantly affected by the absence of either CRY1 or CRY2, compared by their wild type littermate controls.

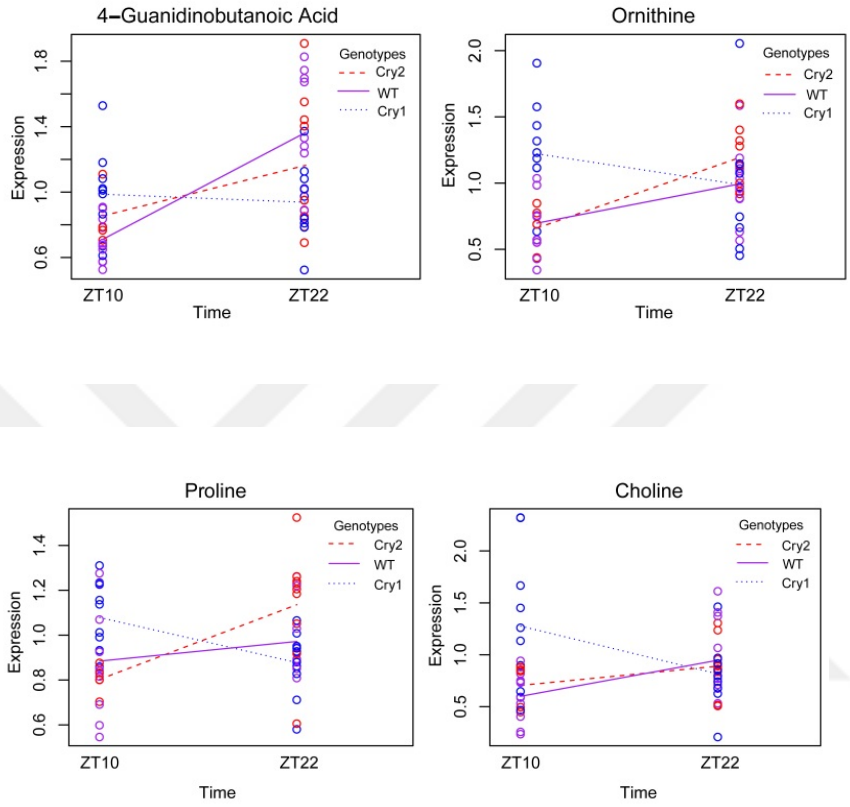


Figure 5-36: Metabolites significantly affected by the absence of either CRY1 or CRY2, compared by their wild type littermate controls.

50 mg liver tissue was used for metabolite extraction experiments. Metabolite extraction step was achieved by using Bligh and Dyer method. In this method, samples were mixed with methanol:chloroform (2:1). Vortex and sonication were applied to dissolve the tissues. Centrifugation were used to separate aqueous and organic layers. Aqueous layers were vacuum-dried and resolved in acetonitrile:water (2:1) for LC-MS (liquid chromatography-mass spectrometry) analysis.

QC (quality control) samples were used to normalize metabolite levels in each sample. Since *Cbs*$^{-/-}$ samples were collected only at one time point (ZT12), two-factor ANOVA for gender and genotype analysis was used for *Cbs*$^{-/-}$ samples. On the other hand, three factor ANOVA was used for *Cry*$^{-/-}$ samples for gender, genotype and time interaction analysis. **Figure 5-37** shows the metabolites significantly affected by gender, genotype and time interaction for *Cry*$^{-/-}$ samples. B-alanine, acetyl choline, citrulline, xhantosine, decadienoylcarnitine, decanoylcarnitine, SAH, NADP+, CoA, Malonyl-CoA, dimethylarginine, N-Acetylaspartate, M-4-Pyr, Lysine, 4-Guanobutiric acid, ornithine, proline and choline are the metabolites affected by cryptochrome 1 and 2 protein deficiency. In these metabolite levels, we clearly see opposite patterns in *Cry1*$^{-/-}$ and *Cry2*$^{-/-}$ samples which further confirms that while CRY1 deficiency reduces CBS activity, more CRY1 (in *Cry2*$^{-/-}$ samples **Figure 5-30 B and D**) increases CBS activity in liver samples. The results of the same metabolomics analysis for *Cbs*$^{-/-}$ samples were represented in page 120. As expected, more metabolites were significantly affected by CBS deficiency. To provide better understanding about which metabolite is in which pathway, and which pathways are affected by both CBS and CRY1 deficiency, **Figure 6-2** was drawn by highlighting CRY1 affected and CBS affected metabolites. Dimethylglycine/2−aminobutyrate, creatinine, acetylglycine, phenylacetylglycine, 3-Methylcrotonylglycine, creatine, homocysteine, cystathionine, SAH, SAM, methionine, aminobenzoates, nicotinamide oxide, acetylserine, guanine, M-2-Pyr, M-4-Pyr, indole-3-carboxylic acid, 1-methyl-histidine, arginine, dimethylarginine, tryptophan, glycine, N2-acetyllysine, phosphoserine, N-acetylaspartate, 3-methyl-histidine, methyl-histidine, trans-4 hydroxyproline, amino sugars, monosaccharide, phosphocholine, N6-acetlyllysine, carnitine, acetylcarnitine, lipoamide, propenoylcarnitine, valerylcarnitine, hydroxyhexanoylcarnitine, octanoylcarnitine, hydroxyhexadecanoylcarnitine, 3-hydroxyisovalerylcarnitine, N-acetyl-tyrosine, cytidine, uridine, uracil, adenine, adenosine, methyl adenosine, 5-methylthioadenosine, dCMP, UMP, CMP, UDP, GDP, AMP, dAMP, cAMP, nicotinamide ribotide, inosine, deoxyinosine, daidzein, CDP-choline, N1-methylnicotinamide, NAD+, NADH, CoA, Acetyl-CoA, Succinyl-CoA, glutathione reduced, glutamate, kynurenine, kynurenic acid, allantoate, ornithine, acetylornithine, betaine, valine, 2-aminoadipate, xanthine, hypoxanthine, oxaloacetate, malate, sorbitol/mannitol, 4-guanidinobutanoic acid, ureidopropionate levels are significantly affected by CBS absence.

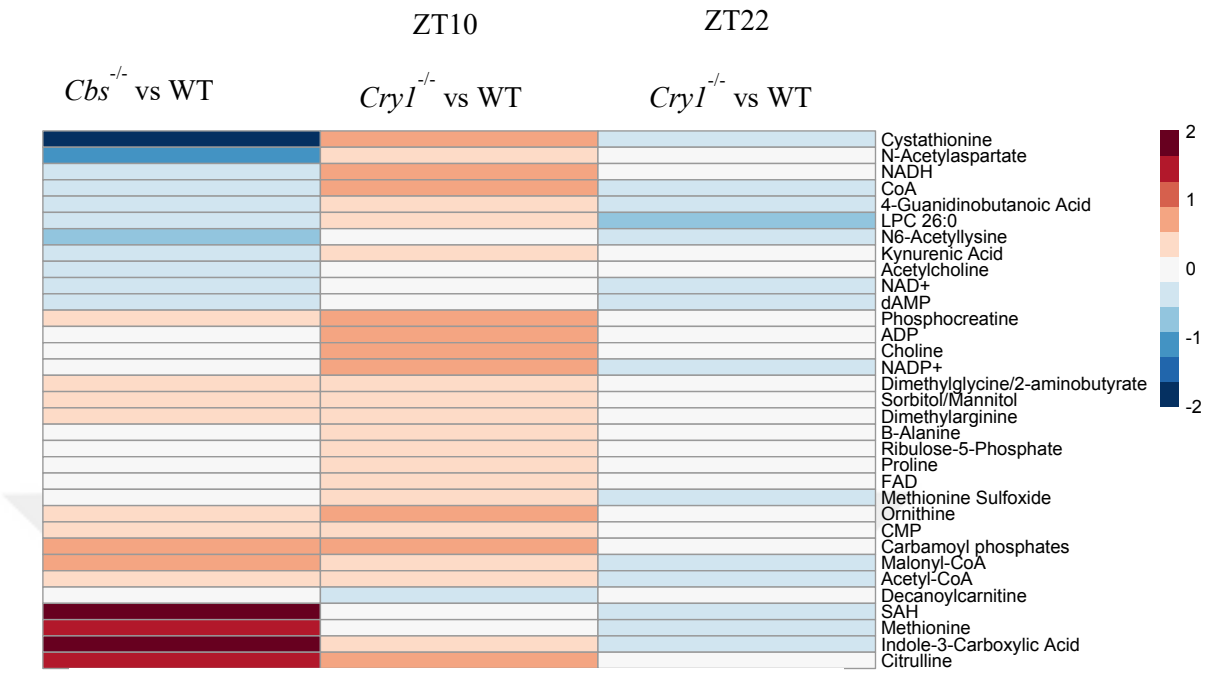


Figure 5-37: Heatmap representing the significance of metabolites in both CBS absence, and CRY1 absence compared to their wild type littermate control.

Figure 5-37 shows the heatmap of the interaction between CBS and CRY1 genotypes. CRY1 genotype analysis shown as two different time points representing peak and through points of CRY1 protein levels (ZT22 and ZT10 respectively). Effect of CRY1 on the same metabolites regulated by CBS detected more significant at ZT22, where total cellular CRY1 is at its peak. In order to show the pathways regulated by the genotypes investigated, Metaboanalyst software was used to apply KEGG pathway analysis. **Figure 5-38A and B** clarifies that cysteine and methionine metabolism was significantly controlled by both CBS and CRY genotypes. Network centrality was used to detect the affected pathways. As further proving our hypothesis, important changes occurred in the same pathways which are cysteine and methionine metabolism and arginine and proline metabolism.

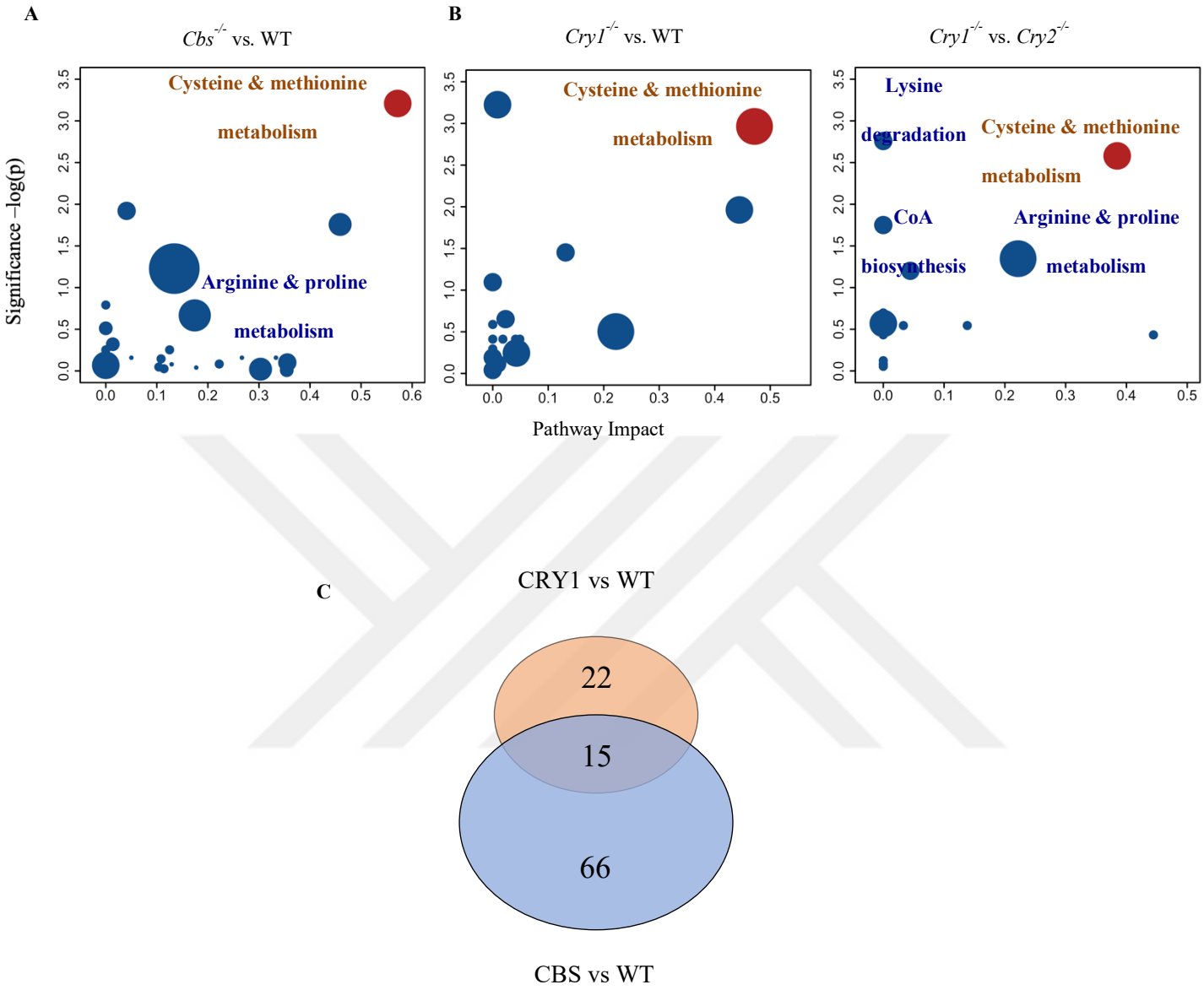


Figure 5-38: Pathways significantly affected by the absence of **(A)** CBS, and **(B)** CRY1 and CRY2. **(C)** 15 out of 37 metabolites are same with the metabolites affected by CBS absence.

Figure 5-38C shows the number of metabolites affected by either CRY1 or CBS absence. More than half of the metabolites regulated by CRY1 are the same metabolites regulated by CBS. These data further support our hypothesis that CRY1 regulates metabolism through its interaction with CBS.

5.10 Analysis of the Effects of CBS and CRY1 Absences on DNA and RNA Methylations

In our study, we proved that CRY1 and CBS physically interacts at both cytosol and nucleus and they regulate the activities of each other. While CBS increases CRY1 repressive function, CRY1 favors the homo-tetramerization and increases CBS enzyme activity. We also showed that these two proteins regulate the same pathways in the metabolism which further proves our findings. Since methyl cycle is one of the most affected pathways by both CRY1 and CBS, we aimed to determine total DNA and RNA methylation statuses in MEF cells. DNA methylation is one of the ways of cells to control gene expression in an inheritable way [137]. There are many different kinds of DNA methylation such as 5-mC (5-methyl cytosine, 5hmC (5-hydroxymethylcytosine), 5fC (5-formylcytosine), 5caC (5-carboxylcytosine), 5hmU (5-hydroxymethyluracil) and 6mA (n6-methyladenine). These methylations have distinct features regulating cell homeostasis and differential gene expressions in different tissues. While 5fc recruits DNA repair machinery to the genome, 6mA regulates nucleosome positioning and correlates with H3K4-methylation. 5-mC DNA methylation highly occurs in active gene bodies and promotes binding of specific proteins [138].

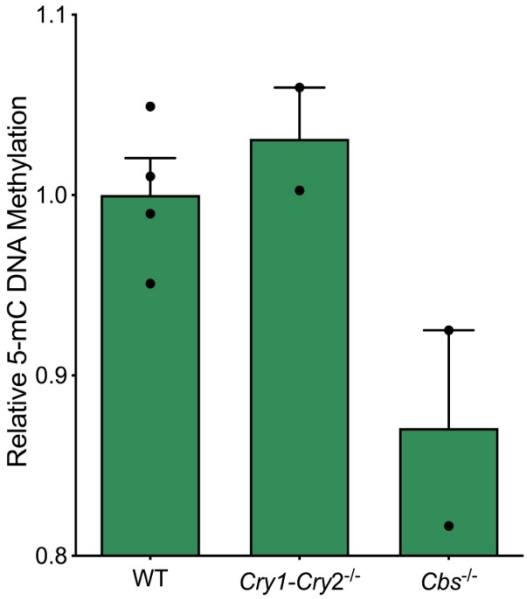


Figure 5-39: 5-mC total DNA methylation in wild type, Cry1 and Cry2$^{-/-}$ and Cbs$^{-/-}$ MEF cells. There is no significant difference between samples.

Changes in DNA methylation levels also related with metabolism. Studies showed that over alcohol consumption changes 5-mC DNA methylation in specific gene promoters regulating addictive behavior [139]. Also, in some genetic conditions leading excess DNA methylation causes DNA methylation at the promoter regions of tumor suppressor genes resulting in repression of tumor suppressor genes and oncogenesis [140]. In order to investigate DNA methylation status, we used Cry1-Cry2 knock-out, Cbs knock-out and their wild type controls. Cells were seeded in 10-cm dishes and collected when they reach to confluency. Collected cells were analyzed for their total 5-mC DNA methylation. As seen in **Figure 5-39**, neither *Cry1-Cry2*$^{-/-}$, nor *Cbs*$^{-/-}$ cells did not show any different 5-mC DNA methylation levels.

After seeing no DNA methylation change in *Cry1-Cry2*$^{-/-}$ and *Cbs*$^{-/-}$, we aimed to detect the RNA methylation in the same cell lines. Even though there are more than 100 RNA modifications regulating gene expression at post-transcriptional level, N6-methyladenosine is one of the most abundant RNA modifications [141] [142]. There are writers (METTL3 (methyltransferase like3), METTL14 (methyltransferase like 14), METTL16 (methyltransferase like 16)), readers (YTHDC1 (YTH domain containing protein-1), HNRNP (heterogeneous ribonucleoprotein particle), YTHDF1 (YTH domain containing family protein-1)), and erasers (FTO (fat mass and obesity associated protein), ALKBH5 (AlkB homolog 5)) to regulate cancer progression and metabolism in cells [143]. In 2013, Jean-Michel Fustin and his colleagues showed that circadian clock is affected by global m6-A RNA methylation changes in cells and methylation disruption inhibits RNA processing of circadian clock genes [67]. In order to detect m6-A RNA methylation in *Cry1-Cry2*$^{-/-}$ and *Cbs* $^{-/-}$ cells, we used EpiQuick m6-A RNA methylation Quantification Kit [144]. Total RNA was isolated from the samples with Qiagen RNA Isolation Kit. 200 ng total RNA was used to detect m6-A RNA quantification. After binding of the RNA to assay wells and several wash steps, color was developed and measured with Bio-Tek Synergy Instrument.

As seen in **Figure 5-40**, while m6-A RNA methylation is significantly lower in *Cry1-Cry2*$^{-/-}$ cells, it is significantly higher in *Cbs*$^{-/-}$ cells. Even though CRY1 and CBS do not regulate DNA methylation, their absence significantly affects m6-A RNA methylation in cells. After detecting their effect in vitro, we aimed to detect their effect in mouse liver samples that we used for metabolomics analyses. RNA methylation analysis in liver samples will allow us to determine de effect of CRY1 specifically, because we used Cry1-Cry2 knock-out cell line.

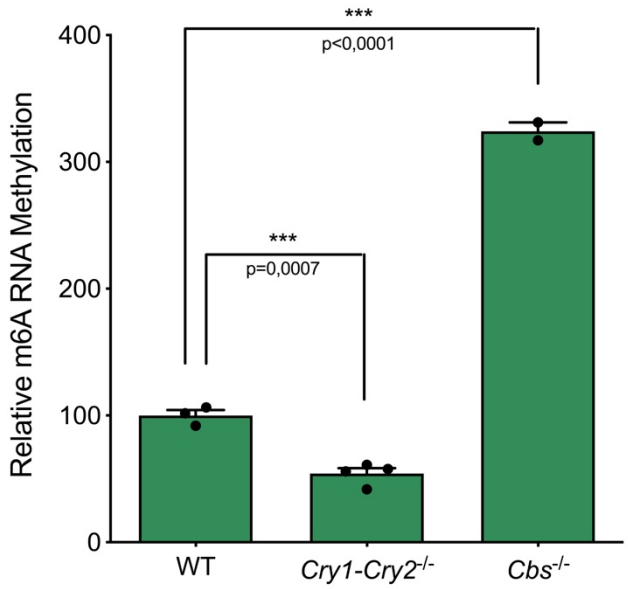


Figure 5-40: m6-A RNA methylation level of Cry1-Cry2$^{-/-}$ and Cbs$^{-/-}$ MEF cells compared with wild type.

Same method was applied to detect m6-A RNA methylation in liver samples belong to *Cry1*$^{-/-}$, *Cry2*$^{-/-}$ and *Cbs*$^{-/-}$ mouse livers. **Figure 5-41** shows the m6-A RNA methylation levels in the absence of CRY1, CRY2 and CBS respectively.

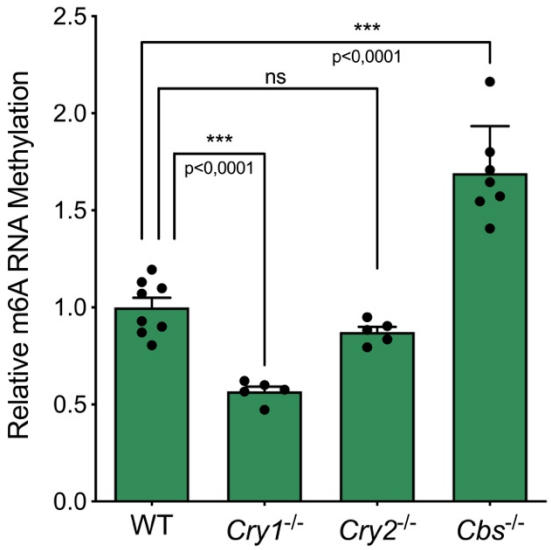


Figure 5-41: m6-A RNA methylation level of Cry1$^{-/-}$, Cry2$^{-/-}$ and Cbs$^{-/-}$ mouse liver samples compared with wild type.

Consistent with cell line results, total m6-A RNA methylation level decreases in the absence of CRY1. On the other hand, CRY2 does not affect m6-A RNA methylation which further support our hypothesis that CRY1 regulates the metabolism through its interaction with CBS, but not CRY2. As seen in the last bar of **Figure 5-41**, lack of CBS in mouse liver causes high m6-A RNA methylation which is expected due to high homocysteine, thus high methionine in CBS deficiency (Page 120).

Chapter 6

DISCUSSION

Mammalian circadian clock is both endogenously controlled, meaning that it persists the circadian rhythm even without any external time cues. In addition to its internal rhythm, it is also very sensitive to environmental changes. The most important synchronization cue for the mammalian circadian rhythm is light. Light is sensed via intrinsically photosensitive retinal ganglion cells (ipRGCs) and transmitted to SCN (suprachiasmatic nucleus). SCN is located in hypothalamus region of the brain and it is considered as circadian rhythm center of the body. When the signal is transmitted from eyes to SCN, neurons are fired, and circadian gene expression starts. BMAL1-CLOCK heterodimer complex drives the expression of clock- controlled genes and negative regulators. PER1/2 and CRY1/2 proteins are negative regulators of molecular circadian clock which repress the BMAL1-CLOCK driven transcription. There is a secondary transcriptional loop controlled by ROR and REV-ERB proteins which positively and negatively regulates BMAL1 expression respectively. The last part of the core molecular circadian clock machinery is a post-translational regulation. CK1ε/δ labels PER proteins for degradation and, FBXL3/21 regulates CRY protein stabilization and degradation. Molecular circadian clock machinery provides 24-hour oscillation of clock-controlled gene expression. However, we still have little information about how central clock regulates differential gene expression in different tissues, since most of the tissues have different circadian peak times [65]. Considering the fact that 50 % of the metabolites show circadian oscillations in their levels, we cannot explain physiological circadian regulation occurs in metabolite level. [5]. Emerging evidences prove that there must be more post-translational regulations controlling circadian physiology [6]. When we identify how critical

enzymatic steps are regulated by circadian clock, we will be able to target those metabolism synchronizers to treat metabolic disorders.

In the current study, we have identified and characterized a novel protein-protein interaction between a prominent metabolic protein, Cystathionine-β-synthase (CBS), and an important circadian clock regulator protein, Cryptochrome 1 (CRY1). In **Figure 5-19**, we showed that this interaction is physical by using co-immunoprecipitation. **Figure 5-20 and Figure 5-22** proved that the interaction occurs at both cytosol and nucleus and these two proteins are located at both cellular compartments. CRY1 is a negative regulator in the mammalian molecular clock machinery. We then investigated the effect of CBS, on CRY1 repression activity on BMAL1/CLOCK transactivation. Repression assay indicated that CBS increases the repressive function of CRY1 **(Figure 5-24)**. On the other hand, we also showed that CRY1 increases tetramerization of CBS, thus, increases its enzyme activity (**Figure 5-32** and **Figure 5-33**). Despite the fact that we have known that post-transcriptional [66] and post-translational [5] controls of circadian clock to regulate metabolism are necessary, we have known little about these regulations. We have known that most of the core clock component proteins' activities are regulated with phosphorylation/ dephosphorylation as post-translational events [145]. The novelty of our work is we have shown that one circadian clock protein directly binds and regulates an activity of an enzyme by favoring its oligomerization (**Figure 6-1**).

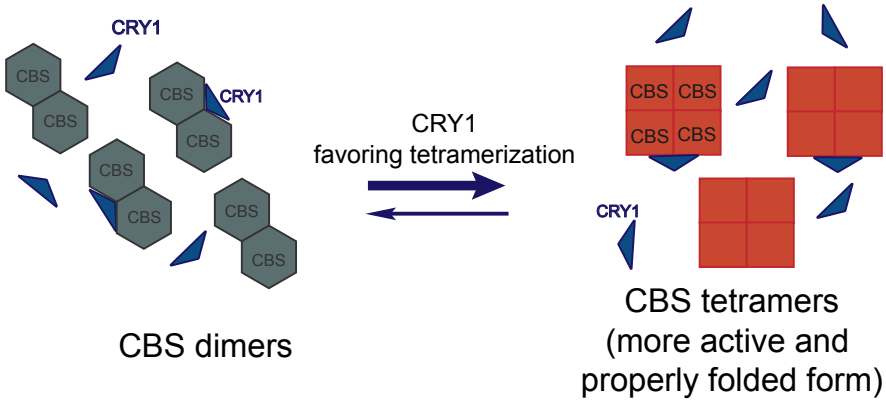


Figure 6-1: CRY1 increases CBS enzyme activity by modulating tetramerization of CBS from dimers.

We also performed untargeted metabolomics screen in *Cry1*$^{-/-}$, *Cry2*$^{-/-}$ and *Cbs*$^{-/-}$ mouse liver samples to investigate that whether CRY1 and CBS regulates same pathways in mouse liver or not. It has been known that many metabolites show rhythmic level changes in both mouse liver and U2-OS (human osteosarcoma cell line) cells [5]. The same study also proved that CRY1 and CRY2 affects the metabolism differently. When we were doing the analyses, we compared the metabolite levels in *Cry1*$^{-/-}$ and *Cbs*$^{-/-}$ mouse liver samples with their wild type littermate controls and we made the heatmap graph based on their significance levels in **Figure 5-37**.

CRY1 protein level was shown to be higher in *Cry2*$^{-/-}$ samples [146]. As seen from **Figure 5-30**, *Cry2*$^{-/-}$ liver samples have more CRY1 and show increased CBS enzyme activity compared to wild type. It is also clear in **Figure 5-34**, **Figure 5-35 and Figure 5-36** that CRY1 and CRY2 regulates metabolism in different ways, in fact, they regulate metabolism with opposite results which is totally reasonable considering our CBS enzyme activity results.

Figure 6-2 shows that one carbon metabolism pathway and urea cycle were significantly regulated by both CBS and CRY1. While metabolites which were significantly affected by CRY1 absence are circled in red, CBS regulated metabolites are circled in blue. These metabolites were also plotted in the heatmap graph based on their significance levels in **Figure 5-37.**

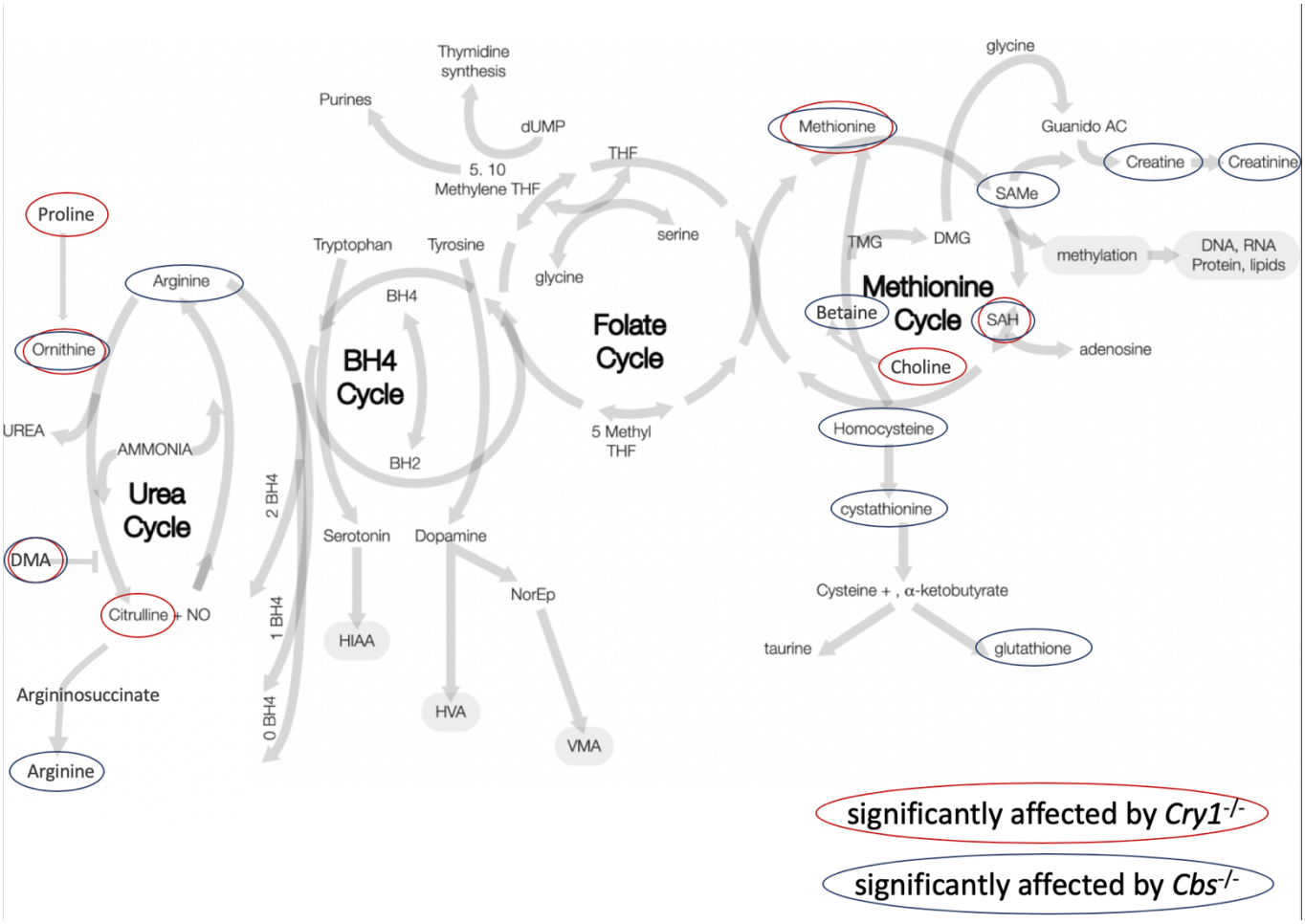


Figure 6-2: Some of the affected metabolites highlighted on one carbon metabolism pathway.

We have also analyzed the effects of CRY1, CRY2 and CBS on m6A-RNA methylation levels *in vitro* and *in vivo*. We saw that m6A-RNA level *in vivo* is affected by CRY1 and CBS absence, but not by CRY2 (**Figure 5-41**). We can conclude that the reduced m6A-RNA level in *Cry1* and *Cry2*$^{-/-}$ MEF cell line might be caused by CRY1 absence (**Figure 5-40**). Even though we weren't able to explain the reverse regulation in m6A-RNA levels by CBS and CRY1, they both significantly regulate epigenetic regulation *in vitro* and *in vivo*. Epigenetic regulation by the interaction of CRY1 and CBS is needed to be further investigated.

We modeled our work in **Figure 6-3** to provide better understanding about the concept. The protein levels of CRY1 and CBS are synchronized in cytosol and nucleus. In cytosol, CRY1 favors CBS oligomerization and induce its enzyme activity at ZT10, when mice are resting. Enzyme activity increasing role of CRY1 provide cellular energy saving. On the other hand, CBS increases CRY1 repression activity on BMAL1-CLOCK transactivation, at ZT22. Altogether, we identified a new post-translational regulatory mechanism providing bi-directional regulation of both circadian clock and metabolism.

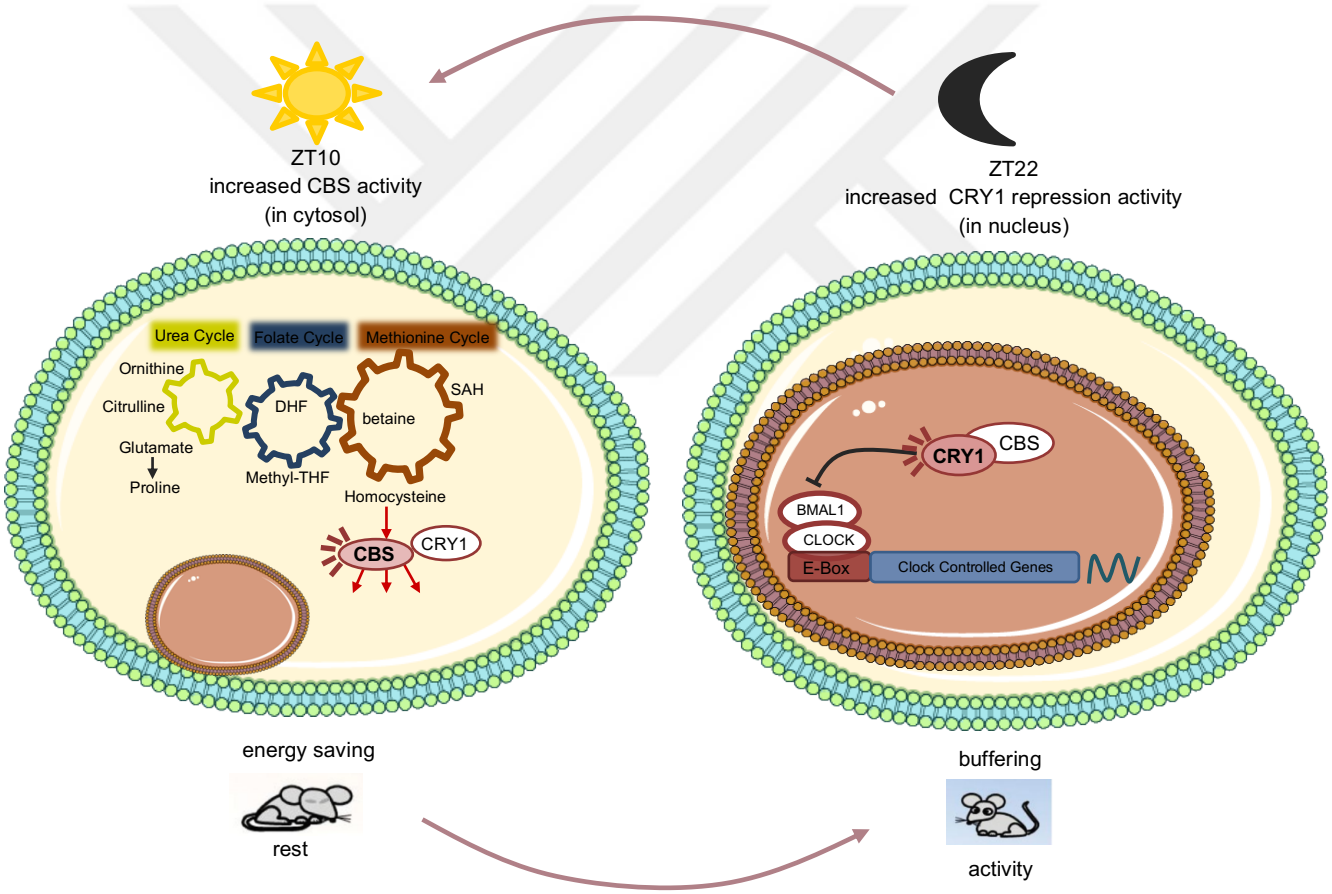


Figure 6-3: Model for the regulation between CRY1 and CBS inducing eachother's activities. CRY1 favors CBS tetramerization and enzyme activity in cytosol at ZT10, while CBS increases CRY1 repression activity in nucleus at ZT22.

Chapter 7

CONCLUSIONS AND FUTURE DIRECTIONS

Since we concluded that one carbon metabolism is strongly controlled by circadian clock through CRY1-CBS interaction, the circadian expressions of important enzymes and post-translational regulations need to be investigated in humans as well. Timing of folic acid supplementation should also be investigated for pregnant women and adults. Even only at transcriptional level, we can get maximum benefit from food or supplements when the enzyme metabolizing them at its highest level. In addition to that, more post-translational level regulations need to be investigated to provide better understanding about how metabolism and circadian clock regulates each other.

Recent homocystinuria studies aim to find drugs to induce proper enzyme activity in CBS-deficient homocystinuria patients [147]. Further studies should also consider the interaction of CRY1 and CBS, because CRY1 increases enzyme activity of CBS.

It has been previously shown that homocystinuria patients show insulin resistance [148] and this resistance is caused by impaired of glycogen synthesis [149]. As known from the literature, CRY1 is a connection between glucose metabolism and circadian clock [150]. Drugs targeting CRY1 or its abundance might be used to improve insulin resistance in homocystinuria patients. Our findings will provide a new perspective for the treatment of hyperhomocysteinemia symptoms. Folic acid and vitamin-B treatment reduce the elevated homocysteine levels [97]. With the knowledge provided by our paper, the timing of these treatments should also be further investigated.

Finally, in order to investigate CRY1-CBS interaction in a more detailed way, CRY1-R602P mutant mice should be generated and physiology and behavior of those mice should be analyzed

Chapter 8

REFERENCES

[1] J. E. Baggs and J. B. Hogenesch, “Genomics and systems approaches in the mammalian circadian clock,” *Current Opinion in Genetics and Development*. 2010.

[2] B. E. McIntosh, J. B. Hogenesch, and C. A. Bradfield, “Mammalian Per-Arnt-Sim Proteins in Environmental Adaptation,” *Annu. Rev. Physiol.*, 2010.

[3] K. L. Eckel-Mahan and D. R. Storm, “Circadian rhythms and memory: Not so simple as cogs and gears,” *EMBO Reports*. 2009.

[4] C. P. Kyriacou and M. H. Hastings, “Circadian clocks: genes, sleep, and cognition,” *Trends in Cognitive Sciences*. 2010.

[5] S. Y. Krishnaiah *et al.*, “Clock Regulation of Metabolites Reveals Coupling between Transcription and Metabolism,” *Cell Metab.*, vol. 25, no. 4, 2017.

[6] D. Mauvoisin, “Circadian rhythms and proteomics : It ’ s all about posttranslational modifications !,” no. December 2018, pp. 1–22, 2019.

[7] R. C. Anafi *et al.*, “Machine Learning Helps Identify CHRONO as a Circadian Clock Component,” *PLoS Biol.*, vol. 12, no. 4, 2014.

[8] V. Kožich *et al.*, “Cystathionine β-synthase mutations: Effect of mutation topology on folding and activity,” *Hum. Mutat.*, 2010.

[9] J. Aschoff, “A Survey on Biological Rhythms,” in *Biological Rhythms*, 1981.

[10] G. Goh, S. Maloney, P. Mark, and D. Blache, “Episodic Ultradian Events—Ultradian Rhythms,” *Biology (Basel).*, vol. 8, no. 1, p. 15, 2019.

[11] E. J. Waite *et al.*, “Ultradian corticosterone secretion is maintained in the absence of circadian cues,” *Eur. J. Neurosci.*, 2012.

[12] F. Weber, “Modeling the mammalian sleep cycle,” *Current Opinion in Neurobiology*. 2017.

[13] D. Cech and S. T. Martin, *Functional Movement Development Across the Life Span*. 2012.

[14] E.Young and A.Korszun, “Stress, the HPA Axis and Depressive Illness.” pp. 543–548, 2009.

[15] J. Rosner and M. S. Sarao, “Physiology, Female Reproduction,” *StatPearls*, pp. 6–9, 2019.

[16] K. Kräuchi, “How is the circadian rhythm of core body temperature regulated?,” *Clinical Autonomic Research*, 2002.

[17] F. C. Baker and H. S. Driver, “Circadian rhythms, sleep, and the menstrual cycle,” *Sleep Med.*, 2007.

[18] S. Labyak, S. Lava, F. Turek, and P. Zee, “Effects of shiftwork on sleep and menstrual function in nurses,” *Health Care Women Int.*, 2002.

[19] D. Farner, “Annual Rhythms,” *Annu. Rev. Physiol.*, 1985.

[20] B. Helm *et al.*, “Annual rhythms that underlie phenology: Biological time-keeping meets environmental change,” *Proceedings of the Royal Society B: Biological Sciences*. 2013.

[21] E. Gwinner, “Circadian and Circannual Programmes in Avian Migration,” *J. Exp. Biol.*, 1996.

[22] E. T. Pengelley and K. C. Fisher, “Onset and cessation of hibernation under constant temperature and light in the golden-mantled ground squirrel (Citellus lateralis) [38],” *Nature*. 1957.

[23] A. Reinberg and M. Lagoguey, “Annual Endocrine Rhythms in Healthy Young Adult Men: Their Implication in Human Biology and Medicine,” pp. 113–121, 2011.

[24] R. A. Hut, S. Paolucci, R. Dor, C. P. Kyriacou, and S. Daan, “Latitudinal clines: An evolutionary view on biological rhythms,” *Proceedings of the Royal Society B: Biological Sciences*. 2013.

[25] W. Lu, Q. J. Meng, N. J. C. Tyler, K. A. Stokkan, and A. S. I. Loudon, “A Circadian Clock Is Not Required in an Arctic Mammal,” *Curr. Biol.*, 2010.

[26] W. Arnold *et al.*, “Circadian rhythmicity persists through the Polar night and midnight sun in Svalbard reindeer,” *Sci. Rep.*, 2018.

[27] F. Halberg, “Circadian (about Twenth-four hour) Rhythms in Experimental Medicine,” pp. 253–257, 1962.

[28] J. Aschoff, “Circadian rhythms in man,” *Science (80-.).*, vol. 148, no. 3676, pp. 1427–1432, 1965.

[29] J. Colin, J. Timbal, C. Boutelier, Y. Houdas, and M. Siffre, “Rhythm of the rectal temperature during a 6-month free-running experiment.,” *J. Appl. Physiol.*, 2017.

[30] C. H. Johnson, C. Zhao, Y. Xu, and T. Mori, “Timing the day: What makes bacterial clocks tick?,” *Nature Reviews Microbiology*. 2017.

[31] Y.-I. Kim, D. J. Vinyard, G. M. Ananyev, G. C. Dismukes, and S. S. Golden, “Oxidized quinones signal onset of darkness directly to the cyanobacterial circadian oscillator,” *Proc. Natl. Acad. Sci.*, 2012.

[32] C. R. McClung, “Plant Circadian Rhythms,” *PLANT CELL ONLINE*, 2006.

[33] S. L. Harmer *et al.*, “Orchestrated transcription of key pathways in Arabidopsis by the circadian clock,” *Science (80-.).*, 2000.

[34] S. G. Fowler, “Low Temperature Induction of Arabidopsis CBF1, 2, and 3 Is Gated by the Circadian Clock,” *PLANT Physiol.*, 2005.

[35] G. Bloch, “The social clock of the honeybee,” *Journal of Biological Rhythms*. 2010.

[36] S. M. Perez, O. R. Taylor, and R. Jander, “A sun compass in monarch butterflies,” *Nature*, 1997.

[37] F. W. Turek *et al.*, “Obesity and metabolic syndrome in circadian Clock mutant mice.,” *Science*, vol. 308, no. 5724, pp. 1043–5, 2005.

[38] K. Nagai, T. Nishio, H. Nakagawa, S. Nakamura, and Y. Fukuda, “Effect of bilateral lesions of the suprachiasmatic nuclei on the circadian rhythm of food-intake,” *Brain Res.*, 1978.

[39] E. D. Buhr, S. H. Yoo, and J. S. Takahashi, “Temperature as a universal resetting cue for mammalian circadian oscillators,” *Science (80-.).*, 2010.

[40] M. Preußner *et al.*, “Body Temperature Cycles Control Rhythmic Alternative Splicing in Mammals,” *Mol. Cell*, 2017.

[41] B. L. Smarr, K. J. Jennings, J. R. Driscoll, and L. J. Kriegsfeld, “A time to remember: The role of circadian clocks in learning and memory,” *Behav. Neurosci.*, 2014.

[42] D. Jakubowicz, M. Barnea, J. Wainstein, and O. Froy, “High Caloric intake at breakfast vs. dinner differentially influences weight loss of overweight and obese women,” *Obesity*, 2013.

[43] K. Gabel *et al.*, “Effects of 8-hour time restricted feeding on body weight and metabolic disease risk factors in obese adults: A pilot study,” *Nutr. Heal. Aging*, 2018.

[44] S. N. Archer *et al.*, “Mistimed sleep disrupts circadian regulation of the human transcriptome,” *Proc. Natl. Acad. Sci.*, 2014.

[45] Y. Dagan, “Circadian rhythm sleep disorders (CRSD),” *Sleep Medicine Reviews*. 2002.

[46] S. Gery and H. P. Koeffler, “Circadian rhythms and cancer,” *Cell Cycle*. 2010.

[47] S. T. Chen, K. B. Choo, M. F. Hou, K. T. Yeh, S. J. Kuo, and J. G. Chang, “Deregulated expression of the PER1, PER2 and PER3 genes in breast cancers,” *Carcinogenesis*, 2005.

[48] T. Sjöblom *et al.*, “The consensus coding sequences of human breast and colorectal cancers,” *Science (80-.).*, 2006.

[49] R. V. Kondratov, A. A. Kondratova, V. Y. Gorbacheva, O. V. Vykhovanets, and M. P. Antoch, “Early aging and age-related pathologies in mice deficient in BMAL1, the core component of the circadian clock,” *Genes Dev.*, 2006.

[50] Y. Shigeyoshi *et al.*, “Light-induced resetting of a mammalian circadian clock is associated with rapid induction of the mPer1 transcript,” *Cell*, 1997.

[51] J. Reznick, E. Preston, D. L. Wilks, S. M. Beale, N. Turner, and G. J. Cooney, “Altered feeding differentially regulates circadian rhythms and energy metabolism in liver and muscle of rats,” *Biochim. Biophys. Acta - Mol. Basis Dis.*, 2013.

[52] G. Bloch, E. D. Herzog, J. D. Levine, and W. J. Schwartz, “Socially synchronized circadian oscillators,” *Proceedings of the Royal Society B: Biological Sciences*. 2013.

[53] B. M. Gabriel and J. R. Zierath, “Circadian rhythms and exercise — re-setting the clock in metabolic disease,” *Nature Reviews Endocrinology*. 2019.

[54] K. I. Honma and S. Honma, “The SCN-independent clocks, methamphetamine and food restriction,” *European Journal of Neuroscience*. 2009.

[55] R. A. B. and S. O. Aleksandar Videnovic, Alpar S. Lazar, “‘The clocks that time us’—circadian rhythms in neurodegenerative disorders,” *Videnovic, A. al. Nat. Rev. Neurol. Adv. online Publ. 11 Novemb. 2014; doi10.1038/nrneurol.2014.206*, 2014.

[56] N. Goldstein *et al.*, “Hypothalamic Neurons that Regulate Feeding Can Influence Sleep/Wake States Based on Homeostatic Need,” *Curr. Biol.*, 2018.

[57] E. Drouyer, C. Rieux, R. A. Hut, and H. M. Cooper, “Responses of Suprachiasmatic Nucleus Neurons to Light and Dark Adaptation: Relative Contributions of Melanopsin and Rod Cone Inputs,” *J. Neurosci.*, 2007.

[58] L. P. Morin and C. N. Allen, “The circadian visual system, 2005,” *Brain Research Reviews*. 2006.

[59] D. K. Welsh, D. E. Logothetis, M. Meister, and S. M. Reppert, “Individual neurons dissociated from rat suprachiasmatic nucleus express independently phased circadian firing rhythms,” *Neuron*, 1995.

[60] J. C. Dunlap, “Molecular bases for circadian clocks,” *Cell*, vol. 96, no. 2, pp. 271–290, 1999.

[61] E. D. Buhr and J. S. Takahashi, “Molecular components of the mammalian circadian clock,” *Handb. Exp. Pharmacol.*, 2013.

[62] A. Missra *et al.*, “The Circadian Clock Modulates Global Daily Cycles of mRNA Ribosome Loading,” *Plant Cell*, 2015.

[63] J. S. Takahashi, “Molecular architecture of the circadian clock in mammals,” *Res. Perspect. Endocr. Interact.*, 2016.

[64] R. Zhang, N. F. Lahens, H. I. Ballance, M. E. Hughes, and J. B. Hogenesch, “A circadian gene expression atlas in mammals: implications for biology and medicine.,” *Proc. Natl. Acad. Sci. U. S. A.*, vol. 111, no. 45, pp. 16219–24, 2014.

[65] R. Zhang, N. F. Lahens, H. I. Ballance, M. E. Hughes, and J. B. Hogenesch, “A circadian gene expression atlas in mammals: Implications for biology and medicine,” *Proc. Natl. Acad. Sci.*, 2014.

[66] M. J. Deery *et al.*, “Proteomic Analysis Reveals the Role of Synaptic Vesicle Cycling in Sustaining the Suprachiasmatic Circadian Clock,” *Curr. Biol.*, 2009.

[67] J. M. Fustin *et al.*, “RNA m6 概日的なスプライシング 阻害で周期延長 岡村研 RNA-methylation-dependent RNA processing controls the speed of the circadian clock,” *Cell*, 2013.

[68] J. Jin, “Folic acid supplementation for prevention of neural tube defects,” *JAMA - Journal*

of the American Medical Association. 2017.

[69] V. Gorelova, O. Bastien, O. De Clerck, S. Lespinats, F. Rébeillé, and D. Van Der Straeten, "Evolution of folate biosynthesis and metabolism across algae and land plant lineages," *Sci. Rep.*, 2019.

[70] V. Gorelova, L. Ambach, F. Rébeillé, C. Stove, and D. Van Der Straeten, "Folates in Plants: Research Advances and Progress in Crop Biofortification," *Front. Chem.*, 2017.

[71] J. M. Mato, M. L. Martínez-Chantar, M. Noureddin, and S. C. Lu, "One-Carbon Metabolism in Liver Health and Disease," *Liver Pathophysiol. Ther. Antioxidants*, vol. 25, no. 1, pp. 761–765, 2017.

[72] M. J. Berg, "The importance of folic acid.," *The journal of gender-specific medicine : JGSM : the official journal of the Partnership for Women's Health at Columbia*, vol. 2, no. 3. pp. 24–8, 1999.

[73] N. D. E. Greene and A. J. Copp, "Neural Tube Defects," *Annu Rev Neurosci.*, pp. 221–242, 2015.

[74] T. J. Lightfoot *et al.*, "Genetic variation in the folate metabolic pathway and risk of childhood leukemia," *Blood*, 2010.

[75] A. S. Tibbetts and D. R. Appling, "Compartmentalization of Mammalian Folate-Mediated One-Carbon Metabolism," *Annu. Rev. Nutr.*, 2010.

[76] K. S. Crider, T. P. Yang, R. J. Berry, and L. B. Bailey, "Folate and DNA methylation: a review of molecular mechanisms and the evidence for folate's role.," *Adv. Nutr.*, 2012.

[77] F. Li *et al.*, "Human betaine-homocysteine methyltransferase (BHMT) and BHMT2: Common gene sequence variation and functional characterization," *Mol. Genet. Metab.*, 2008.

[78] M. A. Pajares and D. Pérez-Sala, "Betaine homocysteine S-methyltransferase: Just a regulator of homocysteine metabolism?," *Cellular and Molecular Life Sciences*. 2006.

[79] J. Malapeira, L. C. Khaitova, and P. Mas, "Ordered changes in histone modifications at the core of the Arabidopsis circadian clock," *Proc. Natl. Acad. Sci.*, 2012.

[80] P. Ciborowski and J. Silberring, *Proteomic Profiling and Analytical Chemistry*. 2013.

[81] S. Zhou, Z. Zhang, and G. Xu, "Notable epigenetic role of hyperhomocysteinemia in atherogenesis," *Lipids in Health and Disease*. 2014.

[82] D. Zhang, X. Wen, W. Wu, Y. Guo, and W. Cui, "Elevated homocysteine level and folate deficiency associated with increased overall risk of carcinogenesis: Meta-analysis of 83 case-control studies involving 35,758 individuals," *PLoS One*, 2015.

[83] G. Almadori *et al.*, "Serum folate and homocysteine levels in head and neck squamous cell carcinoma," *Cancer*, 2002.

[84] S. Sen *et al.*, "Role of cystathionine β-synthase in human breast Cancer.," *Free Radic. Biol. Med.*, vol. 86, pp. 228–238, 2015.

[85] C. Szabo *et al.*, "Tumor-derived hydrogen sulfide, produced by cystathionine- -synthase, stimulates bioenergetics, cell proliferation, and angiogenesis in colon cancer," *Proc. Natl. Acad. Sci.*, 2013.

[86] H. Guo, J. W. Gai, Y. Wang, H. F. Jin, J. B. Du, and J. Jin, "Characterization of hydrogen sulfide and its synthases, cystathionine β-synthase and cystathionine γ-lyase, in human prostatic tissue and cells," *Urology*, 2012.

[87] S. Bhattacharyya *et al.*, "Cystathionine Beta-Synthase (CBS) Contributes to Advanced Ovarian Cancer Progression and Drug Resistance," *PLoS One*, 2013.

[88] N. Takano *et al.*, "Decreased Expression of Cystathionine β-Synthase Promotes Glioma Tumorigenesis," *Mol. Cancer Res.*, 2014.

[89] H. Kimura, "Hydrogen Sulfide-Mediated Cellular Signaling and Cytoprotection," *Hydrog. Sulfide its Ther. Appl.*, pp. 181–202, 2013.

[90] K. Eto, T. Asada, K. Arima, T. Makifuchi, and H. Kimura, "Brain hydrogen sulfide is severely decreased in Alzheimer's disease," *Biochem. Biophys. Res. Commun.*, 2002.

[91] S. C. Lu, "Glutathione synthesis," *Biochimica et Biophysica Acta - General Subjects*. 2013.

[92] T. Finkel, "Signal transduction by reactive oxygen species," *Journal of Cell Biology*. 2011.

[93] P. D. Ray, B.-W. Huang, and Y. Tsuji, "Reactive oxygen species (ROS) homeostasis and redox regulation in cellular signaling.," *Cell. Signal.*, 2012.

[94] K. Brieger, S. Schiavone, F. J. Miller, and K. H. Krause, "Reactive oxygen species: From health to disease," *Swiss Medical Weekly*. 2012.

[95] H. O. Lee, L. Wang, Y. M. Kuo, A. J. Andrews, S. Gupta, and W. D. Kruger, "S-adenosylhomocysteine hydrolase over-expression does not alter S-adenosylmethionine or S-adenosylhomocysteine levels in CBS deficient mice," *Mol. Genet. Metab. Reports*, 2018.

[96] J. P. Kraus *et al.*, "Cystathionine β-synthase mutations in homocystinuria," *Hum. Mutat.*, 1999.

[97] B. A. Maron and J. Loscalzo, "The Treatment of Hyperhomocysteinemia," *Annu. Rev. Med.*, 2009.

[98] D. S. Dimski, "Ammonia Metabolism and the Urea Cycle: Function and Clinical Implications," *Journal of Veterinary Internal Medicine*. 1994.

[99] R. Cunin, N. Glansdorff, A. Piérard, and V. Stalon, "Biosynthesis and metabolism of arginine in bacteria.," *Microbiol. Rev.*, 1986.

[100] N. Ah Mew, K. L. Simpson, A. L. Gropman, B. C. Lanpher, K. A. Chapman, and M. L. Summar, *Urea Cycle Disorders Overview*. 1993.

[101] D. Feng and M. A. Lazar, "Clocks, Metabolism, and the Epigenome," *Molecular Cell*. 2012.

[102] R. Lin *et al.*, "CLOCK Acetylates ASS1 to Drive Circadian Rhythm of Ureagenesis," *Mol. Cell*, 2017.

[103] S. Masri *et al.*, "Circadian acetylome reveals regulation of mitochondrial metabolic pathways," *Proc. Natl. Acad. Sci.*, 2013.

[104] J. S. T. Joseph Bass, "Circadian Integration of Metabolism and Energetics," *Science (80-.).*, vol. 330, no. 6009, pp. 1349–1354, 2010.

[105] T. Manual, "CheckMate ™ Mammalian CheckMate ™ Mammalian Two-Hybrid System," *Reporter*, pp. 0–24.

[106] T. Reagent, "Transfection Reagent," vol. 0747, no. 815, pp. 2–7.

[107] L. Wang, X. Chen, B. Tang, X. Hua, A. Klein-szanto, and D. Warren, "Expression of mutant human cystathionine beta-synthase rescues neonatal lethality but not homocystinuria in a mouse model," *Hum Mol Genet.*, vol. 14, no. 15, pp. 2201–2208, 2005.

[108] E. G. . D. W. J. Bligh, "A Rapid Method Of Total Lipid Extraction and Purification," *Can. J. Biochem. Physiol.*, 1959.

[109] N. Tambellini, V. Zaremberg, R. Turner, and A. Weljie, "Evaluation of Extraction Protocols for Simultaneous Polar and Non-Polar Yeast Metabolite Analysis Using Multivariate Projection Methods," *Metabolites*, 2013.

[110] J. Chong *et al.*, "MetaboAnalyst 4.0: Towards more transparent and integrative metabolomics analysis," *Nucleic Acids Res.*, 2018.

[111] A. Pizarro, K. Hayer, N. F. Lahens, and J. B. Hogenesch, "CircaDB: A database of mammalian circadian gene expression profiles," *Nucleic Acids Res.*, 2013.

[112] R. He and X. Li, "Mammalian two-hybrid assay for detecting protein-protein interactions in vivo," *Methods Mol. Biol.*, 2008.

[113] A. J. Pratt and I. J. MacRae, "The RNA-induced silencing complex: A versatile gene-silencing machine," *J. Biol. Chem.*, vol. 284, no. 27, pp. 17897–17901, 2009.

[114] A. Fire, S. Xu, M. K. Montgomery, S. A. Kostas, S. E. Driver, and C. C. Mello, "Potent and specific genetic interference by double-stranded RNA in Caenorhabditis elegans.," *Nature*, 1998.

[115] S. Yamazaki and J. S. Takahashi, "Real-time luminescence reporting of circadian gene expression in mammals," *Methods Enzymol.*, 2005.

[116] E. E. Zhang *et al.*, "A Genome-wide RNAi Screen for Modifiers of the Circadian Clock in Human Cells," *Cell*, vol. 139, no. 1, pp. 199–210, 2009.

[117] P. M. Holland, R. D. Abramson, R. Watson, and D. H. Gelfand, "Detection of specific polymerase chain reaction product by utilizing the 5'----3' exonuclease activity of Thermus aquaticus DNA polymerase.," *Proc. Natl. Acad. Sci. U. S. A.*, 1991.

[118] F. Ponchel *et al.*, "Real-time PCR based on SYBR-Green I fluorescence: An alternative to the TaqMan assay for a relative quantification of gene rearrangements, gene amplifications and micro gene deletions," *BMC Biotechnol.*, 2003.

[119] F. H. Stephenson and F. H. Stephenson, "Chapter 9 – Real-Time PCR," in *Calculations*

for Molecular Biology and Biotechnology, 2016.

[120] A. C. Newman and O. D. K. Maddocks, "One-carbon metabolism in cancer," *British Journal of Cancer*. 2017.

[121] I. H. Kavakli *et al.*, "The Photolyase/Cryptochrome Family of Proteins as DNA Repair Enzymes and Transcriptional Repressors," *Photochemistry and Photobiology*. 2017.

[122] P. Gao *et al.*, "Phosphorylation of the cryptochrome 1 C-terminal tail regulates circadian period length," *J. Biol. Chem.*, 2013.

[123] S. Gahoi, A. L, R. Anil, and M. SS, "DPPrimer – A Degenerate PCR Primer Design Tool," *Bioinformation*, 2013.

[124] S. Lacks and B. Greenberg, "A deoxyribonuclease of Diplococcus pneumoniae specific for methylated DNA," *J. Biol. Chem.*, 1975.

[125] T. K. Kerppola, "Design and implementation of bimolecular fluorescence complementation (BiFC) assays for the visualization of protein interactions in living cells," *Nat. Protoc.*, 2006.

[126] O. Kabil, Y. Zhou, and R. Banerjee, "Human cystathionine β-synthase is a target for sumoylation," *Biochemistry*, vol. 45, no. 45, pp. 13528–13536, 2006.

[127] B. Chazotte, "Labeling nuclear DNA using DAPI," *Cold Spring Harb. Protoc.*, 2011.

[128] S. J. Sacharow, J. D. Picker, and H. L. Levy, *Homocystinuria Caused by Cystathionine Beta-Synthase Deficiency*. 1993.

[129] J. Ereno-Orbea, T. Majtan, I. Oyenarte, J. P. Kraus, and L. A. Martinez-Cruz, "Structural basis of regulation and oligomerization of human cystathionine -synthase, the central enzyme of transsulfuration," *Proc. Natl. Acad. Sci.*, 2013.

[130] L. R. Singh, X. Chen, V. Kožich, and W. D. Kruger, "Chemical chaperone rescue of mutant human cystathionine β-synthase," *Mol. Genet. Metab.*, 2007.

[131] S. Mani, W. Cao, L. Wu, and R. Wang, "Hydrogen sulfide and the liver," *Nitric Oxide - Biol. Chem.*, vol. 41, pp. 62–71, 2014.

[132] A. Asimakopoulou *et al.*, "Selectivity of commonly used pharmacological inhibitors for cystathionine β synthase (CBS) and cystathionine γ lyase (CSE)," *Br. J. Pharmacol.*, vol. 169, no. 4, pp. 922–932, 2013.

[133] G. W. Luther *et al.*, "Thermodynamics and kinetics of sulfide oxidation by oxygen: A look at inorganically controlled reactions and biologically mediated processes in the environment," *Front. Microbiol.*, 2011.

[134] M. Koutmos, O. Kabil, J. L. Smith, and R. Banerjee, "Structural basis for substrate activation and regulation by cystathionine beta-synthase (CBS) domains in cystathionine -synthase," *Proc. Natl. Acad. Sci.*, 2010.

[135] R. Banerjee, R. Evande, Ö. Kabil, S. Ojha, and S. Taoka, "Reaction mechanism and regulation of cystathionine β-synthase," in *Biochimica et Biophysica Acta - Proteins and*

Proteomics, 2003.

[136] H.-O. L. W.-M. K. G. J. S. L. J. A. D. KrugerEmail, "Lack of global epigenetic methylation defects in CBS deficient mice," *J. Inherit. Metab. Dis.*, pp. 1–8, 2016.

[137] E. Li and Y. Zhang, "DNA methylation in mammals," *Cold Spring Harb. Perspect. Biol.*, 2014.

[138] A. Breiling and F. Lyko, "Epigenetic regulatory functions of DNA modifications: 5-methylcytosine and beyond," *Epigenetics and Chromatin*. 2015.

[139] T. D. M. Berkel and S. C. Pandey, "Emerging Role of Epigenetic Mechanisms in Alcohol Addiction," *Alcoholism: Clinical and Experimental Research*. 2017.

[140] C. C. Wong, Y. Qian, and J. Yu, "Interplay between epigenetics and metabolism in oncogenesis: Mechanisms and therapeutic approaches," *Oncogene*. 2017.

[141] Z. Li, H. Weng, H. Huang, X. Deng, J. Chen, and R. Su, "RNA N6-methyladenosine modification in cancers: current status and perspectives," *Cell Res.*, 2018.

[142] P. K. Yadav, P. K. Rajvanshi, and R. Rajasekharan, "The role of yeast m6A methyltransferase in peroxisomal fatty acid oxidation," *Current Genetics*. 2018.

[143] Y. Yang, P. J. Hsu, Y. S. Chen, and Y. G. Yang, "Dynamic transcriptomic m6A decoration: Writers, erasers, readers and functions in RNA metabolism," *Cell Research*. 2018.

[144] Q. K. Colorimetric and B. C. P-, "Complete Solutions for Epigenetics EpiQuik ™ m 6 A RNA Methylation Complete Solutions for Epigenetics," pp. 1–11.

[145] S. Reischl and A. Kramer, "Kinases and phosphatases in the mammalian circadian clock," *FEBS Letters*. 2011.

[146] S. J. Papp *et al.*, "DNA damage shifts circadian clock time via hausp-dependent cry1 stabilization," *Elife*, vol. 2015, no. 4, pp. 1–19, 2015.

[147] T. Majtan *et al.*, "Potential pharmacological chaperones for cystathionine beta-synthase-deficient homocystinuria," in *Handbook of Experimental Pharmacology*, 2018.

[148] M. Schachter, A. Raziel, S. Friedler, D. Strassburger, O. Bern, and R. Ron-El, "Insulin resistance in patients with polcystic ovary syndrome is associated with elevated plasma homocysteine," *Hum. Reprod.*, 2003.

[149] W. J. Liu, L. Q. Ma, W. H. Liu, W. Zhou, K. Q. Zhang, and C. G. Zou, "Inhibition of hepatic glycogen synthesis by hyperhomocysteinemia mediated by TRB3," *Am. J. Pathol.*, 2011.

[150] E. E. Zhang *et al.*, "Cryptochrome mediates circadian regulation of cAMP signaling and hepatic gluconeogenesis.," *Nat. Med.*, vol. 16, no. 10, pp. 1152–6, 2010.

Chapter 9

APPENDICES

9.1 Supplementary Tables

Table 7: Period, relative amplitude and circadian power raw data obtained from locomotor activity analysis

Gender	Genotype	Period	RelAmp	Power
Female	WT	23.77	0.948	0.290833
		23.98	0.881	0.331655
		23.63	0.93	0.375238
		23.67	0.947	0.208958
		23.67	0.998	0.417655
		23.58	0.83	0.344354
		23.68	0.964	0.456287
		23.68	0.852	0.434127
		23.72	0.933	0.38062
		23.85	0.977	0.430421
		23.65	0.956	0.416996
	Cbs-/-	23.95	0.881	0.032317
		23.4	0.599	0.242118
		23.82	0.802	0.026243
		23.47	0.802	0.308849
		23.98	0.846	0.054124
		23.83	0.908	0.13958
		23.6	0.816	0.131822
		23.53	0.703	0.170435
		23.6	0.766	0.136397
		23.32	0.636	0.261014
		23.88	0.579	0.005612
		23.63	0.745	0.251861
		23.68	0.485	0.009998
		23.6	0.747	0.066536
		23.83	0.975	0.054036

Gender	Genotype	Period	RelAmp	Power
Male	WT	23.65	0.99	0.465515
		23.55	0.946	0.376805
		23.65	0.944	0.338214
		23.48	0.831	0.419876
		23.55	0.746	0.335057
		23.57	0.935	0.318144
		23.77	0.839	0.260767
		23.28	0.533	0.31191
		23.25	0.544	0.360891
		23.85	0.863	0.133785
	Cbs-/-	23.45	0.67	0.235851
		23.48	0.816	0.273836
		23.82	0.891	0.078104
		23.58	0.444	0.160222
		23.65	0.542	0.106838
		23.07	0.223	0.183994
		23.98	0.642	0.083745
		23.98	0.838	0.130037
		23.57	0.891	0.24478
		23.8	0.598	0.061703
		23.68	0.808	0.207746

Table 8: Q-PCR primer sequences used in this project.

Primer Name	Sequence (5' to 3')
had-RT-Fwd	TGCACCACCAACTGCTTAGC
hGAPDH-RT-Rev	ACAGTCTTCTGGGTGGCAGTG
hDbp-RT-Fwd	GAGGAACTTAAGCCCCAGCC
hDbp-RT-Rev	CTCGTTGTTCTTGTACCGCC
hCry1-RT-Fwd	ACAGGTGGCGATTTTTGCTTC
hCry1-RT-Rev	TCCAAAGGGCTCAGAATCATACT
hPer2-RT-Fwd	AGTTGGCCTGCAAGAACCAG
hPer2-RT-Rev	ACTCGCATTTCCTCTTCAGGG
hCbs-RT-Fwd	CCTAGACCAGTACCGCAACG
hCbs-RT-Rev	CTCCTTCAGCTTCCTGGCAA
mGAPDH-RT-Fwd	AACTTTGGCATTGTGGAAGG
mGAPDH-RT-Rev	ACACATTGGGGGTAGGAACA
mDbp-RT-Fwd	GCTGCTTGGGCTGAGGAG
mDbp-RT-Rev	TGAGGGCAGAGTTGCCTTG
mCry1-RT-Fwd	CAACGTGGGCATCAACAGG
mCry1-RT-Rev	GATGTTCCATTCCTTGAAAAGCC
mPer2-RT-Fwd	GAGCGCCACCAAGTGACGG
mPer2-RT-Rev	GGTGGGACTTGGGGAGAAGT
mCbs-RT-Fwd	ATCCAATCACGAGACCAGGC
mCbs-RT-Rev	GCAGTGACAACCCCAAACAC

Table 9: Primer sequences which used to make degenerate mutations in the last 20 amino acids of CRY1. Last two primers were used to make site-directed mutagenesis on R602 point.

Primer Name	Sequence (5` to 3`)
mCRY1-deg1	GGTACCTGCGGCCGCTCANTTACTGMTCTGCVGCTGVACTTTSGGGCCGACACTCTGGGCATCCTCTTCCTGACTAGG
mCRY1-deg2	GGTACCTGCGGCCGCTCAGTTRCTGCTCWGCCGMTGGACNTTGGGGCCGACACTCTGGGCATCCTCTTCCTGACTAGG
mCRY1-deg3	GGTACCTGCGGCCGCTCAGTTACTGCTCTGCCGCTGGACTTTGGGRCCGACAMTCTGGKCATCHTCTTCCNGACTAGG
mCRY1-deg4	GGTACCTGCGGCCGCTCAGTTACTGCTCTGCCGCTGGACTTTGGGGCCGNCACTDTGGGCARCCTCVTCCTGMCTAGG
mCRY1-R602P-fwd	GTCGGCCCCAAAGTCCAGCCGCAGAGCAGTAACTGGCGG
mCRY1-R602P-rev	CCGCCAGTTACTGCTCTGCGGCTGGACTTTGGGGCCGAC

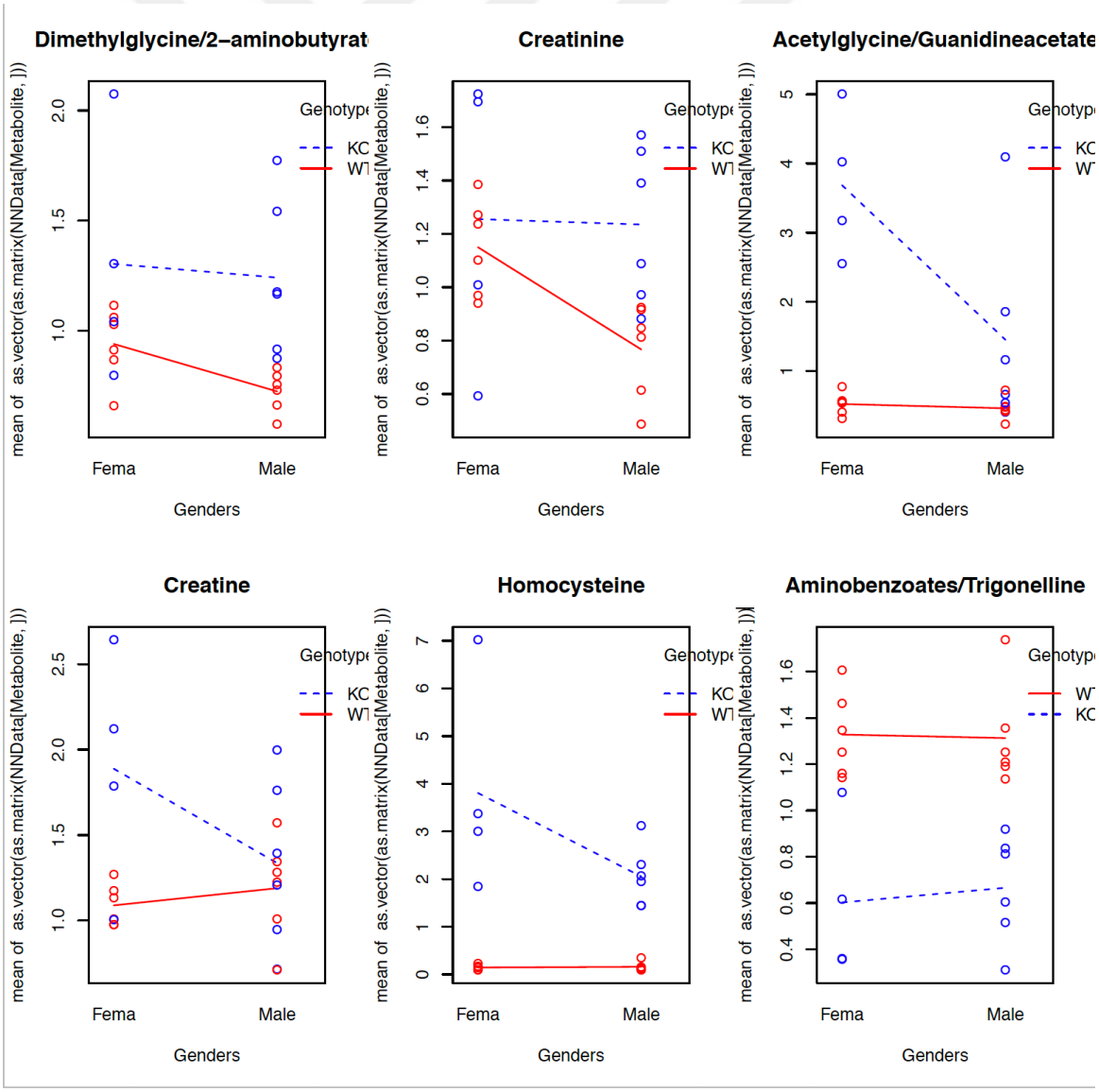
Table 10: IUPAC codes and their base meanings

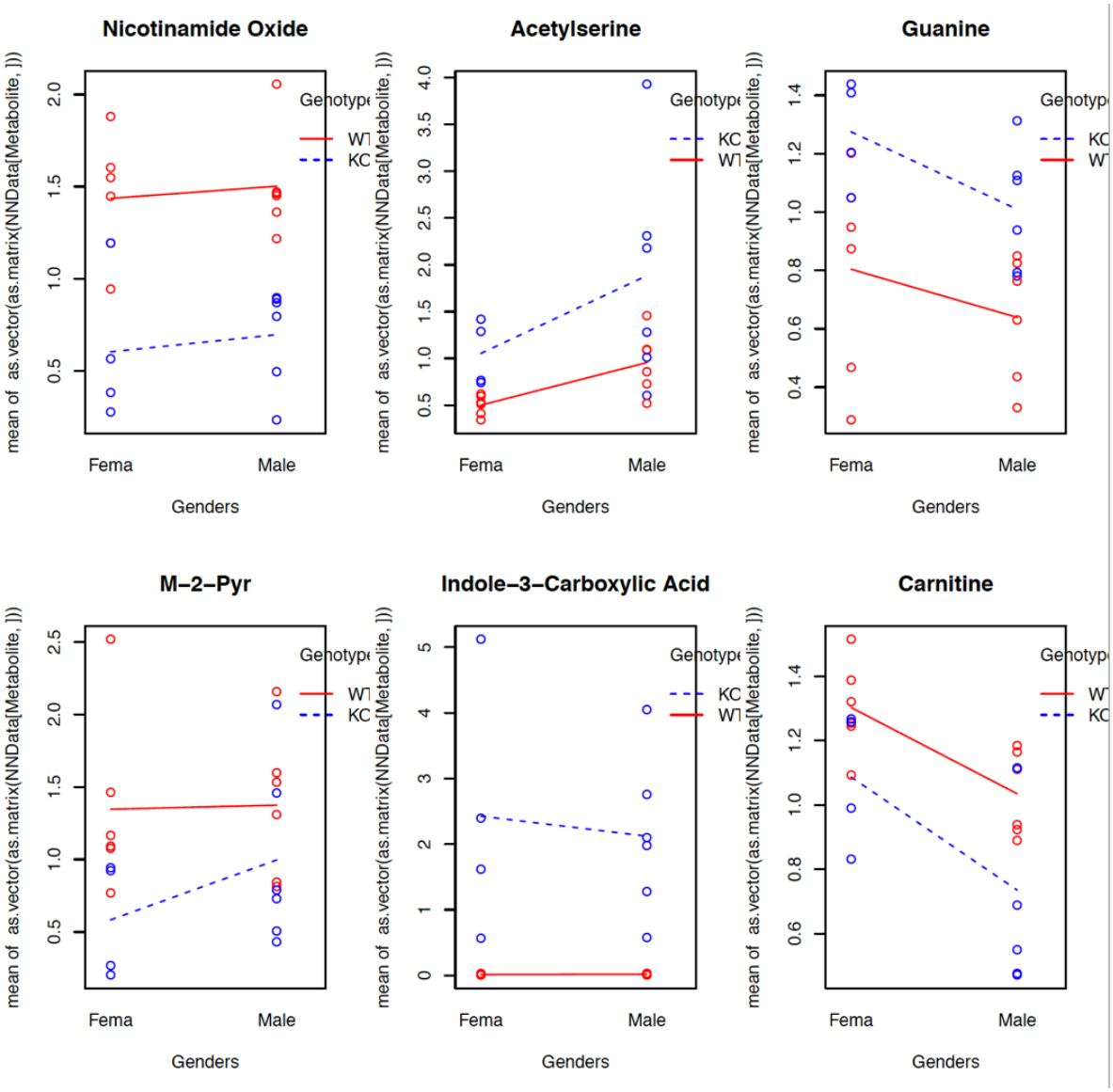
IUPAC nucleotide code	Base
R	A or G
Y	C or T
S	G or C
W	A or T
K	G or T
M	A or C
B	C or G or T
D	A or G or T
H	A or C or T
V	A or C or G
N	Any base

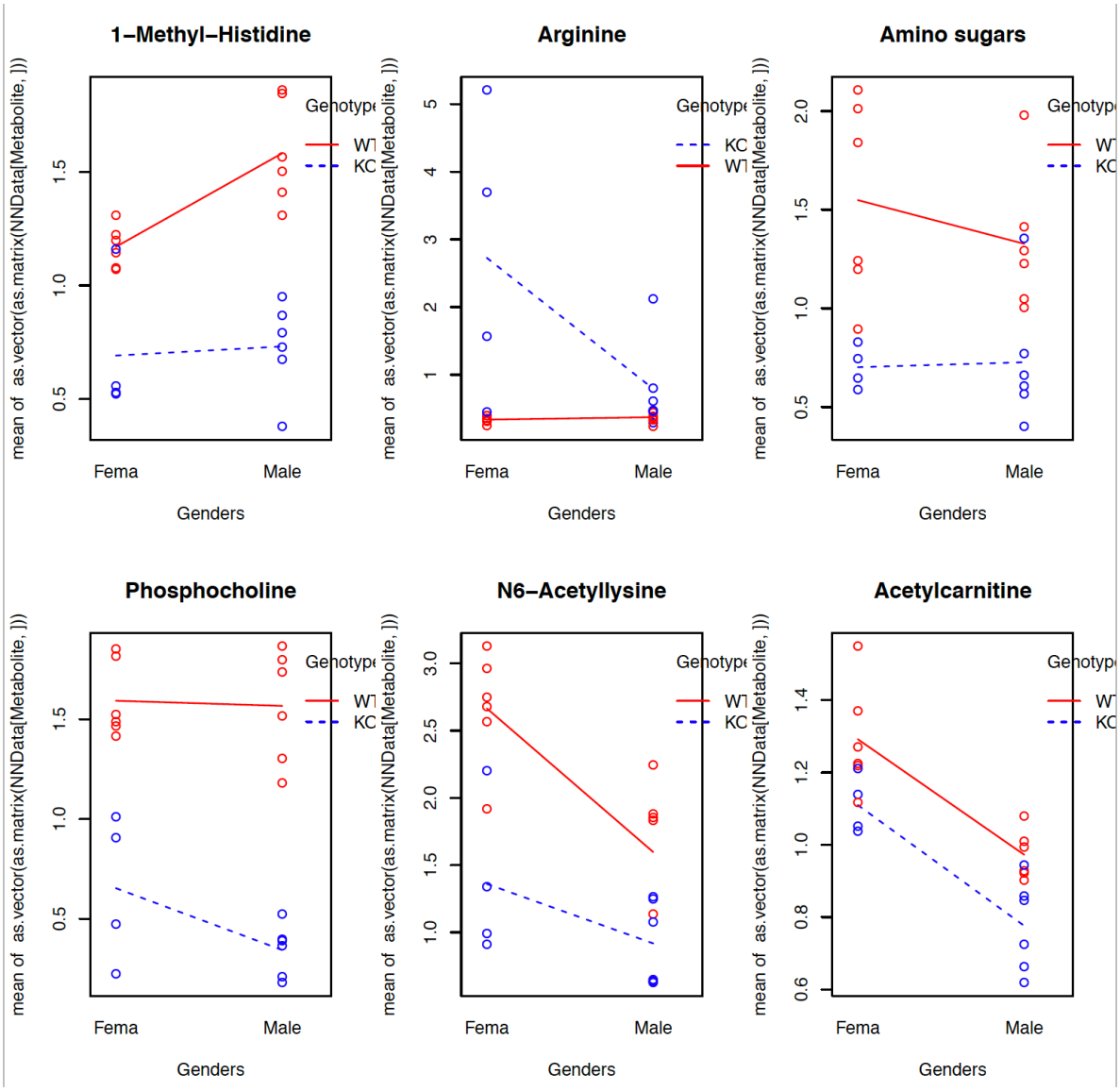
9.2 Supplementary documents

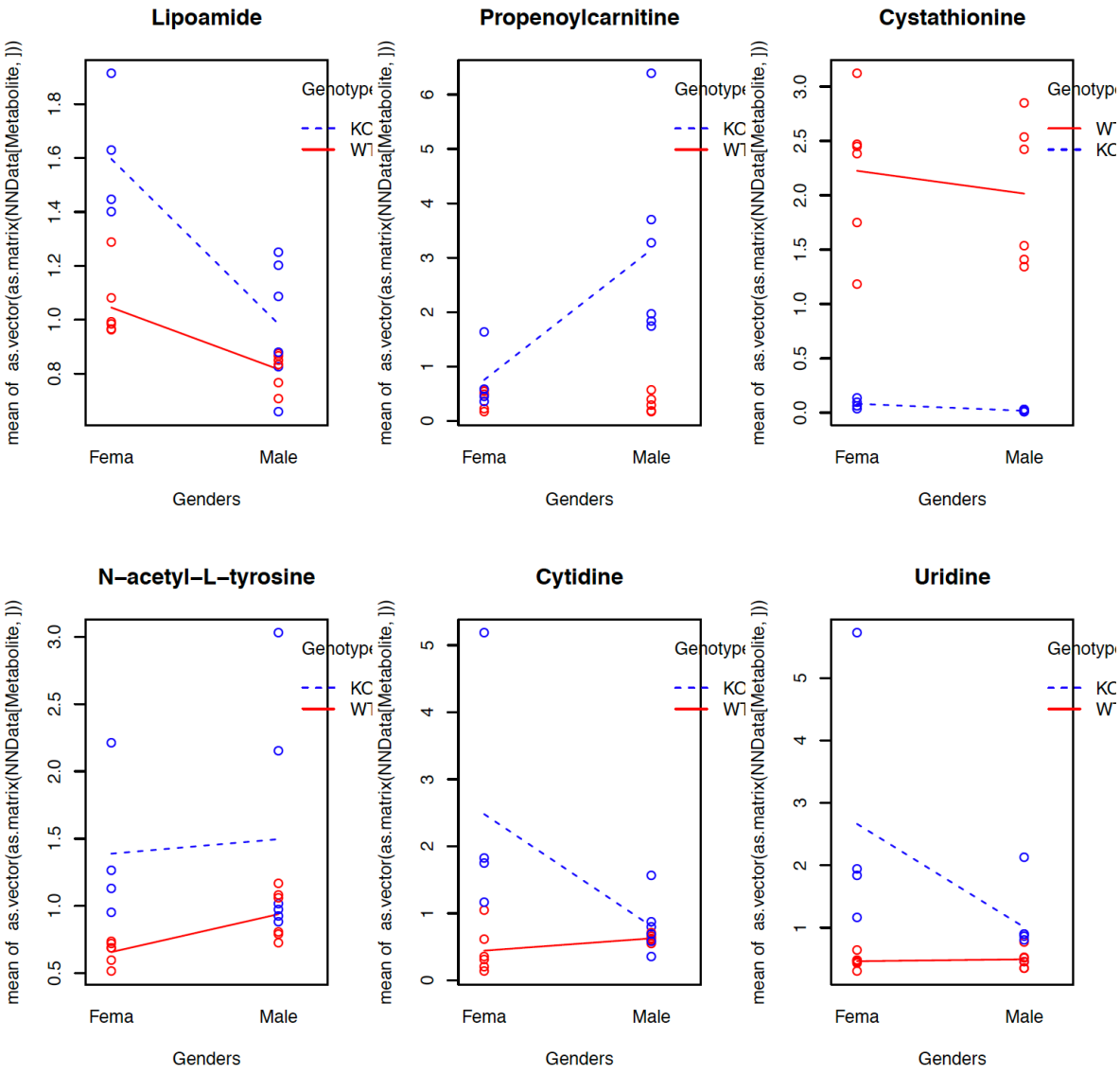
9.2.1 Metabolites Significantly Changed in CBS knock out liver samples, compared with wild type

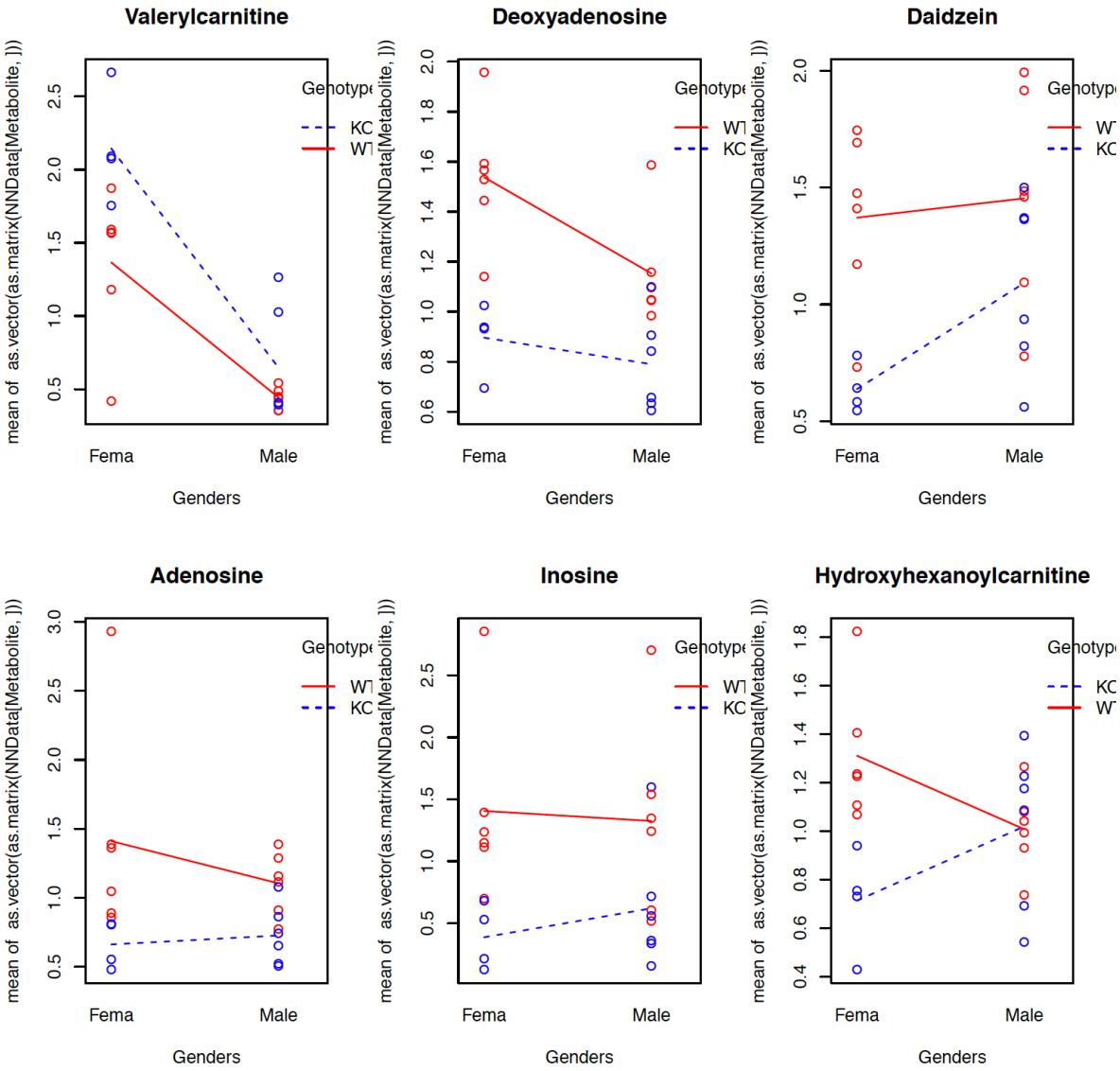
Significantly affected metabolites in *Cbs*$^{-/-}$ mouse liver samples as the result of untargeted high throughput metabolomics screen. Solid red line shows indicated metabolite levels in wild type female and male mice, while dashed blue line shows *Cbs*$^{-/-}$ female and male mice results.

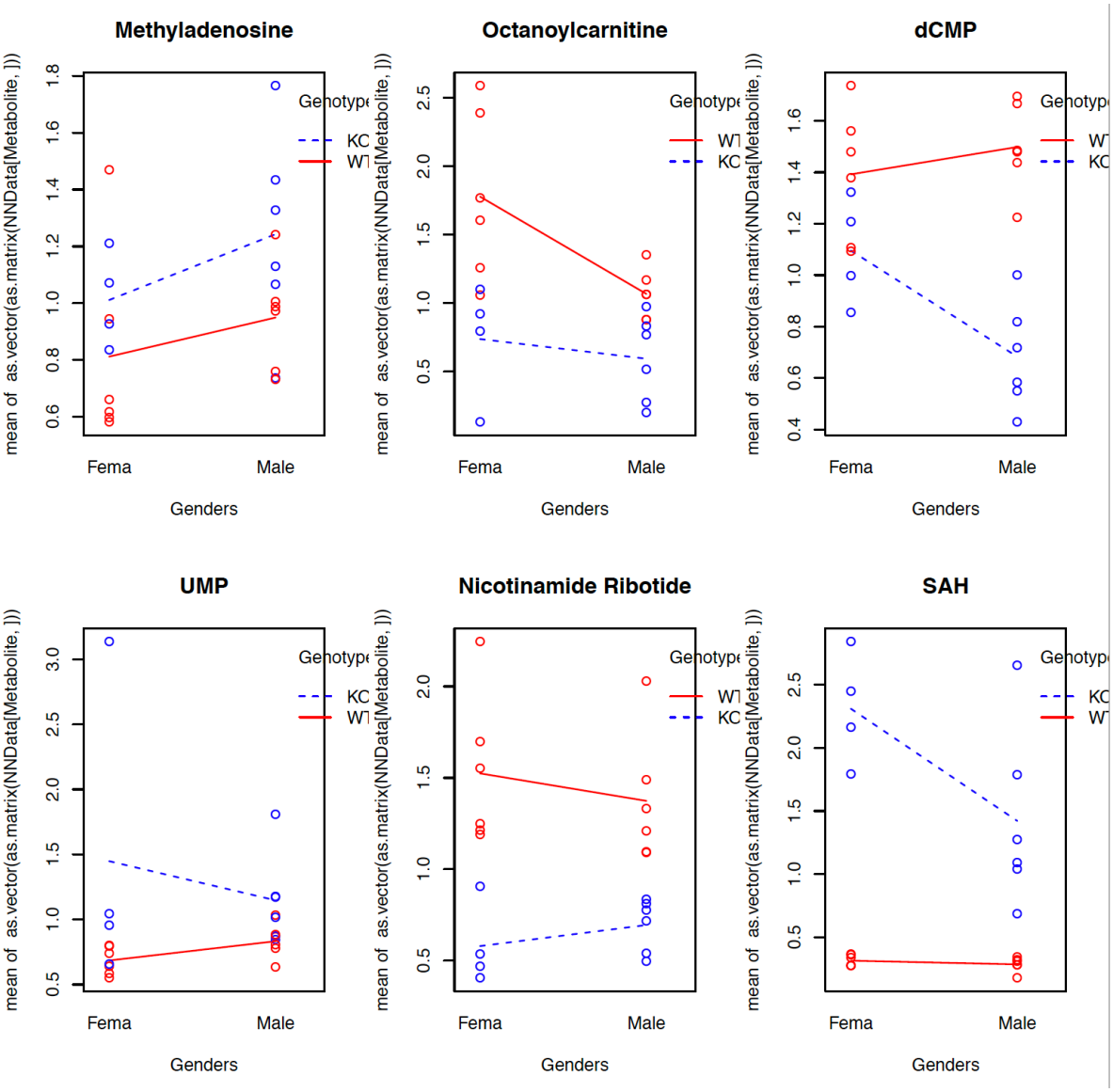


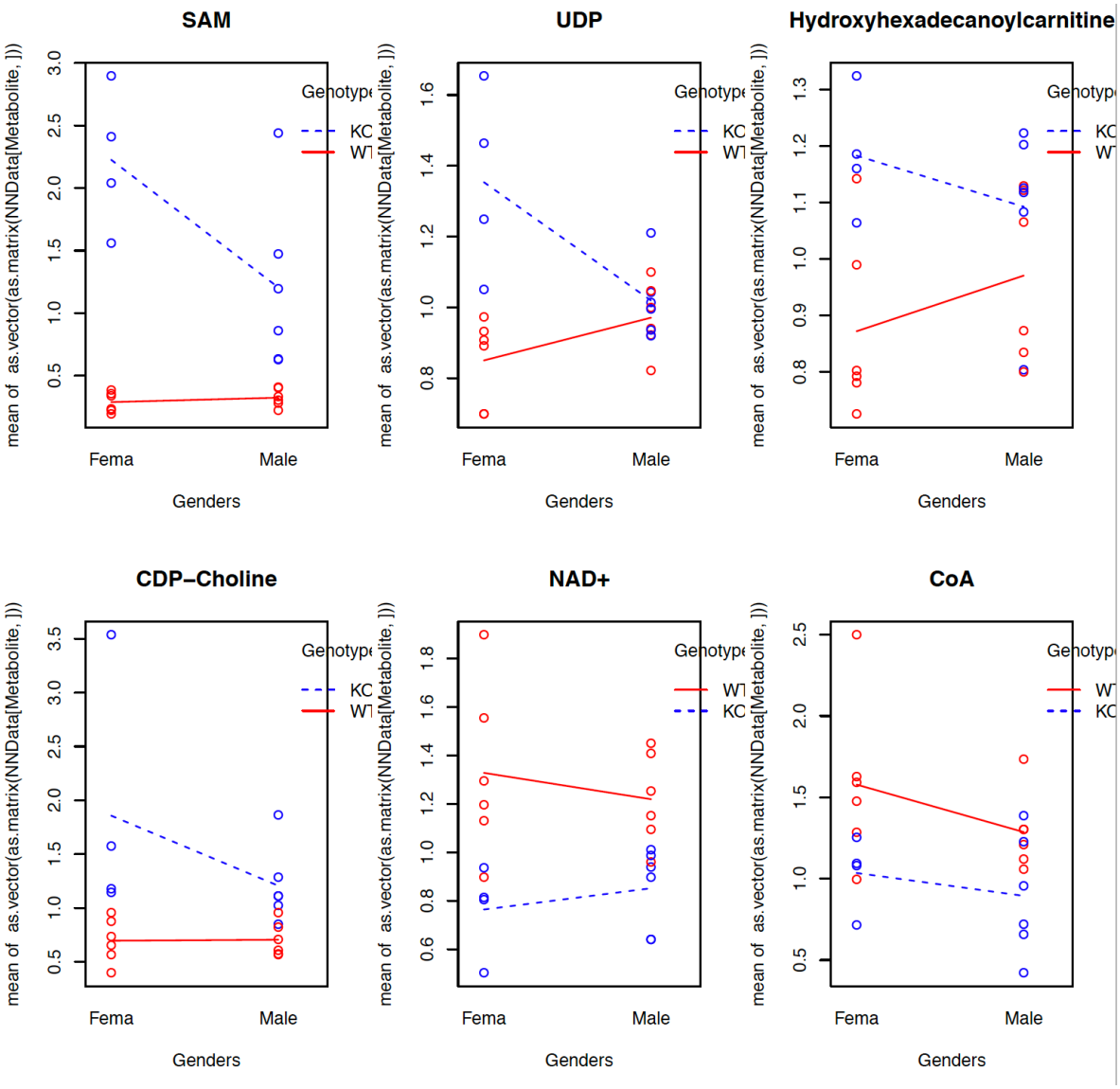

Nicotinamide Oxide
Acetylserine
Guanine
M−2−Pyr
Indole−3−Carboxylic Acid
Carnitine
mean of as.vector(as.matrix(NNData[Metabolite,]))
Genotype
WT
KO
Fema
Male
Genders

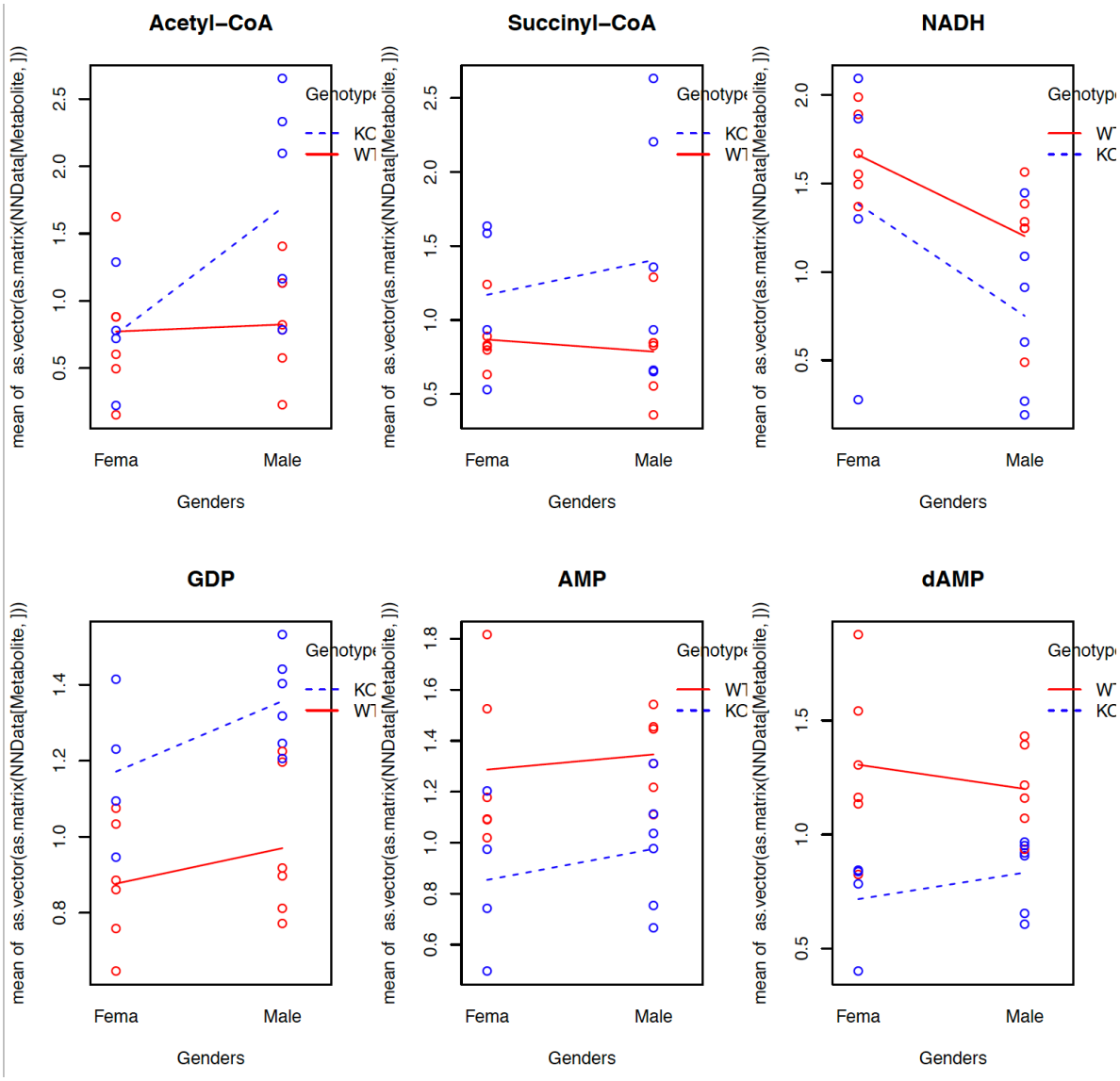

1−Methyl−Histidine
Arginine
Amino sugars
Phosphocholine
N6−Acetyllysine
Acetylcarnitine
mean of as.vector(as.matrix(NNData[Metabolite,]))
Genotype
WT
KO
Fema
Male
Genders

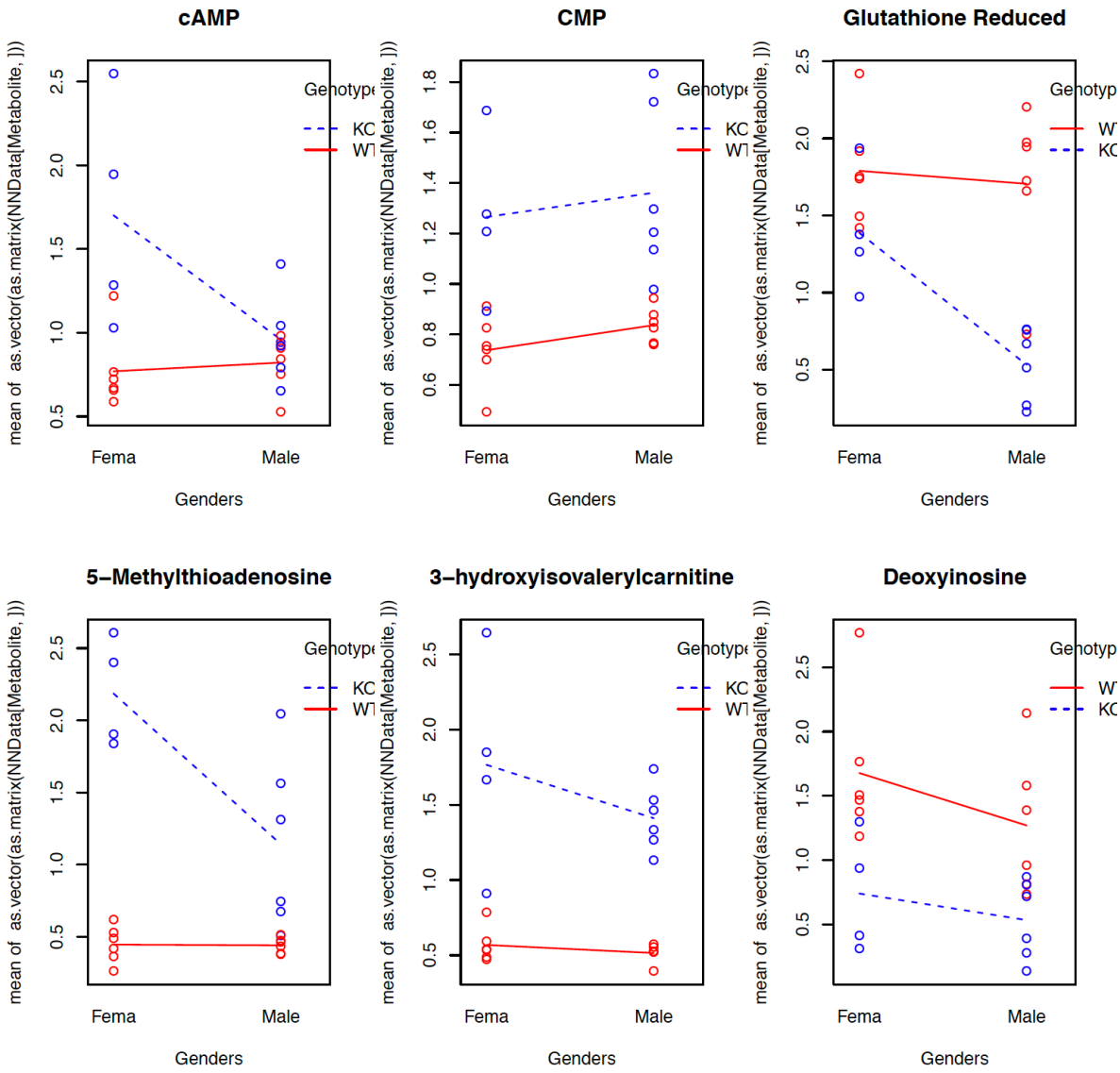

Lipoamide
Propenoylcarnitine
Cystathionine
N–acetyl–L–tyrosine
Cytidine
Uridine
mean of as.vector(as.matrix(NNData[Metabolite,]))
Genotype
KC
WT
Fema
Male
Genders

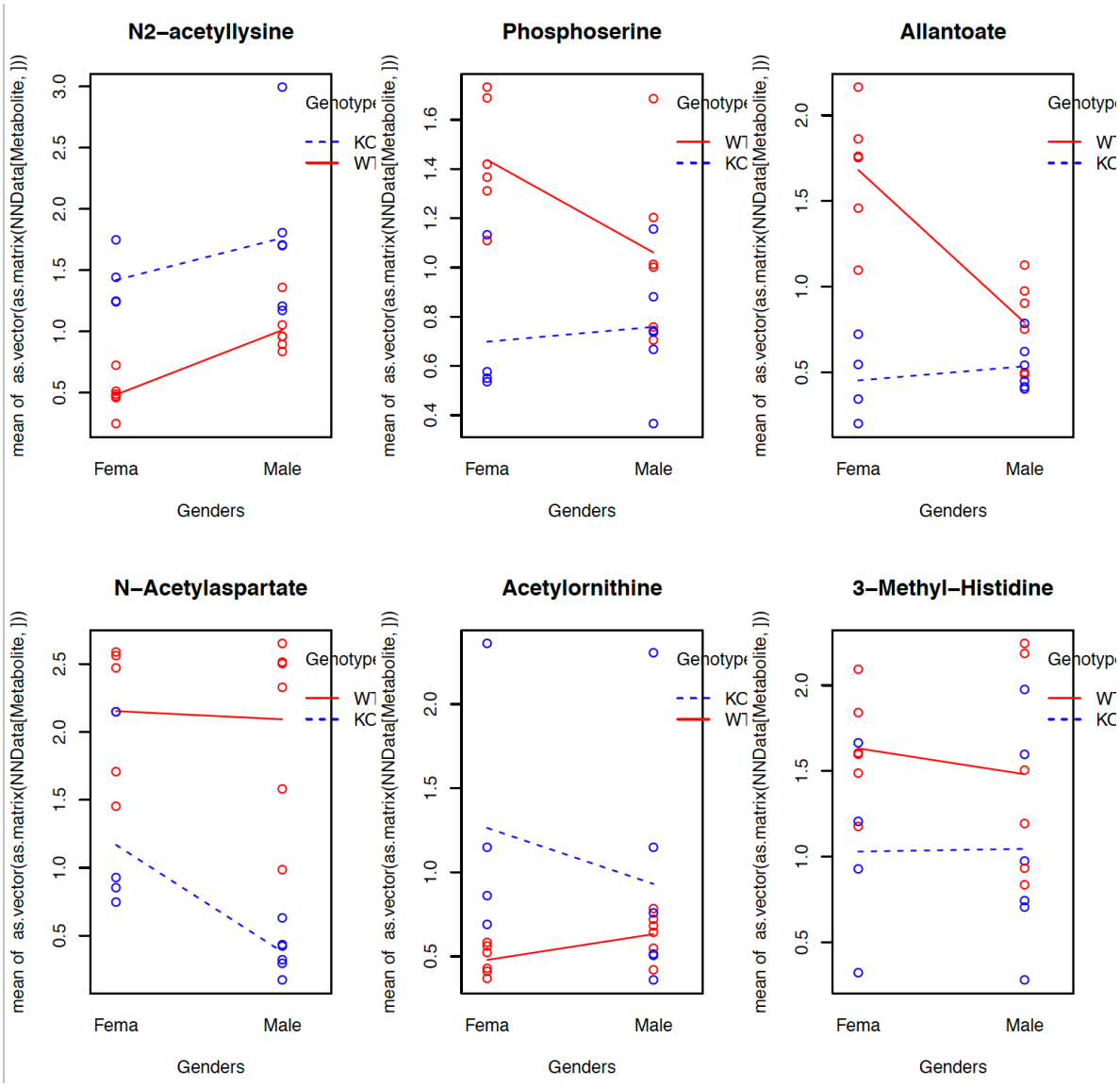

Valerylcarnitine
Deoxyadenosine
Daidzein
Adenosine
Inosine
Hydroxyhexanoylcarnitine
mean of as.vector(as.matrix(NNData[Metabolite,]))
Genotype
KO
WT
Fema
Male
Genders

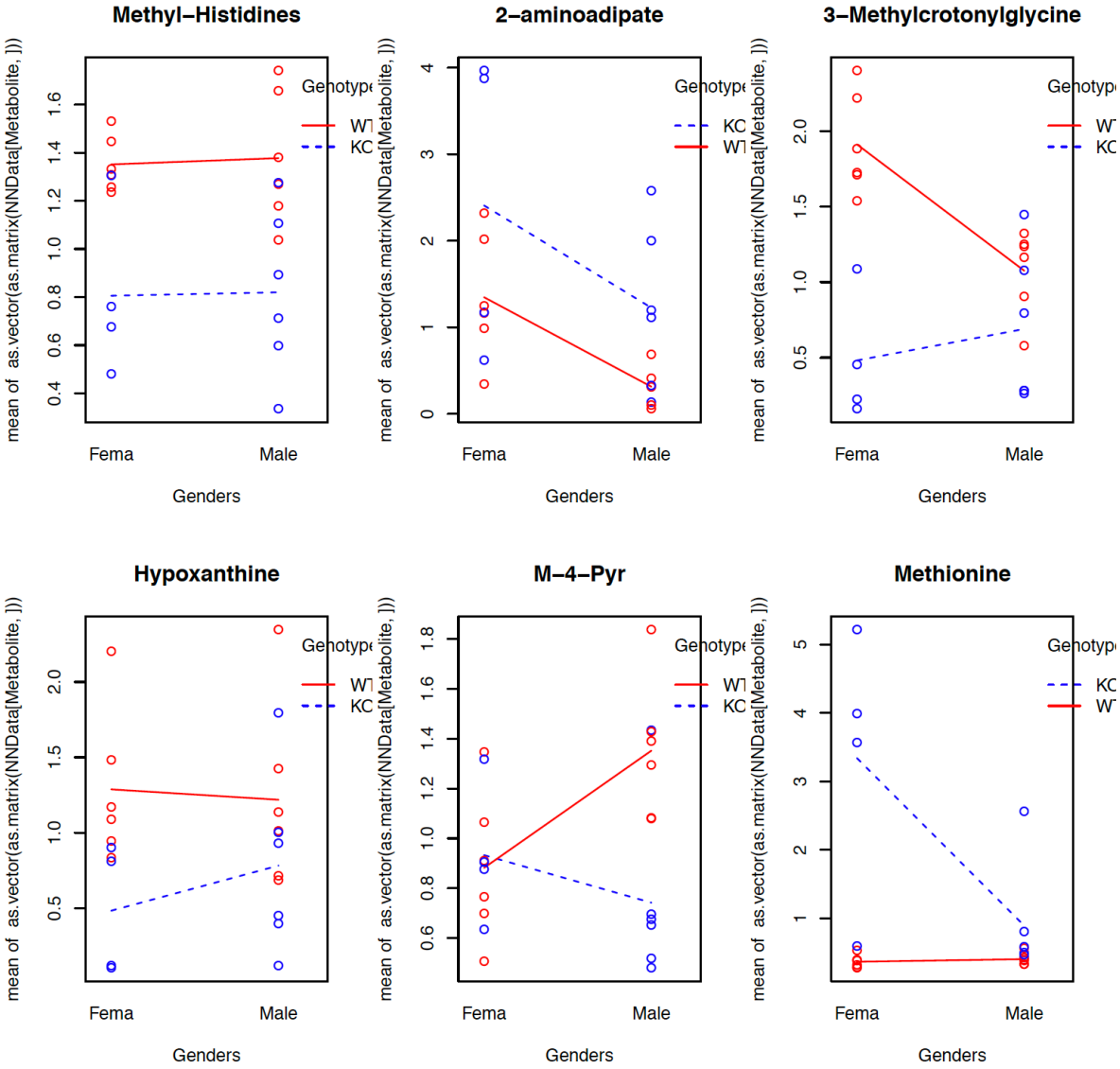

Methyladenosine
Octanoylcarnitine
dCMP
UMP
Nicotinamide Ribotide
SAH
mean of as.vector(as.matrix(NNData[Metabolite,]))
Genders
Fema
Male
Genotype
KC
WT

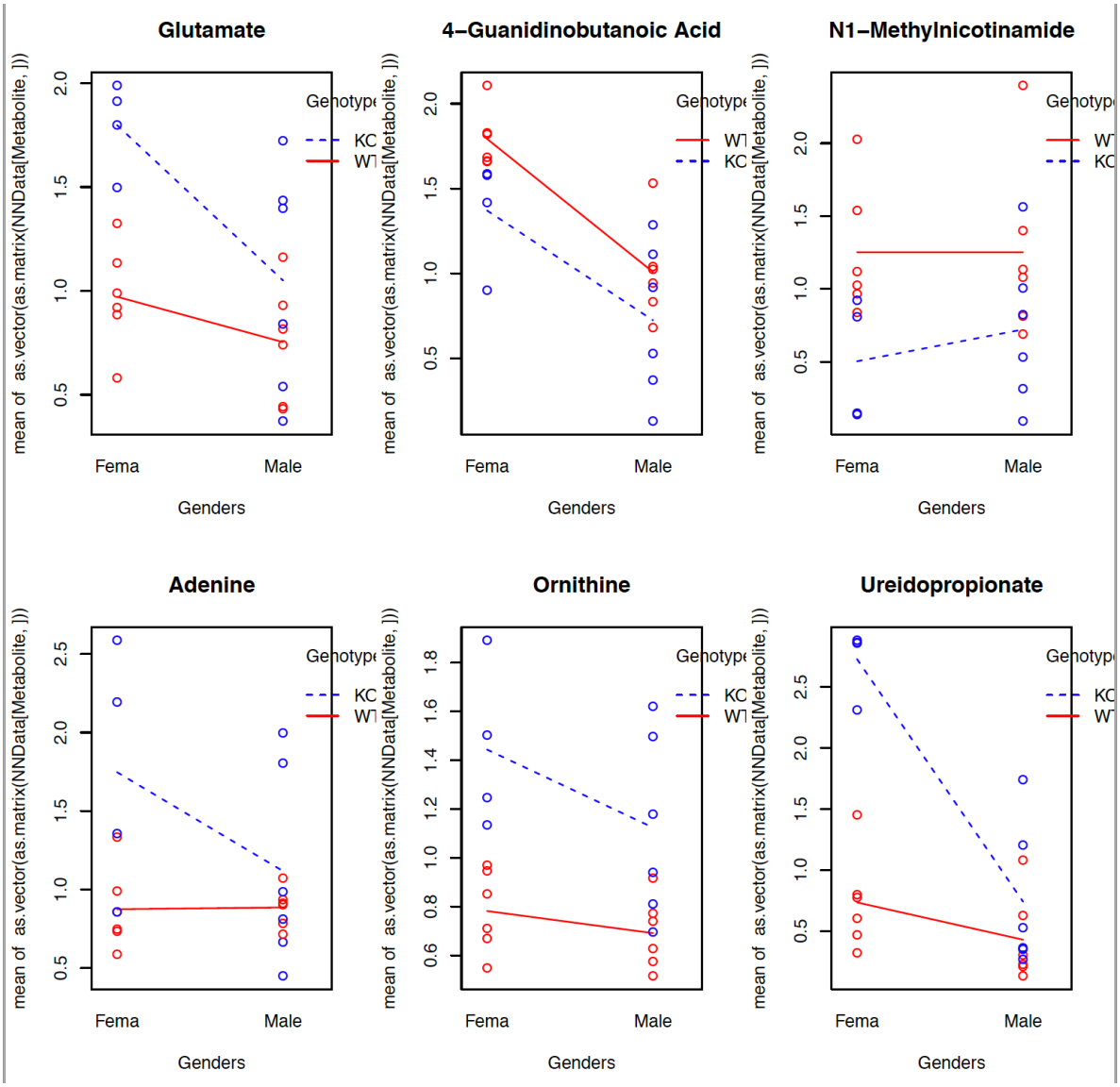

SAM
UDP
Hydroxyhexadecanoylcarnitine
CDP−Choline
NAD+
CoA
mean of as.vector(as.matrix(NNData[Metabolite,]))
Genotype
KO
WT
Fema
Male
Genders

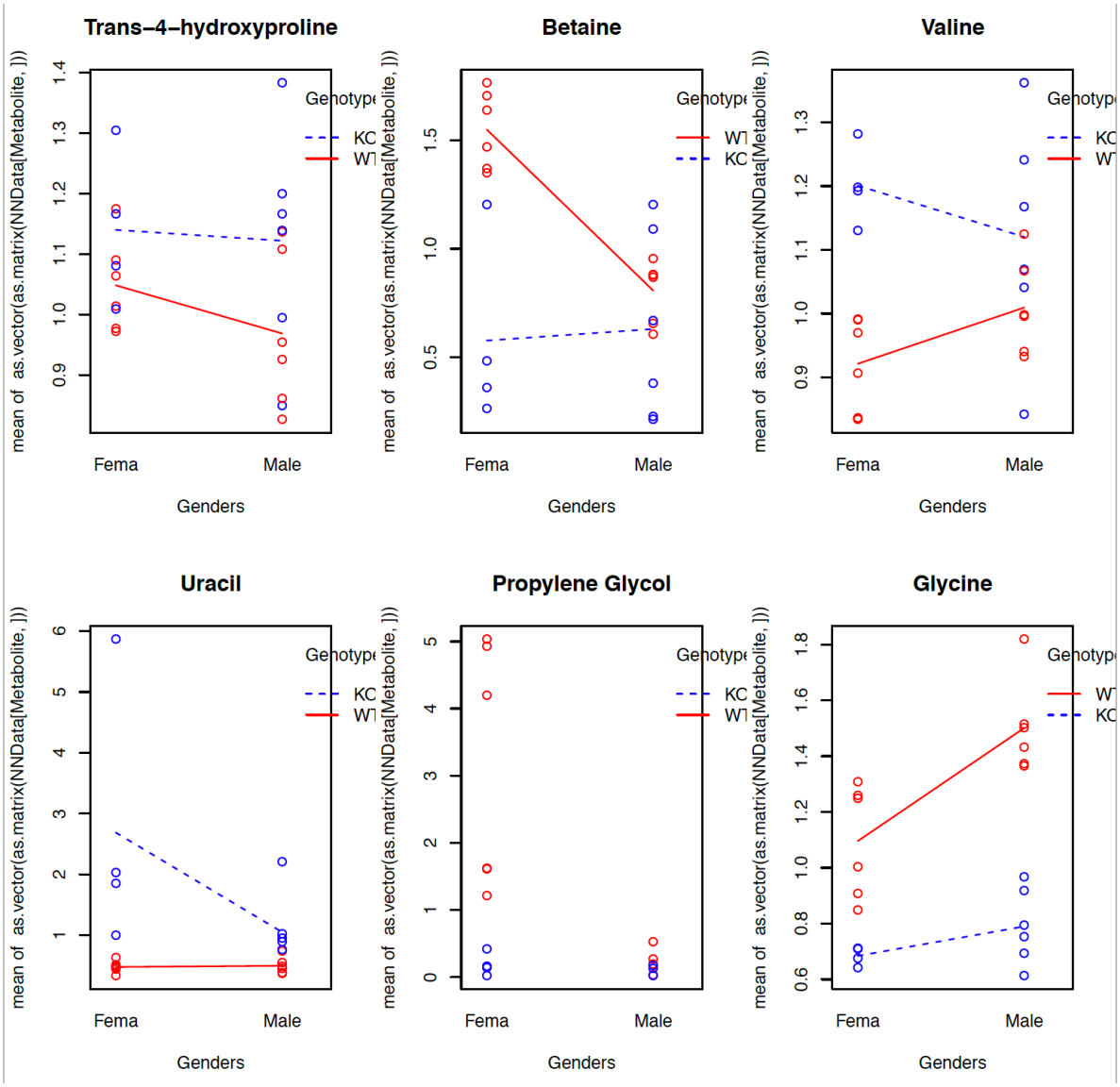

Acetyl−CoA
Succinyl−CoA
NADH
GDP
AMP
dAMP
mean of as.vector(as.matrix(NNData[Metabolite,]))
Genotype
KO
WT
Fema
Male
Genders

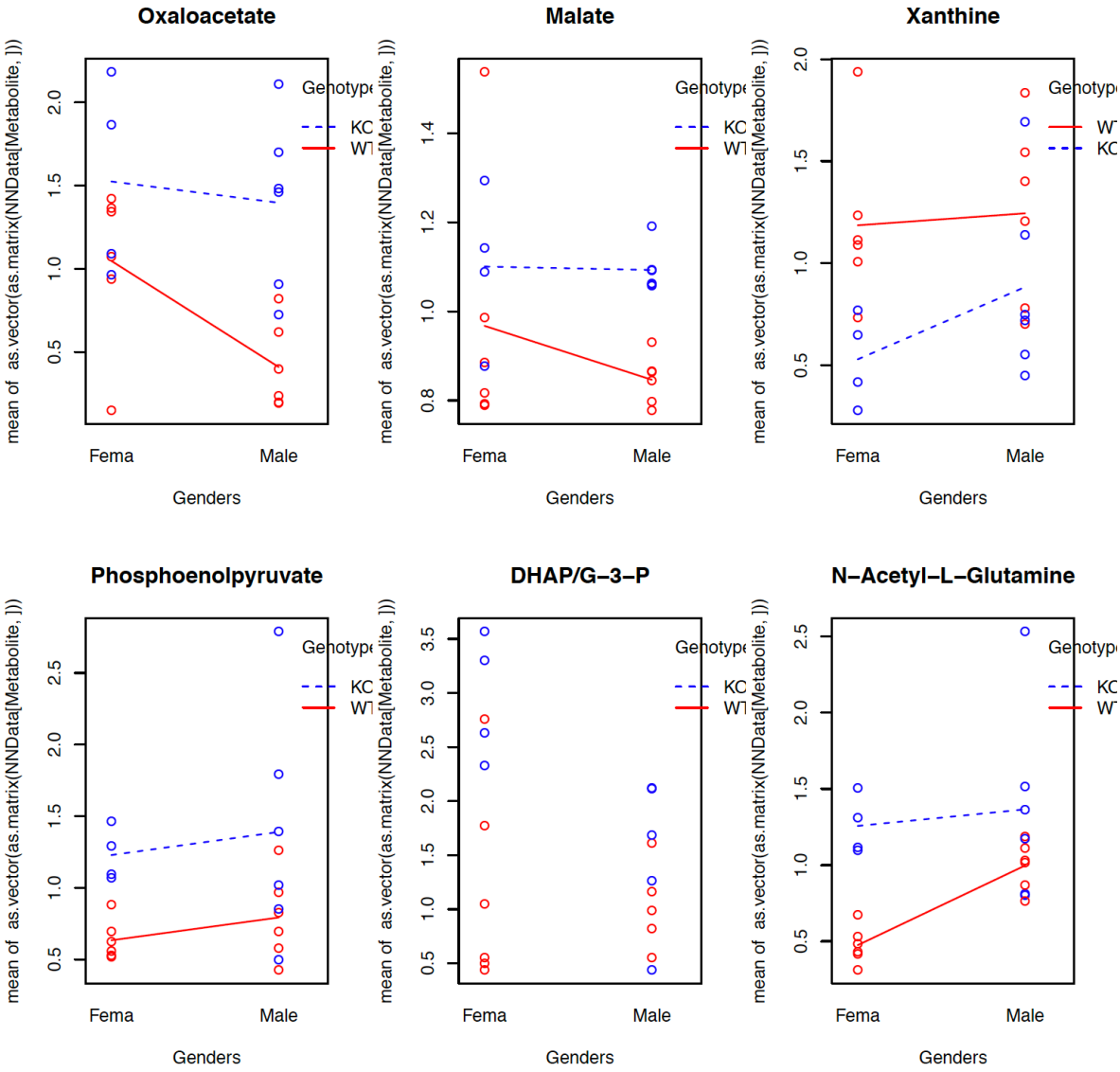

cAMP
CMP
Glutathione Reduced
5–Methylthioadenosine
3–hydroxyisovalerylcarnitine
Deoxyinosine
mean of as.vector(as.matrix(NNData[Metabolite,]))
Genotype
KO
WT
Fema
Male
Genders

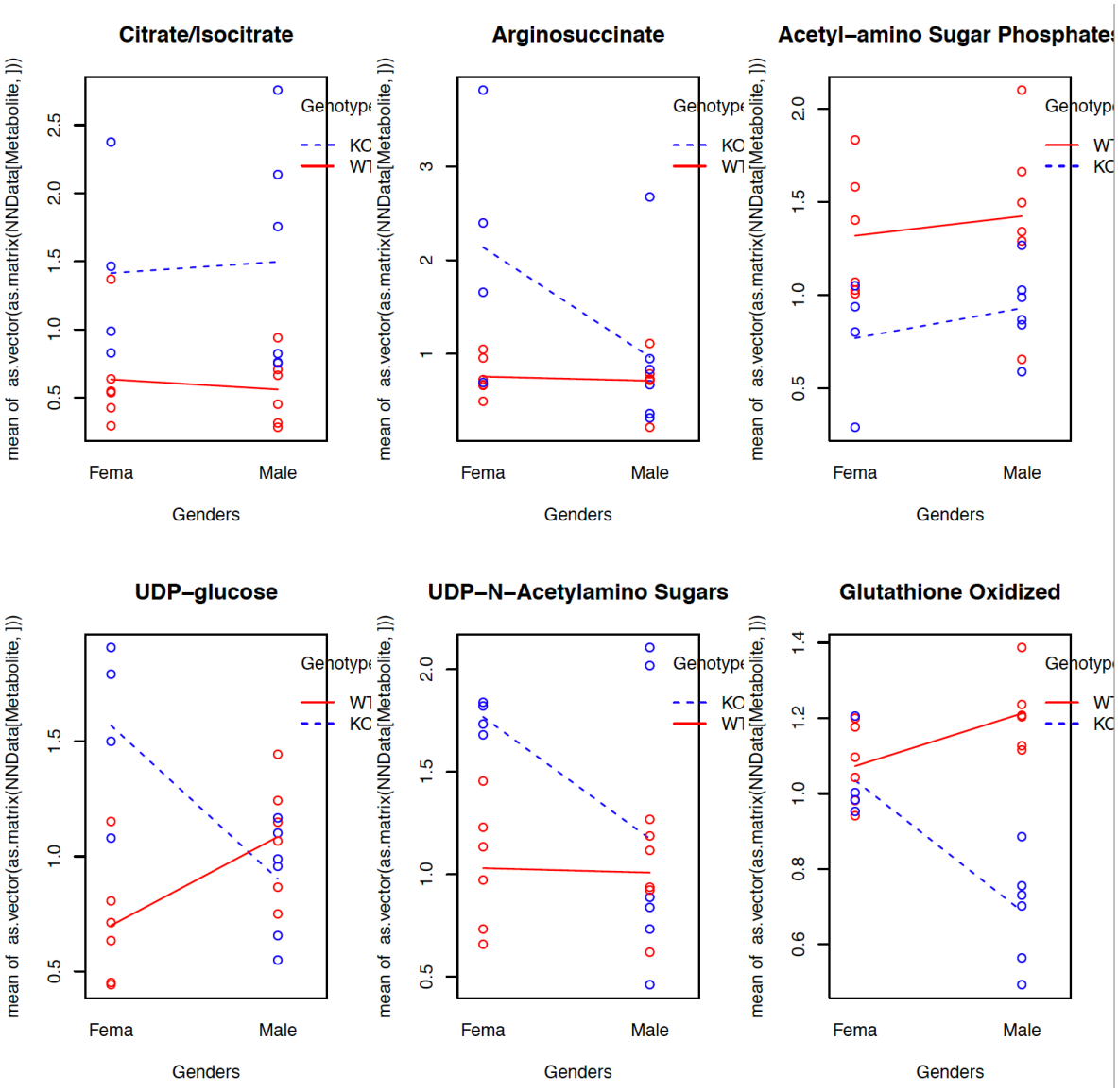

N2–acetyllysine
Phosphoserine
Allantoate
N–Acetylaspartate
Acetylornithine
3–Methyl–Histidine
mean of as.vector(as.matrix(NNData[Metabolite,]))
Genotype
KO
WT
Fema
Male
Genders

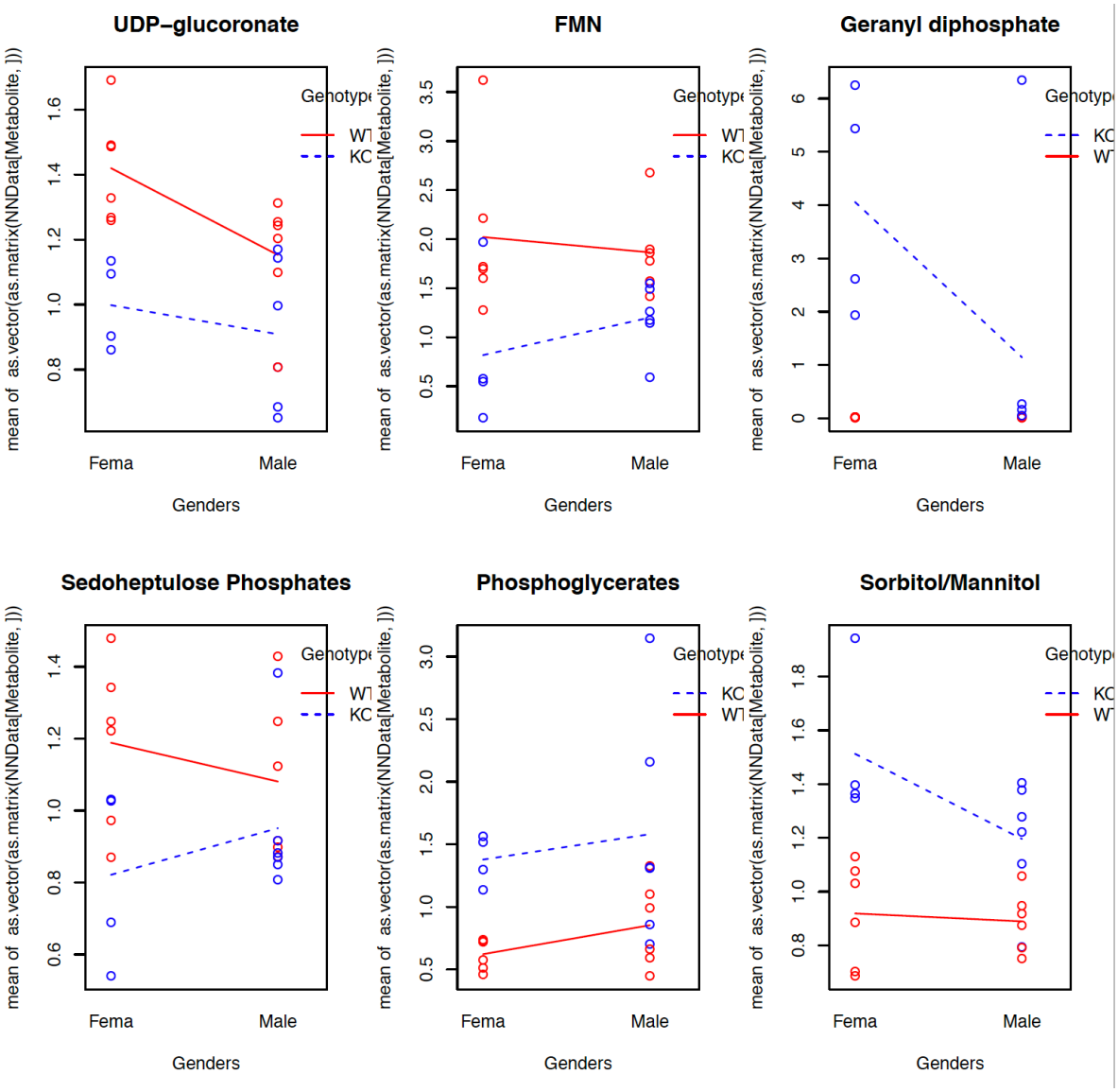

Methyl–Histidines
2–aminoadipate
3–Methylcrotonylglycine
Hypoxanthine
M–4–Pyr
Methionine
mean of as.vector(as.matrix(NNData[Metabolite,]))
Genotype
WT
KO
Fema
Male
Genders

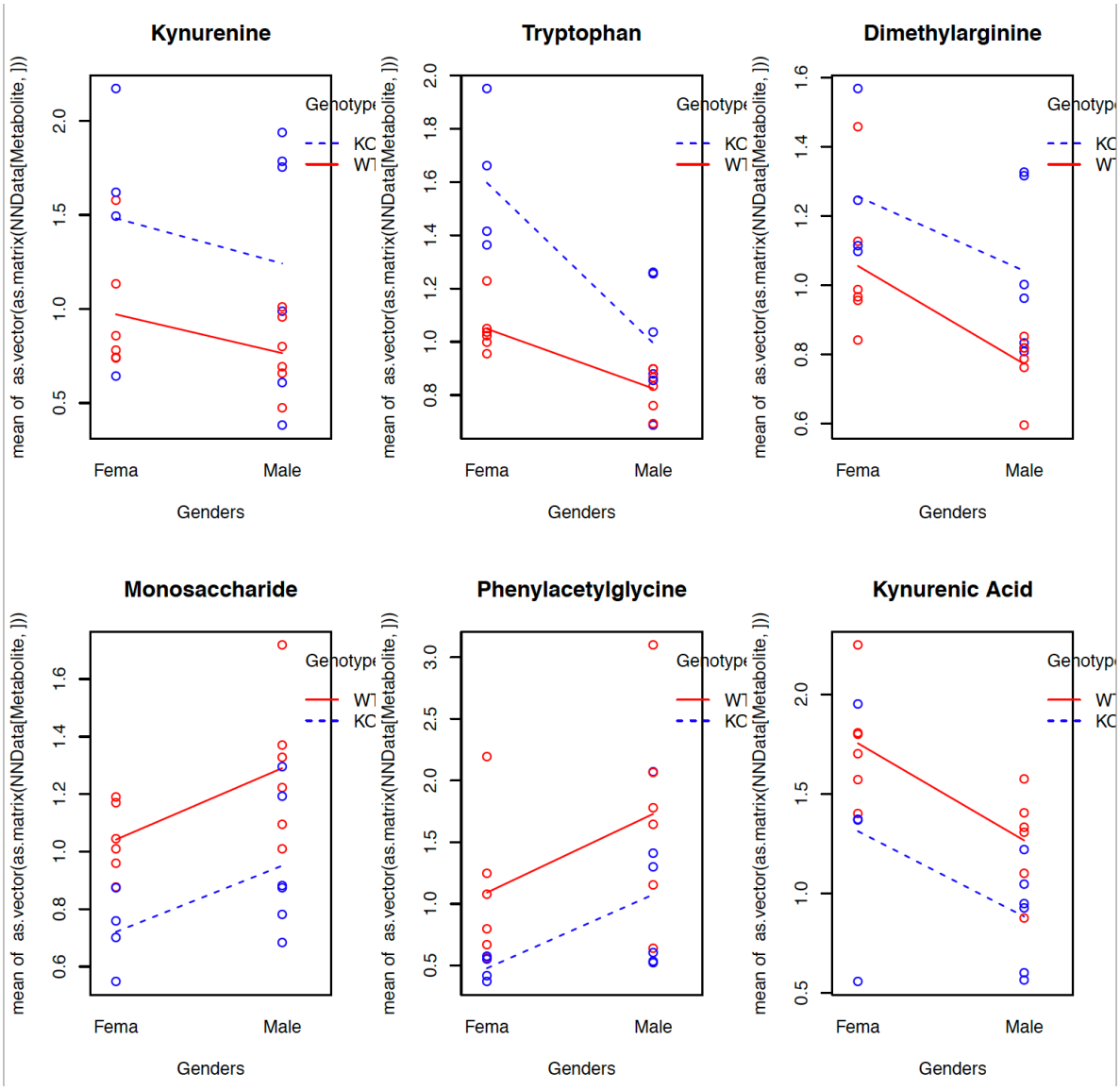

Glutamate
4−Guanidinobutanoic Acid
N1−Methylnicotinamide
Adenine
Ornithine
Ureidopropionate
mean of as.vector(as.matrix(NNData[Metabolite,]))
Genotype
KO
WT
Fema
Male
Genders

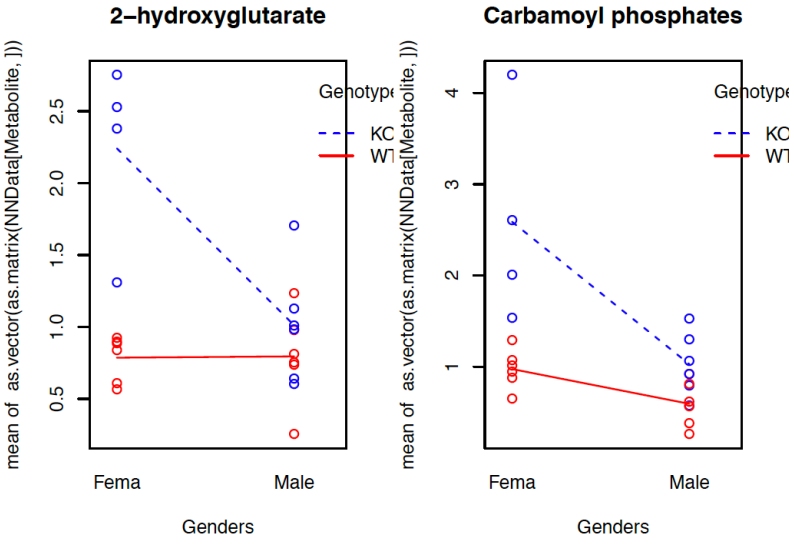

Trans–4–hydroxyproline
Betaine
Valine
Uracil
Propylene Glycol
Glycine
mean of as.vector(as.matrix(NNData[Metabolite,]))
Genotype
KO
WT
Fema
Male
Genders


Oxaloacetate
Malate
Xanthine
Phosphoenolpyruvate
DHAP/G−3−P
N−Acetyl−L−Glutamine
mean of as.vector(as.matrix(NNData[Metabolite,]))
Genotype
KC
WT
Fema
Male
Genders

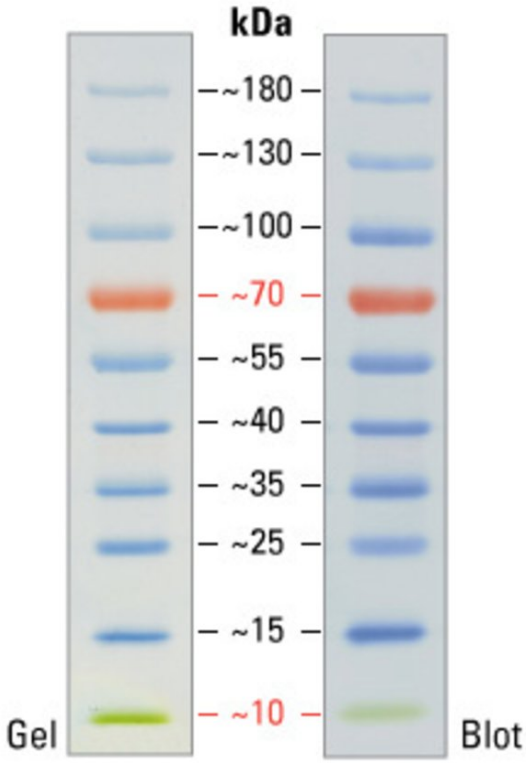

Citrate/Isocitrate
Arginosuccinate
Acetyl−amino Sugar Phosphates
UDP−glucose
UDP−N−Acetylamino Sugars
Glutathione Oxidized
mean of as.vector(as.matrix(NNData[Metabolite,]))
Genotype
KO
WT
Fema
Male
Genders


UDP−glucoronate
FMN
Geranyl diphosphate
Sedoheptulose Phosphates
Phosphoglycerates
Sorbitol/Mannitol
mean of as.vector(as.matrix(NNData[Metabolite,]))
Genotype
WT
KO
Fema
Male
Genders


Kynurenine
Tryptophan
Dimethylarginine
Monosaccharide
Phenylacetylglycine
Kynurenic Acid
mean of as.vector(as.matrix(NNData[Metabolite,]))
Genotype
KO
WT
Fema
Male
Genders


2–hydroxyglutarate
mean of as.vector(as.matrix(NNData[Metabolite,]))
0.5
1.0
1.5
2.0
2.5
Fema
Male
Genders
Genotype
KC
WT
Carbamoyl phosphates
mean of as.vector(as.matrix(NNData[Metabolite,]))
1
2
3
4
Fema
Male
Genders
Genotype
KC
WT

9.2.2 Thermo Prestained page ruler used in all western blot experiments as molecular weight indicator.



9.2.3 Permissions to use published figures in literature review section



Copyright Clearance Center

Confirmation Number: 11827562
Order Date: 06/28/2019

Customer Information

Customer: Sibel Cal Kayitmazbatir
Account Number: 3001476145
Organization: Koc University
Email: cal.sibel@gmail.com
Phone: +90 (543)6642191
Payment Method: Invoice

This is not an invoice

Order Details

Current opinion in neurobiology

Billing Status: **N/A**

Order detail ID: 71933645
ISSN: 0959-4388
Publication Type: Journal
Volume:
Issue:
Start page:
Publisher: ELSEVIER LTD.

Permission Status: Granted
Permission type: Republish or display content
Type of use: Thesis/Dissertation
Order License Id: 4617511272853
Order ref number: N/A

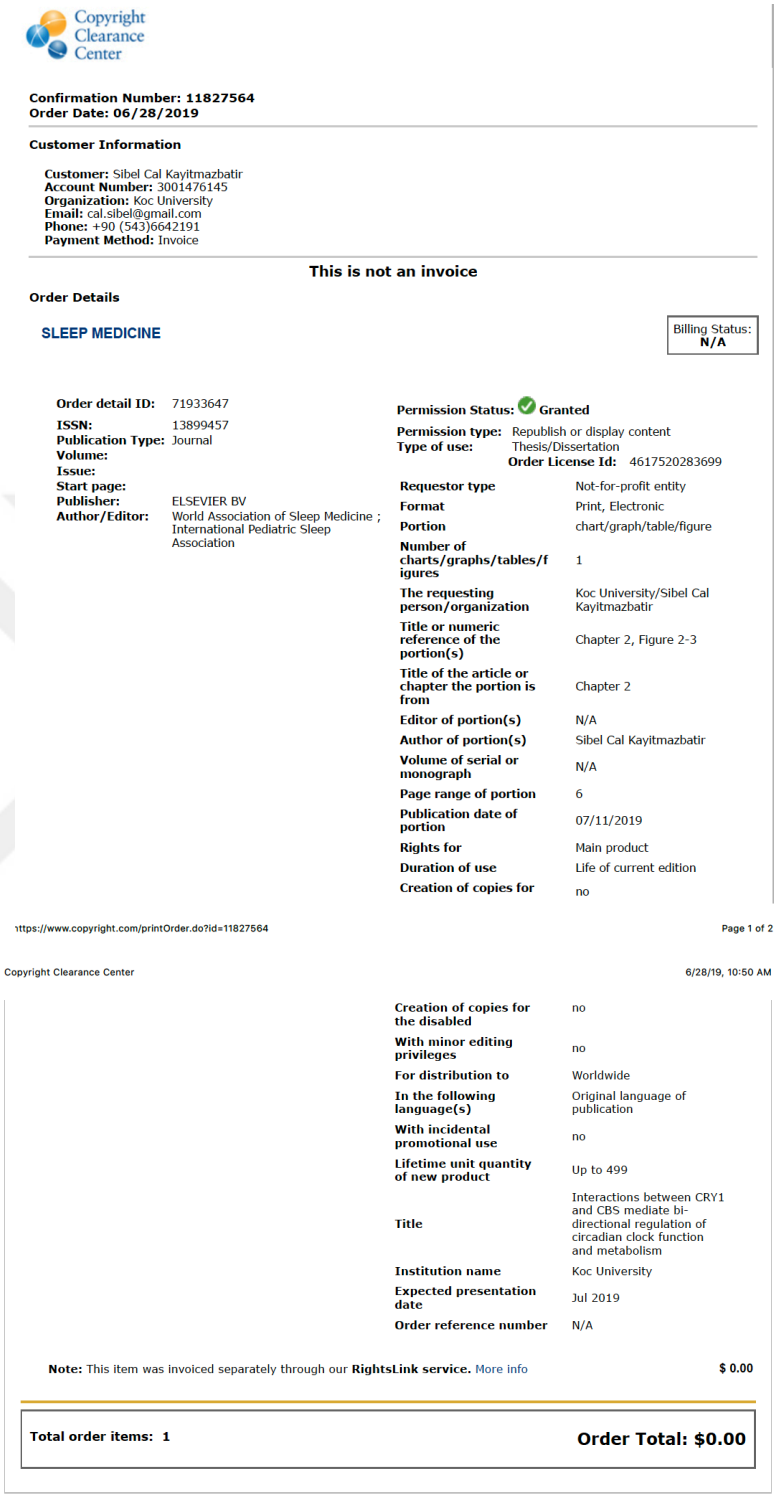
Requestor type	Not-for-profit entity
Format	Print
Portion	chart/graph/table/figure
Number of charts/graphs/tables/figures	1
The requesting person/organization	Koc University/Sibel Cal Kayitmazbatir
Title or numeric reference of the portion(s)	Chapter 2, Figure 2-1
Title of the article or chapter the portion is from	N/A
Editor of portion(s)	N/A
Author of portion(s)	Sibel Cal Kayitmazbatir
Volume of serial or monograph	N/A
Page range of portion	4
Publication date of portion	07/11/2019
Rights for	Main product
Duration of use	Life of current edition

Creation of copies for the disabled	no
With minor editing privileges	no
For distribution to	Worldwide
In the following language(s)	Original language of publication
With incidental promotional use	no
Lifetime unit quantity of new product	Up to 499
Title	Interactions between CRY1 and CBS mediate bi-directional regulation of circadian clock function and metabolism
Institution name	Koc University
Expected presentation date	Jul 2019
Order reference number	N/A

Note: This item was invoiced separately through our **RightsLink service.** More info **$ 0.00**

Total order items: 1 **Order Total: $0.00**

About Us | Privacy Policy | Terms & Conditions | Pay an Invoice
Copyright 2019 Copyright Clearance Center



Copyright Clearance Center

Confirmation Number: 11827564
Order Date: 06/28/2019

Customer Information

Customer: Sibel Cal Kayitmazbatir
Account Number: 3001476145
Organization: Koc University
Email: cal.sibel@gmail.com
Phone: +90 (543)6642191
Payment Method: Invoice

This is not an invoice

Order Details

SLEEP MEDICINE

Billing Status: **N/A**

Order detail ID:	71933647
ISSN:	13899457
Publication Type:	Journal
Volume:	
Issue:	
Start page:	
Publisher:	ELSEVIER BV
Author/Editor:	World Association of Sleep Medicine ; International Pediatric Sleep Association

Permission Status: Granted

Permission type: Republish or display content
Type of use: Thesis/Dissertation
Order License Id: 4617520283699

Requestor type	Not-for-profit entity
Format	Print, Electronic
Portion	chart/graph/table/figure
Number of charts/graphs/tables/figures	1
The requesting person/organization	Koc University/Sibel Cal Kayitmazbatir
Title or numeric reference of the portion(s)	Chapter 2, Figure 2-3
Title of the article or chapter the portion is from	Chapter 2
Editor of portion(s)	N/A
Author of portion(s)	Sibel Cal Kayitmazbatir
Volume of serial or monograph	N/A
Page range of portion	6
Publication date of portion	07/11/2019
Rights for	Main product
Duration of use	Life of current edition
Creation of copies for	no

Creation of copies for the disabled	no
With minor editing privileges	no
For distribution to	Worldwide
In the following language(s)	Original language of publication
With incidental promotional use	no
Lifetime unit quantity of new product	Up to 499
Title	Interactions between CRY1 and CBS mediate bi-directional regulation of circadian clock function and metabolism
Institution name	Koc University
Expected presentation date	Jul 2019
Order reference number	N/A

Note: This item was invoiced separately through our **RightsLink service.** More info **$ 0.00**

Total order items: 1 **Order Total: $0.00**

About Us | Privacy Policy | Terms & Conditions | Pay an Invoice

Copyright 2019 Copyright Clearance Center

Copyright Clearance Center

Confirmation Number: 11827566
Order Date: 06/28/2019

Customer Information

Customer: Sibel Cal Kayitmazbatir
Account Number: 3001476145
Organization: Koc University
Email: cal.sibel@gmail.com
Phone: +90 (543)6642191
Payment Method: Invoice

This is not an invoice

Order Details

Nature Reviews Neurology

Billing Status: **N/A**

Order detail ID: 71933649
ISSN: 1759-4766
Publication Type: e-Journal
Volume:
Issue:
Start page:
Publisher: Nature Publishing Group

Permission Status: Granted
Permission type: Republish or display content
Type of use: Thesis/Dissertation
Order License Id: 4617520883506

Requestor type	Not-for-profit entity
Format	Print, Electronic
Portion	chart/graph/table/figure
Number of charts/graphs/tables/figures	1
The requesting person/organization	Koc University/Sibel Cal Kayitmazbatir
Title or numeric reference of the portion(s)	Chapter 2, Figure 2-6
Title of the article or chapter the portion is from	Chapter 2
Editor of portion(s)	N/A
Author of portion(s)	Sibel Cal Kayitmazbatir
Volume of serial or monograph	N/A
Page range of portion	14
Publication date of portion	07/11/20197
Rights for	Main product
Duration of use	Life of current edition
Creation of copies for	no

Creation of copies for the disabled	no
With minor editing privileges	no
For distribution to	Worldwide
In the following language(s)	Original language of publication
With incidental promotional use	no
Lifetime unit quantity of new product	Up to 499
Title	Interactions between CRY1 and CBS mediate bi-directional regulation of circadian clock function and metabolism
Institution name	Koc University
Expected presentation date	Jul 2019
Order reference number	N/A

Note: This item was invoiced separately through our **RightsLink service.** More info **$ 0.00**

Total order items: 1 **Order Total: $0.00**

About Us | Privacy Policy | Terms & Conditions | Pay an Invoice

Copyright 2019 Copyright Clearance Center

Copyright Clearance Center

Confirmation Number: 11827573
Order Date: 06/28/2019

Customer Information

Customer: Sibel Cal Kayitmazbatir
Account Number: 3001476145
Organization: Koc University
Email: cal.sibel@gmail.com
Phone: +90 (543)6642191
Payment Method: Invoice

This is not an invoice

Order Details

Cell

Billing Status: **N/A**

Order detail ID: 71933656
ISSN: 0092-8674
Publication Type: Journal
Volume:
Issue:
Start page:
Publisher: CELL PRESS
Author/Editor: National Institute for Medical Research

Permission Status: Granted
Permission type: Republish or display content
Type of use: Thesis/Dissertation
Order License Id: 4617521416931

Requestor type	Not-for-profit entity
Format	Print, Electronic
Portion	chart/graph/table/figure
Number of charts/graphs/tables/figures	1
The requesting person/organization	Koc University/ Sibel Cal Kayitmazbatir
Title or numeric reference of the portion(s)	Chapter 2, Figure 2-7
Title of the article or chapter the portion is from	N/A
Editor of portion(s)	N/A
Author of portion(s)	Sibel Cal Kayitmazbatir
Volume of serial or monograph	N/A
Page range of portion	15
Publication date of portion	07/11/2019
Rights for	Main product
Duration of use	Life of current edition
Creation of copies for	no

Creation of copies for the disabled	no
With minor editing privileges	no
For distribution to	Worldwide
In the following language(s)	Original language of publication
With incidental promotional use	no
Lifetime unit quantity of new product	Up to 499
Title	Interactions between CRY1 and CBS mediate bi-directional regulation of circadian clock function and metabolism
Institution name	Koc University
Expected presentation date	Jul 2019
Order reference number	N/A

Note: This item was invoiced separately through our **RightsLink service.** More info **$ 0.00**

Total order items: 1 **Order Total: $0.00**

About Us | Privacy Policy | Terms & Conditions | Pay an Invoice

Copyright 2019 Copyright Clearance Center

Copyright Clearance Center

Confirmation Number: 11827576
Order Date: 06/28/2019

Customer Information

Customer: Sibel Cal Kayitmazbatir
Account Number: 3001476145
Organization: Koc University
Email: cal.sibel@gmail.com
Phone: +90 (543)6642191
Payment Method: Invoice

This is not an invoice

Order Details

Science

Billing Status: **N/A**

Order detail ID:	71933663
ISSN:	1095-9203
Publication Type:	e-Journal
Volume:	
Issue:	
Start page:	
Publisher:	AMERICAN ASSOCIATION FOR THE ADVANCEMENT OF SCIENCE
Author/Editor:	American Association for the Advancement of Science

Permission Status: Granted
Permission type: Republish or display content
Type of use: Republish in a thesis/dissertation
Order License Id: 4617530132927

Requestor type	Not-for-profit entity
Format	Print, Electronic
Portion	chart/graph/table/figure
Number of charts/graphs/tables/figures	1
The requesting person/organization	Koc University/Sibel Cal Kayitmazbatir
Title or numeric reference of the portion(s)	Chapter 2, Figure 2-8
Title of the article or chapter the portion is from	Chapter 2
Editor of portion(s)	N/A
Author of portion(s)	Sibel Cal Kayitmazbatir
Volume of serial or monograph	N/A
Page range of portion	16
Publication date of portion	07/11/2019
Rights for	Main product
Duration of use	Life of current edition
Creation of copies for	no

Creation of copies for the disabled	no
With minor editing privileges	no
For distribution to	Worldwide
In the following language(s)	Original language of publication
With incidental promotional use	no
Lifetime unit quantity of new product	Up to 499
Title	Interactions between CRY1 and CBS mediate bi-directional regulation of circadian clock function and metabolism
Institution name	Koc University
Expected presentation date	Jul 2019
Order reference number	N/A

Note: This item was invoiced separately through our **RightsLink service.** More info **$ 0.00**

Total order items: 1 **Order Total: $0.00**

About Us | Privacy Policy | Terms & Conditions | Pay an Invoice

Copyright 2019 Copyright Clearance Center

Copyright Clearance Center

Confirmation Number: 11827590
Order Date: 06/28/2019

Customer Information

Customer: Sibel Cal Kayitmazbatir
Account Number: 3001476145
Organization: Koc University
Email: cal.sibel@gmail.com
Phone: +90 (543)6642191
Payment Method: Invoice

This is not an invoice

Order Details

Trends in cell biology

Billing Status: **N/A**

Order detail ID: 71933678
ISSN: 0962-8924
Publication Type: Journal
Volume:
Issue:
Start page:
Publisher: ELSEVIER LTD.

Permission Status: Granted
Permission type: Republish or display content
Type of use: Thesis/Dissertation
Order License Id: 4617550104582

Requestor type	Not-for-profit entity
Format	Print, Electronic
Portion	chart/graph/table/figure
Number of charts/graphs/tables/figures	1
The requesting person/organization	Koc University/Sibel Cal Kayitmazbatir
Title or numeric reference of the portion(s)	Chapter 2, Figure 2-9
Title of the article or chapter the portion is from	N/A
Editor of portion(s)	N/A
Author of portion(s)	Sibel Cal Kayitmazbatir
Volume of serial or monograph	N/A
Page range of portion	18
Publication date of portion	07/11/2019
Rights for	Main product
Duration of use	Life of current edition
Creation of copies for	no

Creation of copies for the disabled	no
With minor editing privileges	no
For distribution to	Worldwide
In the following language(s)	Original language of publication
With incidental promotional use	no
Lifetime unit quantity of new product	Up to 499
Title	Interactions between CRY1 and CBS mediate bi-directional regulation of circadian clock function and metabolism
Institution name	Koc University
Expected presentation date	Jul 2019
Order reference number	N/A

Note: This item was invoiced separately through our **RightsLink service.** More info **$ 0.00**

Total order items: 1 **Order Total: $0.00**

Copyright 2019 Copyright Clearance Center